

Dynamic Modelling and Simulation of (Pulsed and Stirred) Liquid-Liquid Extraction Columns using the Population Balance Equation

Dem Fachbereich Maschinenbau und Verfahrenstechnik
der Technischen Universität Kaiserslautern
zur Erlangung des akademischen Grades

Doktor-Ingenieur (Dr.-Ing.)

genehmigte
Dissertation

von Herrn

M. Sc. Eng. Moutasem Jaradat

aus Irbid – Jordanien

Tag der mündlichen Prüfung: 06. 07. 2012

Dekan: Prof. Dr.-Ing. B. Sauer

Prüfungskommission:

Vorsitzender: Prof. Dr.-Ing. M. Böhle

Referenten: Prof. Dipl.-Ing. Dr. techn. H.-J. Bart

Prof. Dr. N. M. Faqir

D 386

Kaiserslautern, 2012

DEDICATIONS

First and foremost, I humbly thank *Allah Almighty*, the *Merciful* and the *Beneficent* for giving every opportunity I have had to succeed and for surrounding me with so many wonderful people that support me throughout my life. Everything I have achieved is because of Him. I would like to thank my whole family for their love and support. One of the many things my parents instilled in me is the importance of a good education and work ethic, and for that I am forever grateful.

I would like to dedicate this work to my parents, my coming babies, my wife, my brothers and my sisters. Without their support, I would not be where I am today.

ACKNOWLEDGMENT

The research work of this doctoral thesis was carried out at the Technical University Kaiserslautern, in the Institute of Separation Science and Technology chaired by Prof. Dipl.-Ing. Dr. techn. Hans-Jörg Bart, during the years 2008-2011. I'm grateful and thankful for Prof. Hans-Jörg Bart for giving me the opportunity of studying this interesting and challenging research work and for supervising this thesis.

I am deeply indebted to my advisor Prof. Hans-Jörg Bart for his guidance, collaboration and his permanent and extensive support as well as encouraging me to accomplish this hard work. I highly appreciate his trust and his excellent advice and guidance during all stages of this long term research, in particularly for his contributions to my publications encouragement throughout my research. I would like to gratefully thank him for his guidance and collaboration. I am very grateful to Prof. Naim Faqir for his serving as committee member and to Prof. Böhle for taking the chairmanship of the examination committee. I am equally indebted to my advisory committee members, Prof. Hans-Jörg Bart and Prof. Naim Faqir, for their providing invaluable suggestions towards this research.

I would also like to express my thanks to Dr. M. Attarakih from the University of Jordan for his support and technical consulting and for granting me access to his mathematical models, discrete population balance algorithm, and source codes during his summer visits (from 2008 to 2010) at the Chair Separation & Science Technology at the University of Kaiserslautern/ Germany. I gratefully acknowledge Dr. Hussein Allaboun and Prof. Naim Faqir for their advice and guidance; they provided me unflinching encouragement and support in various ways. I am deeply indebted to all my colleagues and co-authors for their cooperation, ideas and contribution on this project, also for the pleasant working atmosphere at the institute. I also wish to thank Dr. Krätz and the secretaries of the Institute. Also, my special thanks to the Simulation and CFD group for the cooperation encouragements and valuable suggestions, advices and discussions.

My special grateful is for my parents, my coming babies, my wife, my brothers and my sisters. They have been suffering for patience to see me getting my Ph.D. To the whole family members who are waiting for my successful comeback to my home country Jordan.

This work is supported by the precious financial support by Graduiertenkolleg of TU Kaiserslautern, Deutsche Forschungsgemeinschaft (DFG), DAAD (Deutscher Akademischer Austauschdienst), the Federal State Research Centre of Mathematical and Computational Modelling (CM)²- TU Kaiserslautern, and to Prof. Hans-Jörg Bart, to all those I gratefully acknowledge this support.

Finally, I wish to express my deep appreciation and warmest thanks to my dear parents, my coming babies, my wife, my brothers and my sisters for their support, affection, patience, trust, support and inspiration throughout my research and education. Special thanks to my wife for her love, patience and support.

Kaiserslautern, 2012

Moutasem Jaradat

ABSTRACT

The discrete nature of the dispersed phase (swarm of droplet) in stirred and pulsed liquid-liquid extraction columns makes its mathematical modelling of such complex system a tedious task. The dispersed phase is considered as a population of droplets distributed randomly with respect to their internal properties (such as: droplet size and solute concentration) at a specific location in space. Hence, the population balance equation has been emerged as a mathematical tool to model and describe such complex behaviour. However, the resulting model is too complicated. Accordingly, the analytical solution of such a mathematical model does not exist except for particular cases. Therefore, numerical solutions are resorted to in general. This is due to the inherent nonlinearities in the convective and diffusive terms as well as the appearance of many integrals in the source term. However, modelling and simulation of liquid extraction columns is not an easy task because of the discrete nature of the dispersed phase, which consist of population of droplets. The natural frame work for taking this into account is the population balance approach.

In part of this doctoral thesis work, a rigours mathematical model based on the bivariate population balance frame work (the base of LLECMOD ‘‘Liquid-Liquid Extraction Column Module’’) for the steady state and dynamic simulation of pulsed (sieve plate and packed) liquid-liquid extraction columns is developed. The model simulates the coupled hydrodynamic and mass transfer for pulsed (packed and sieve plate) extraction columns. The model is programmed using visual digital FORTRAN and then integrated into the LLECMOD program. Within LLECMOD the user can simulate different types of extraction columns including stirred and pulsed ones. The basis of LLECMOD depends on stable robust numerical algorithms based on an extended version of a fixed pivot technique after Attarakih et al., 2003 (to take into account interphase solute transfer) and advanced computational fluid dynamics numerical methods. Experimental validated correlations are used for the estimation of the droplet terminal velocity in extraction columns based on single and swarm droplet experiments in laboratory scale devices. Additionally, recent published correlations for turbulent energy dissipation, droplet breakage and coalescence frequencies are discussed as been used in this version of LLECMOD. Moreover, coalescence model from literature derived from a stochastical description have been modified to fit the deterministic population model. As a case study, LLECMOD is used here to simulate the steady state performance of pulsed extraction columns under different operating conditions, which include pulsation intensity and volumetric flow rates are simulated. The effect of pulsation intensity (on the holdup, mean droplet diameter and solute concentration) is found to have more profound effect on systems of high interfacial tension. On the hand, the variation of volumetric flow rates have substantial effect on the holdup, mean droplet diameter and solute concentration profiles for chemical systems with low interfacial tension. Two chemical test systems recommended by the European Federation of Chemical Engineering (water-acetone (solute)-n-butyl acetate and water-acetone (solute)-toluene) and an industrial test system are used in the simulation. Model predictions are successfully validated against steady state and transient

experimental data, where good agreements are achieved. The simulated results (holdup, mean droplet diameter and mass transfer profiles) compared to the experimental data show that LLECMOD is a powerful simulation tool, which can efficiently predict the dynamic and steady state performance of pulsed extraction columns.

In other part of this doctoral thesis work, the steady state performance of extraction columns is studied taking into account the effect of dispersed phase inlet condition (light or heavy phase is dispersed) and the direction of mass transfer (from continuous to dispersed phase and vice versa) using the population balance framework. LLECMOD, a program that uses multivariate population balance models, is extended to take into account the direction of mass transfer and the dispersed phase inlet. As a case study, LLECMOD is used to simulate pilot plant RDC columns where the steady state mean flow properties (dispersed phase hold up and droplet mean diameter) and the solute concentration profiles are compared to the available experimental data. Three chemical systems were used: sulpholane–benzene–n-heptane, water–acetone–toluene and water–acetone–n-butyl acetate. The dispersed phase inlet and the direction of mass transfer as well as the chemical system physical properties are found to have profound effect on the steady state performance of the RDC column. For example, the mean droplet diameter is found to persist invariant when the heavy phase is dispersed and the extractor efficiency is higher when the direction of mass transfer is from the continuous to the dispersed phase. For the purpose of experimental validation, it is found that LLECMOD predictions are in good agreement with the available experimental data concerning the dispersed phase hold up, mean droplet diameter and solute concentration profiles in both phases.

In a further part of this doctoral thesis, a mathematical model is developed for liquid extraction columns based on the multivariate population balance equation (PBE) and the primary secondary particle method (PSPM) introduced by Attarakih, 2010 (US Patent Application: 0100106467). It is extended to include the momentum balance for the dispersed phase. The advantage of momentum balance is to eliminate the need for often conflicting correlations used in estimating the terminal velocity of single and swarm of droplets. The resulting mathematical model is complex due to the integral nature of the population balance equation. To reduce the complexity of this model, while maintaining most of the information drawn from the continuous population balance equation, the concept of the PSPM is used. Based on the multivariate population balance equation and the PSPM a mathematical model is developed for any liquid extraction column. The secondary particle could be envisaged as a fluid particle carrying information about the distribution as it is evolved in space and time, in the meanwhile the primary particles carry the mean properties of the population such as total droplet concentration; mean droplet diameter dispersed phase hold up and so on. This information reflects the particle-particle interactions (breakage and coalescence) and transport (convection and diffusion). The developed model is discretized in space using a first-order upwind method, while semi-implicit first-order scheme in time is used to simulate a pilot plant RDC extraction column. Here the effect of the number of primary particles (classes) on the final predicted solution is investigated. Numerical results show that the solution converge fast even as the number of primary particle is increased. The terminal droplet velocity of the individual primary particle is found the most sensitive to the number of

primary particles. Other mean population properties like the droplet mean diameter, mean hold up and the concentration profiles are also found to converge along the column height by increasing the number of primary particles. The predicted steady state profiles (droplet diameter, holdup and the concentration profiles) along a pilot RDC extraction column are compared to the experimental data where good agreement is achieved.

In addition to this a robust rigorous mathematical model based on the bivariate population balance equation is developed to predict the steady state and dynamic behaviour of the interacting hydrodynamics and mass transfer in Kühni extraction columns. The developed model is extended to include the momentum balance for the calculation of the droplet velocity. The effects of step changes in the important input variables (such as volumetric flow rates, rotational speed, inlet solute concentrations etc.) on the output variables (dispersed phase holdup, mean droplet diameter and the concentration profiles) are investigated.

The last topic of this doctoral thesis is developed to transient problems. The unsteady state analysis reveals the fact that the largest time constant (slowest response) is due to the mass transfer. On the contrary, the hydrodynamic response of the dispersed phase holdup is very fast when compared to the mass transfer due to the relative fast motion of the dispersed droplets with respect to the continuous phase. The dynamic behaviour of the dispersed and continuous phases shows a lag time that increases away from the feed points of both phases. Moreover, the solute concentration response shows a highly nonlinear behaviour due to both positive and negative step changes in the input variables. The simulation results are in good agreement with the experimental ones and show the usefulness of the model.

ZUSAMMENFASSUNG

Die diskrete Natur der dispersen Phase (Schwarm von Tröpfchen) in gerührten und gepulsten Flüssig-Flüssig-Extraktionskolonnen macht aus ihrer mathematischen Modellierung solcher komplexer Systeme eine mühsame Aufgabe. Die disperse Phase wird als eine Population von Tröpfchen betrachtet, die zufällig in Bezug auf ihre inneren Werte an einem bestimmten Ort im Raum verteilt ist. Daher ist die Populationsbilanzgleichung als mathematisches Werkzeug zur Modellierung entstanden und beschreibt ein solch komplexes Verhalten. Allerdings ist das resultierende Modell zu kompliziert und dementsprechend gibt es die analytische Lösung eines solchen mathematischen Modells nur für bestimmte Fälle. Daher wird im Allgemeinen auf numerische Lösungen zurückgegriffen. Dies liegt an inhärenten Nichtlinearitäten in den konvektiven und diffusiven Bedingungen sowie an dem Erscheinungsbild vieler Integrale im Quellterm. Allerdings ist die Modellierung und Simulation von Flüssig-Flüssig-Extraktionskolonnen keine leichte Aufgabe, aufgrund der diskreten Natur der dispersen Phase mit ihrer Tropfengrößenverteilung.

In dieser Arbeit wird ein rigoroses mathematisches Modell basierend auf der bivariaten Populationsbilanz für den stationären Zustand und die dynamische Simulation der gepulsten Flüssig-Flüssig-Extraktionskolonnen entwickelt. Das Modell simuliert den gekoppelten hydrodynamischen Transport und Stofftransport für gepulste Packungs- und Siebbodenextraktionskolonnen. Das Modell wurde programmiert im "Visual Digitalen FORTRAN" und dann in das LLECMOD Programm integriert. Innerhalb LLECMOD kann der Anwender verschiedene Arten von Extraktionskolonnen simulieren, die gerührt oder gepulst werden. LLECMOD nutzt zur Lösung der Populationsbilanz die "general fixed pivot method" von Attarakih et al., 2003. Es enthält experimentell validierte Korrelationen für die Tropfenendgeschwindigkeit in Extraktionskolonnen basierend auf Experimenten von Einzel- und Schwarmtropfen. Darüber hinaus werden kürzlich veröffentlichte Korrelationen für turbulente Energiedissipation, Tropfenbruch und Koaleszenzfrequenzen diskutiert und modifiziert.

Als Fallstudie wird LLECMOD genutzt, um den stationären Zustand von gepulsten Extraktionskolonnen unter verschiedenen Betriebsbedingungen zu simulieren. Die Änderung der Pulsationsintensität hat eine tiefgreifende Auswirkung auf Systeme mit hoher Grenzflächenspannung. Die Variation der Volumenströme hat einen wesentlichen Einfluss auf den Hold-up, den mittleren Tropfendurchmesser und die Konzentrationsprofile für chemische Systeme mit niedriger Grenzflächenspannung. Zwei chemische Testsysteme von der European Federation of Chemical Engineering (Wasser-Aceton-n-Butylacetat und Wasser-Aceton-Toluol) und ein industrielles Testsystem werden in der Simulation verwendet. Modellvorhersagen wurden erfolgreich gegen stationäre und transiente experimentelle Daten validiert, wo gute Übereinstimmung erreicht werden konnte. Die simulierten Ergebnisse im Vergleich zu den experimentellen Daten zeigen, dass LLECMOD ein leistungsstarkes Simulations-Tool ist, welches effizient das dynamische und stationäre Verhalten von gepulsten Extraktionskolonnen vorhersagen kann.

Ein weiterer Schwerpunkt lag bei gerührten Kolonnen, wo die Wirkung der dispergierten Phase (leichte oder schwere Phase ist dispergiert) und der Richtung des Stoffaustauschs (von der kontinuierlichen zur dispersen Phase und umgekehrt) mit Hilfe der Populationsbilanz simuliert wird. LLECMOD wird um die Berücksichtigung der Richtung des Stofftransports und des dispergierten Phaseneinlasses erweitert, wobei eine Drehscheibenkolonne (RDC, Rotating Disk Contactor) mit verfügbaren experimentellen Daten verglichen wird. Drei chemische Systeme wurden verwendet: Sulfolan-Benzol-n-Heptan, Wasser-Aceton-Toluol und Wasser-Aceton-n-Butylacetat. Der disperse Phaseneinlass und die Richtung des

Stofftransports sowie physikalischen Eigenschaften des chemischen Systems haben ergeben, dass z.B. der reduzierte mittlere Tropfendurchmesser sich nicht ändert, wenn die schwere Phase dispergiert ist und der Wirkungsgrad höher ist, wenn die Richtung des Stoffübergangs von der kontinuierlichen zur dispersen Phase ist. Für die Zwecke der experimentellen Validierung stellt man fest, dass die LLECMOD Vorhersagen in guter Übereinstimmung mit den experimentellen Daten stehen (mittlerer Tropfendurchmesser, Konzentrationsprofile und Dispersphaseanteil in der Kolonne).

Als weiterer Teil der Arbeit wird ein mathematisches Modell der multivariaten Populationsbilanzgleichung (PBE) entwickelt. Es basiert auf dem OPOSPM (Attarakih 2010) und wird erweitert, um die Impulsbilanz für die disperse Phase zu enthalten. Der Vorteil ist damit unabhängig von Korrelation für Tropfenaufstieg zu werden. Um die Komplexität des Modells zu reduzieren wird das Konzept der primären und sekundären Partikel-Methode (PSPM) von Attarakih, 2010 verwendet. Basierend auf der multivariaten Populationsbilanzgleichung und dem primären und sekundären Teilchenkonzept wird ein mathematisches Modell für Flüssig-Flüssig Extraktionskolonnen entwickelt. Die sekundären Partikel tragen Informationen über die Verteilung, wie sie sich in Raum und Zeit entwickelt hat. Die primäre Partikel tragen die mittleren Eigenschaften der Population, wie totale Tropfenkonzentration oder mittlerer Tropfendurchmesser der dispergierten Phase. Sie spiegeln die Teilchen-Teilchen-Wechselwirkungen (Bruch und Koaleszenz) und Transport (Konvektion und Diffusion) wieder. Das Modell wurde räumlich mit Hilfe eines Upwind-Verfahrens 1.Ordnung diskretisiert während ein semi-implizites Schema 1.Ordnung in der Zeitintegration verwendet wird, um eine Pilot-RDC Extraktionskolonne zu simulieren. Hier wird die Wirkung der Anzahl der primären Partikel (Klassen) auf die Qualität der vorhergesagte Lösung untersucht. Numerische Ergebnisse zeigen, dass die Lösung umso langsamer konvergiert wie sich die Anzahl der primären Partikel erhöht. Die terminale Tropfengeschwindigkeit hat sich als der am empfindlichste Parameter für die primären Partikel herausgestellt. Andere mittlere Eigenschaften (Tropfendurchmesser, Dispersphasenanteil und die Konzentrationsprofile) entlang einer Pilot-RDC Extraktionskolonne sind mit den experimentellen Daten in guter Übereinstimmung.

Das Modell der RDC-Kolonne wird weiter entwickelt um Hydrodynamik und Stofftransport in Kühni-Extraktionskolonnen vorherzusagen. Für die transienten Analyse wird die Auswirkungen der schrittweisen Veränderungen in den wichtigen Input-Variablen (wie Volumenströme, Drehzahl, Einlasskonzentration etc.) auf der Ausgangsvariablen (Anteile der dispersen Phase, mittlerer Tropfendurchmesser und Konzentrationsprofile) untersucht. Die instationäre Analyse zeigt, dass die größte Zeitkonstante (langsamste Reaktion) bei der Stoffübertragung liegt. Im Gegenteil, dazu ist das hydrodynamische Verhalten der dispersen Phase sehr schnell im Vergleich zum Stofftransport. Das dynamische Verhalten der dispergierten und der kontinuierlichen Phase zeigt eine Zeitverzögerung, die umso größer wird, je weiter man vom Ort der Phasenaufgabe entfernt ist. Darüber hinaus zeigt die Konzentrationsverläufe der gelösten Stoffe ein stark nichtlineares Sprungverhalten bei abrupten Konzentrationsänderungen. Die Simulationsergebnisse sind in guter Übereinstimmung mit den experimentellen und zeigen den Nutzen des Modells.

TABLE OF CONTENTS

1. INTRODUCTION	1
1.1. Significance of this work	4
2. POPULATION BALANCE EQUATION	6
2.1. Homogenous population balance equation	7
2.2. Breakage and coalescence functions	9
2.2.1. Breakage models	9
2.2.2. Coalescence models	9
2.3. Bivariate Spatially Distributed Population Balance Equation	10
2.4. Population balance equation solution methods	11
2.4.1. Monte Carlo simulations	13
2.4.2. Moment Methods	14
2.4.3. Quadrature Method of Moments	14
2.4.4. The Direct Quadrature Method of Moments	15
2.4.5. Classes Method	15
2.4.6. Sectional Quadrature Method of Moments	16
2.4.6.1. The SQMOM: Primary and Secondary Particles Concept	17
2.4.6.2. The One Primary and One Secondary Particle Methods (OPSPM)	18
2.4.6.3. The Multi Primary and One Secondary Particle Methods (MPSPM)	18
2.4.7. A Multivariate Sectional Quadrature Method Of Moments for the solution of the population balance equation (BVSQMOM)	19
2.4.8. Solution of the population balance equation using the Cumulative Quadrature Method of Moments (CQMOM)	20
2.4.9. Integral Formulation of the Population Balance Equation using the Cumulative Quadrature Method of Moments (CQMOM)	20
3. MATHEMATICAL MODELLING	22
3.1. Introduction	22
3.1.1. The Population Balance Equation (PBE)	22
3.1.2. Continuous and dispersed phase's solute balance	23
3.2. The Multi Primary One Secondary Particle Model	23
3.2.1. Number balance	24
3.2.2. Volume balance	25
3.2.3. The momentum balance equation	26
3.2.4. Continuous and dispersed phase's solute balance	27
3.3. Numerical solution of the MPOSPM	28
3.4. Population balance sub models	29
3.4.1. Daughter droplet distribution and mean number of daughter droplets	29
3.4.2. Breakage frequency	30
3.4.3. Droplet coalescence frequency	31

3.4.4. The terminal droplet velocity	32
3.4.5. Effect of internal column geometry on rising droplet velocity	33
3.4.6. Continuous phase velocity models	34
3.4.7. Mass transfer models	35
3.4.8. Axial dispersion coefficients	36
3.5.LLECMOD program	36
4. STEADY STATE MODELLING AND SIMULATION OF EXTRACTION COLUMNS	39
4.1.Stirred extraction columns	39
4.1.1. RDC and Kühni columns	39
4.2.Pulsed extraction columns	45
4.2.1. Sieve plate and packed columns	46
4.2.1.1. <i>Steady state column hydrodynamics: pulsed sieve plate column</i>	48
4.2.1.2. <i>Steady state column hydrodynamics: pulsed packed column</i>	50
4.2.1.3. <i>Steady state mass transfer profiles: pulsed (packed and sieve plate) columns</i>	54
4.3.Effect of phase dispersion and mass transfer direction	57
5. DYNAMIC MODELLING AND SIMULATION OF EXTRACTION COLUMNS	66
5.1.Dynamic behaviour of stirred extraction column	67
5.1.1. Dynamic behaviour due to a disturbance in the flow rate of both phases	68
5.1.2. Column dynamic behaviour due to the variation in the rotor speed	74
5.1.3. Dynamic behaviour due to a disturbance in both phases inlet concentrations	76
5.1.4. Dynamic behaviour during start-up of the extractor	78
5.2.Dynamic behaviour of pulsed columns	81
6. CONCLUSIONS	83
List of symbols	86
References	90
Own publications	104
Oral and poster presentations	106
Appendices	I
Appendix I: Figures and Tables	II

1. INTRODUCTION

Dynamic Modelling and Simulation of (Pulsed and Stirred) Liquid-Liquid Extraction Columns using the Population Balance Equation

1. Introduction

Liquid-liquid or solvent extraction is a mass transfer operation in which a liquid solution (the feed) is contacted with an immiscible or nearly immiscible liquid (solvent) that exhibits preferential affinity or selectivity towards one or more of the components in the feed. As a result, two flow streams are produced from this contact: the extract, which is the solvent rich solution containing the desired extracted solute, and the raffinate, the residual feed solution containing little solute (Treybal, 1963; 1980; Lo et al., 1983; Perry and Green, 2008). For optimal and optimized design and operation of liquid-liquid extraction columns the following items must be carefully evaluated: solvent selection, operating conditions, mode of operation, extractor type and design criteria.

The most important parameters that govern solvent selection are the distribution coefficient and selectivity. The solvents must satisfy the following properties: high distribution coefficients, good selectivity towards solute and immiscibility with feed solution. If it exhibits some miscibility with feed solution it should be easily recoverable. Consequently, while extracting larger quantities of solute, the solvent could also extract significant amount of feed solution.

Designing an extractor is usually a fine balance between capital and operating costs. Other important factors that affecting solvent selection are boiling point, density, interfacial tension, viscosity, corrosiveness, flammability, toxicity, stability, compatibility with product, availability and costs Bart and Stevens, (2004). Interfacial tension has the most profound effect on the hydrodynamic parameters such as droplet formation, coalescing tendency, droplet rise velocity and size, and therefore is an important factor affecting the holdup. Taken into account that these parameters vary the interfacial area available and the contact time between phases, the interfacial tension is one of the most important parameter to be considered when studding mass transfer in extraction.

Selection of extraction conditions is depending on the extraction process itself, the temperature, pH and residence time. These parameters affect the yield and selectivity. However, most of extraction processes take place at atmospheric pressure since the operating pressure has a negligible effect on extraction performance. Other parameters to be considered are selectivity, mutual solubility. In some extraction process temperature is considered as manipulation variable to improve the selectivity. In order to keep low viscosity and thereby minimizing the mass-transfer resistance sometimes higher temperatures are preferred. However, usually the processes are performed at ambient temperature.

In metal and bio-extractions processes the pH value is very significant (Dutta, 2007; Perry and Green, 2008). The pH value is maintained to improve the distribution coefficient and to minimize the product degradation like in bio-extractions and agrochemicals. In metals extraction the pH value is governed by the kinetic considerations. The pH value is playing a significant role in dissociation-based extraction of organic molecules (e.g., cresols separation). Under certain pH conditions the solvent itself may participate in undesirable reactions (e.g., ethyl acetate may undergo hydrolysis in presence of mineral acids to acetic acid and ethanol). In reactive extraction processes and in processes involving decomposable components (e.g., antibiotics or vitamins) the residence time is a very important parameter leading to choice expensive centrifuge as extractors. Liquid-liquid extraction is a very important separation processes that has many and wide applications in atomic energy, food, nuclear, petroleum, petrochemical, pharmaceutical and metallurgical industries (Treybal, 1963, Hanson, 1971, Bailes and Winward, 1972, Treybal, 1980; Lo et al., 1983; Bart, 2001; Perry and Green, 2008). The number and variety of liquid-liquid extraction contactors that have been described in the literature are considerable. These can be classified according to type of agitation into (Brandt et al., 1978; Dutta, 2007):

- a) Unagitated columns: spray column, packed column and perforated plate or sieve tray.
- b) Pulsed columns: Pulsed, packed column and sieve tray.
- c) Mechanically agitated columns:
 - i- Rotary agitated contactors (Scheibel column, Oldshue-Rushton column, Rotating Disk Contactor and Kühni column)
 - ii- Pulsed perforated or sieve plate columns, reciprocating plate columns

Modelling of liquid-liquid extraction columns (LLEC) aid to develop a computer simulation program that is capable to simulate the coupled hydrodynamic and mass transfer (steady state and dynamic) behaviour of the extraction columns in order to avoid long and expensive pilot plant tests.

Modelling of liquid extraction columns is not as well established as that of distillation columns and still demands improvement. Nevertheless, the design and control of extraction column has not yet been fulfilled and is still based on laboratory scale pilot plants and depends on scale up methods which are time consuming and expensive (Bart et al., 2008; Drumm, 2010). The scale up and design of an extraction column is mainly based on manufacturer's prior knowledge and simplified models like: stage-wise models, flow models such as the dispersion or backmixing model to describe the non-ideal flow, where in these models one parameter accounts for all deviations from the ideal plug flow behaviour (Thornton, 1992). These models are over simplified by severe assumptions that limit their application to only very limited cases of the process range of operation and not able to describe the real hydrodynamics behaviour, where one of the liquid phases is normally dispersed as droplets in the second continuous phase (Bart & Stevens, 2004).

In multiphase flow systems that are encounter the presence of particulate, droplet, or bubble such as liquid-liquid extraction, crystallization, combustion, aerosol, etc. The population balance framework has been emerged as a powerful approach for modelling of such systems. Nowadays, for the industrial sector and also for the academic there is strong demand for robust, rigours,

straight forward, faster and money-saving simulation methods to reduce efforts with pilot plant tests.

Hulburt and Katz (1964) were the first who formulated the population balance model (PBM) for chemical engineering purposes particularly in crystallization, in the last decades PBM has drawn an exceptional attention from both the academic and industrial quarters that has a wide applicability in variety of particulate processes (Ramkrishna & Mahoney, 2002). Many researcher has been emerged the PBM to describe and simulate the droplets and the discrete nature of the dispersed phase in liquid-liquid systems and bubbles in gas-liquid systems, which showed the great potential of PBM in such systems (Kostoglou & Karabelas, 1997; Millies & Mewes, 1999; Colella et al., 1999; Lehr & Mewes, 2001; Ramkrishna, 2000; Pohorecki et al., 2001; Garthe, 2006; Bart et al., 2008).

Under the PBM framework the scale-up of extraction columns is obtained successfully from single droplet experiments (Bart, 2006). Recently, the industrial sector assert great attention in regard to process intensification to use the PBM for high precision engineering and accurate modelling of industrial scale column design (Bart et al., 2006; Pfennig et al., 2006; Schmidt, 2006; Bart et al., 2008; Reay et al., 2008). The interaction of a droplet with the turbulent continuous phase leads to transmit the turbulent kinetic energy to the droplet; if this energy exceeds the droplet surface energy the droplet undergoes breakage (Coulaloglou & Tavlarides, 1977; Borba Costa et al., 2007; Aarts and Lekkerkerker, 2008; Liao and Lucas, 2010). On the contrary, droplet coalescence is expected to occur due to the interaction between two droplets and the surrounding turbulent continuous phase. The coalescence reduces the total interfacial area and is driven by the interfacial tension. The coalescence between these two droplets is considered to occur due to the rupture and disappearance of the separating continuous film between these two droplets (Chatzi & Lee, 1987; Liao and Lucas, 2010). The droplet breakage process can be described in terms of a breakage rate function and the daughter distribution function (Narsimhan and Gupta, 1979; Coulaloglou and Tavlarides, 1977; Liao and Lucas, 2009).

Consequently, the modelling of these phenomena under the population balances framework furnishes all the detailed information that is required in the engineering applications. This information includes the dispersed number and volume concentration (phase holdup) and any other integral property associated with the resulting droplet size distribution such as the mean droplet diameter, accordingly the interfacial area required for the calculation of mass and heat fluxes (Al Khani et al., 1988; Tsouris et al., 1994; Alopaeus et al., 2002).

The behaviour of the interacting liquid-liquid dispersions could be modelled successfully under the framework of population balance either in stagewise or in differential approach. In the stagewise (Tsouris et al., 1994; Kentish et al., 1998; Steiner et al., 1999; Bastani, 2004) the multistage column is considered as a sequence of completely mixed and interacting stirred tanks. To compensate for the nonideal behaviour of each tank the forward and backward flow components is considered. Practical examples of such columns are the sieve plate column, Scheibel column and mixer-settler cascades. Therefore, for each stirred tank a population balance equation has to be written with the corresponding boundary conditions. However, in the differential approach the continuous and the dispersed phases are in a continuous contacted

domain through the active part of the column. Practical examples of such columns are the spray column, the rotating disc contactor (RDC), sieve plate column, packed column, Kühni column and the Oldshue-Rushton column. In such equipment, the PBE is usually formulated as a conservation law in terms of volume concentration (Casamatta & Vogelpohl, 1985; Al Khani et al., 1988, 1989; Cabassud et al., 1990; Modes et al., 1999; Attarakih et al., 2006, 2008). The resulting differential model takes into account the droplet transport; breakage, coalescence and mass transfer as well as the necessary boundary conditions, though the latter are not clearly stated in the published literature. For a comprehensive review of mathematical modelling of liquid-liquid extraction columns, their advantages and disadvantages, the interested reader could refer to (Mohanty, 2000; Attarakih et al., 2004a, 2008a).

1.1. Significance of this work

The aim of this work is to provide robust rigorous mathematical models under the population balance modelling framework for better understanding of complex behaviour of the coupled hydrodynamic and mass transfer in (pulsed and stirred) liquid-liquid extraction columns for both steady state and dynamic analysis. These models can ingeniously be used to increase the reliability in the design of extraction (pulsed and stirred) columns (Oliveira et al., 2008; Attarakih et al., 2008a). These models are helpful to predict the influence of various operational and process parameters on the performance of such types of equipment in order to avoid long and expensive pilot tests (Blass and Zimmerman, 1982; Grinbaum, 2006).

New solution methods for the population balance equation based on OPOSPM (Attarakih, 2010) and SQMOM (Attarakih et al., 2009) were studied and reproduced in this work: The One Primary One Secondary Particle Method (OPOSPM) [XVI; XVII; XVIII, Attarakih et al., 2009b, 2009c, 2008b]¹ and the Multi Primary One Secondary Particle Method (MPOSPM) [I; II; IV; X, Jaradat et al., 2012a, 2012b, 2012d, 2010b].

The LLECMOD program is further developed and modified to include more features such as the mass direction and phase dispersion [IX, Jaradat et al., 2010a]. Moreover, the LLECMOD is modified and developed to satisfy the industrial demand by including the pulsed (sieve plate and packed) liquid-liquid extraction columns [III; V; VI; VII; VIII, Jaradat et al., 2012c, 2011a, 2011b, 2011c, 2011d]. To provide a complete modelling and study of the liquid-liquid extraction columns performance, the transient study and analysis is done for stirred and pulsed columns [I; II; III, Jaradat et al., 2012a, 2012b, 2012c].

The structure of the work is as follows: In each main chapter a short introduction and a literature survey on the topic are given. For the details of theory and results the interested reader could refer to the relevant publications. The homogeneous population balance equation is introduced in chapter 2. The spatially distributed population balance equation is given in chapter 3. Steady state modelling and simulation of stirred (RDC & Kühni) and pulsed (packed & sieve plate) extraction columns are presented in chapter 4. In chapter 5 the dynamic modelling and simulation of extraction columns is given. Conclusions are given in chapter 6.

¹ I to XXIII are own publications (see pages 104 & 105)

2. POPULATION BALANCE EQUATION

Population balances are a powerful and widely used tool in engineering applications, mainly in branches with particulate entities such as aerosols, crystallisation, liquid-liquid extraction, gas-liquid dispersions, liquid-liquid reactions, pharmaceutical industry, polymerization, soot formation in flames and growth of microbial and cell populations. Wherever the interaction of a large number of particles (bubbles, liquid droplets or solid particles) is studied, population balance equation is necessary to determine the properties of the resulting product and its dependence on processes such as coalescence, breakage, nucleation or growth.

Hulburt & Katz, (1964) and Randolph (1964) were among the first who propose the Droplet Population Balance Modelling (DPBM) in chemical engineering, particularly in crystallization. Utilizing the DPBM the droplet-droplet interactions, namely; droplet motion, droplet breakage and droplet coalescence of the dispersed phase is taking into account and consider the particulate behaviour in an extraction column (Gourdon et al., 1994; Schmidt et al., 2006; Garth, 2006; Attarakih et al., 2006a, 2008a). Valentas & Amundson, (1966) and Bayens and Laurence, (1969) were the first who described the steady drop size distribution for liquid-liquid dispersions in a continuous stirred tank under the framework of PBM. Casamatta, (1981) was the first who developed a differential model for hydrodynamics and mass transfer in liquid-liquid extraction column relying on a DPBM. However, the resulting differential models are too complex that take into account the droplet –droplet interactions such as: breakage, coalescence, interphase mass. However, this model includes the axial dispersion term to account the deviation from the plug flow due to droplet random motion due to the energy inputs (agitation or pulsation) and the internals (Gourdon et al. 1994, Bart et al., 2008).

Based on the Spatially Distributed Population Balance Equation (SDBPBE), Attarakih et al., (2006a, 2008a) developed a software package (LLECMOD) for the simulation of coupled hydrodynamics and mass transfer in the agitated (RDC and Kühni) liquid-liquid extraction columns. LLECMOD has validated extensively against experimental data in RDC and Kühni columns (Steinmetz et al. 2005; Schmidt et al. 2006) this validation shows the usefulness of LLECMOD to predict the hydrodynamics and mass transfer behaviour in the agitated liquid-liquid extraction columns. In this work [IX, Jaradat et al., 2010a], LLECMOD has been modified to provide new features like the direction of mass transfer (continuous to dispersed or vice versa) and the dispersion type (heavy or light). However, the LLECMOD is modified and developed to include the pulsed (sieve plate and packed) extraction column [III; V; VI; VII; VIII, Jaradat et al., 2012c, 2011a, 2011b, 2011c, 2011d]. Despite the enormous advantages of the population balance modelling over the currently used design methods (simplified models), the experiments in small lab-scale devices are still necessary. Such type of experiments are necessary to provide the correlations to describe the droplet-droplet interactions, such as droplet rising velocities, the dispersion coefficient in the dispersion model, mass transfer coefficients and to fit adjustable parameters in the coalescence and breakage kernels. To get rid from the experimental work to determine the droplet velocity, in [IV; X, Jaradat et al., 2012d, 2010b] a modified momentum

balance equation is developed to calculate the dispersed phase velocity under the population balance equation.

This chapter outlines the modelling framework that has been used to describe the mathematical modelling of hydrodynamic and mass transfer behaviour relying on the SDBPBE, and to describe droplet-droplet interaction, namely; breakage, coalescence, droplet velocity and mass transfer in the PBM approach. A brief introduction about the population balance equation is presented. A review of the available popular solution methods is given as well as the new solution methods which were used for the PBM. A review of different breakage and coalescence frequencies and other correlations and models that describe the droplet-droplet interactions are given.

PBEs define how populations of separate entities (bubbles, droplets, particles, etc.) develop in specific properties over time and space. They are a set of integro-partial differential equations which gives the behaviour of a population of particles from the analysis of behaviour of single particle in local conditions. Particulate systems are characterized by the birth and death of particles. For example, consider extraction process which has the sub processes agglomeration, breakage, etc., that result in the increase or decrease of the number of particles of a droplet size (assuming formation of spherical droplets). Population balance is nothing but a balance on the number of particles of a particular state (in this example, size). The population balance equation (PBE) is a continuity statement. The superstructure of the PBE and the general derivation based on the Reynolds transport theorem is given in Ramkrishna (2000), an intensive review of the state-of-the-art in population balances could be found in Ramkrishna, 2000; Attarakih et al., 2004a.

In this work new numerical methods were used OPOSPM [XVI; XVII; XVIII, Attarakih et al., 2009b, 2009c, 2008b] and developed MPOSPM [I; II; IV; X, Jaradat et al., 2012a, 2012b, 2012d, 2010b] for the solution of multivariate population balances with and without spatial dependence. These methods are based on the concept of primary and secondary particle concept. Moreover, other new methods were developed [XIII; XIV; XV, Attarakih et al., 2011, 2010a, 2010b] that are based on the cumulative distribution and the integral cumulative distribution.

2.1.Homogenous population balance equation

In liquid-liquid dispersion the droplets may change their properties due to several droplets interaction. However, the most common interactions in liquid extraction are breakage and coalescence. A short description of coalescence and breakage mechanisms is given below.

Coalescence, agglomeration or aggregation processes occur commonly in nature and engineering processes. In this process two or more droplets coalesce together to form a large droplets. Breakage: in a breakage process, droplets breakup into two or many smaller droplets. Breakage has a significant effect on the number of droplets. Breakage of droplets will influence and may control the final droplet size distribution, especially at higher energy input (agitation / pulsation). As a result of the above mentioned processes, droplets change their properties continuously. Therefore the mathematical population balance model is emerged to describe the change of droplet property distribution. Population balances describe the dynamic evolution of the distribution of one or more properties. The evolution of the droplet number density $f(v, r; t)$ take

into account the droplet-droplet interactions that control the droplet size such as breakage, coalescence and convective transport. Thus, $f(v, r; t)dv$ represent the average number of droplets having internal properties (diameter, concentration, etc.) in the range of v and $v + dv$ per unit volume in the point r in the time t . The dynamic and simultaneous change of droplet number density, $f = f(v, r; t)$ as a function of droplet internal (v) and external (r) properties and time (t) in a homogeneous liquid dispersion system undergoing breakage and coalescence processes is described by the population balance equation (Ramkrishna, 2000):

$$\frac{\partial}{\partial t} f(v, x; t) + \nabla \cdot [\vec{u} f(v, x; t)] = \Upsilon(v, x; t) \quad (1)$$

In this equation, v is the droplet volume, $f(v, x; t)dv = N(\zeta) f(v) \delta v$ is the average number density associated with droplets having a volume between v and $v \pm \delta v$ at the time instant t and position in space x , where $N(\zeta)$ is the total number concentration and $f(v)$ is the average number density. The last term in the above equation, is the source term Υ that is represent the net rate of droplets generation due to birth and death due to breakage and coalescence of the droplets per unit time and unit volume. The source term is written as:

$$\Upsilon(v, x; t) = B^b(v, x; t) - D^b(v, x; t) + B^c(v, x; t) - D^c(v, x; t) \quad (2)$$

Thus, the source term can be further written as (Valentas & Amundson, 1966):

$$\begin{aligned} \Upsilon(v, x; t) = & -\Gamma(v, \phi) f(v, x; t) + \int_v^{v_{\max}} \Gamma(v', \phi) \beta_n(v | v') f(v', x; t) \delta v' \\ & - f(v, x; t) \int_{v_{\min}}^{v_{\max}-v} \omega(v, v - v', \phi) f(v - v', x; t) \delta v' \\ & + \frac{1}{2} \int_v^{v_{\max}} \omega(v, v - v', \phi) f(v - v', x; t) f(v', x; t) \delta v' \end{aligned} \quad (3)$$

In the above equation, the first term on the right hand side represents the rate of death of drops of volume v due to breakage. The second term denotes the rate of birth of drops of size v due to breakage of drops of size larger than v . The third term describes the rate at which drops of volume v are lost due to their coalescence with other drops. The fourth term signifies the rate of formation of drops of size v due to coalescence between droplets of volume $v - v'$ and v' . The breakage frequency $\Gamma(v, \phi)$, the daughter droplet size distribution $\beta_n(v | v')$, the mean number of daughter droplets formed upon breakage, and the coalescence frequency $\omega(v, v', \phi)$ are needed in order to solve the population balance equation. The distribution of the daughter droplets, given that a mother droplet of volume v' is broken and is assumed independent of time, but it is a function of the energy input (agitation/ pulsation) and the system physical properties. The breakage and coalescence frequencies are dependent on the agitation or pulsation intensity, internal vessel (column) geometry and the dispersed phase holdup that is given by:

$$\phi(\zeta) = \int_{v_{\min}}^{v_{\max}} v f(v; \zeta) \delta v \quad (4)$$

In the above equation, $\zeta = [r, t]$ is a vector of external and time coordinates specifying the variation of the droplet number density, $f = f(v, \zeta)$.

2.2. Breakage and coalescence functions

The population balance model describes the droplet population in terms of droplet properties, such as size, concentration and residence time (droplet age) during droplet interaction events with themselves and with the surrounding environment. For example, droplet coalescence, breakage, and inlet-outlet transport phenomena which are distributed randomly in time. These interactions are described satisfactory by the PBE model along with the continuously occurring mass transfer between the two phases. The droplet breakage and coalescence frequency functions employed to accomplish the PBE for the analysis of extraction columns. Breakage and coalescence processes results in birth and death of droplets.

2.2.1. Breakage models

In addition to the droplet number density $f = f(v, r; t)$, the breakage frequency $\Gamma(v, \phi)$ is crucial to close the breakage source term. The distribution $\beta_n(v, v')$ appearing in the source term is the daughter droplet distribution function upon breakage of mother droplet of a definite size (v'). The breakage frequency is defined as the relative change in the number of droplets per unit time.

$$\Gamma(v', \phi) \beta(v | v') \quad (5)$$

The breakage term describe the interaction of a single droplet with the surrounding turbulent continuous phase. Coualoglou & Tavlarides, (1977) describe the droplet breakage to occur if the turbulent kinetic energy transmitted to the droplet exceeds its surface energy. Several models have been proposed to describe the droplets or bubbles breakage frequency (Alopaeus et al., 2002; Coualoglou & Tavlarides, 1977; Hagesaether et al., 2002; Lehr et al., 2002; Luo & Svendsen, 1996; Martínez-Bazán et al., 1999a; Prince & Blanch, 1990; Andersson & Andersson; 2006a; Zacccone et al., 2007). Several models were proposed to determine the daughter droplet distribution (Coualoglou and Tavlarides, 1977; Konno et al., 1980; Diemer and Olson, 2002; Martínez-Bazán et al., 1999b. Coualoglou and Tavlarides, (1977) started from an early work of Valentas et al., (1966). Assumes binary breakage Valentas et al., (1966) used a normal density function for the daughter droplet distribution. To describe more than two daughter droplets, Bahmanyar et al., (1991) used the beta distribution function. Liao and Lucas et al., 2009; Patruno et al., 2009a,b; Zacccone et al., 2007; Wang et al., 2003; Lasheras et al., 2002 provided an intensive review of daughter size distributions and breakage models.

2.2.2. Coalescence models

The coalescence source term is described by analogy to the breakage source term. To describe the coalescence frequency, different approaches in the literature are proposed (Coualoglou & Tavlarides, 1977; Chesters, 1991; Luo, 1993; Prince & Blanch, 1990; Tsouris & Tavlarides, 1994; Sovová, 1981; Henschke, 2004; Liao and Lucas, 2010). Coalescence rate analysis and modelling has been paid greater attention. Many authors proposed phenomenological models

based on the concept of collision frequency and coalescence efficiency, where the latter assumed to be a function of the two coalesce droplets, an intensive review on the coalescence models is provided by Liao and Lucas, (2010) which support this assumption. The classical model describes the coalescence as a result of the collision of two droplets of sizes v and v' , and the rupture and disappearance of the separating continuous film between these two droplets. Note that the number of coalescence events between droplets with volumes v and v' per unit volume and unit time is proportional to the product of coalescence frequency $\omega(v, v')$ and the number concentration function of droplets of volumes v and v' .

$$\omega(v, v') = h(v, v') \cdot \lambda(v, v') \quad (6)$$

In the above equation, the coalescence frequency is denoted by $\omega(v, v')$, which is defined as the relative change in the number of droplets per unit time and volume.

In modelling and simulation of this work the reputable models by Coulaloglou & Tavlarides (1977) was used for stirred (RDC and Kühni) [I; II; IV; X, Jaradat et al., 2012a, 2012b, 2012d, 2010b] and the modified Henschke, (2004) for pulsed (packed and sieve plate) [III; V; VI; VII; VIII; IX, Jaradat et al., 2012c, 2011a, 2011b, 2011c, 2011d, 2010a] extraction columns.

2.3. Bivariate Spatially Distributed Population Balance Equation

A general, spatially homogeneous population balance equation that describes the dispersed phase behaviour in a continuous flow system is written as (Ramkrishna, 2000):

$$\frac{\partial f_{d,c_y}(\psi)}{\partial t} + \frac{\partial [u_y f_{d,c_y}(\psi)]}{\partial z} + \sum_{i=1}^2 \frac{\partial [\dot{\zeta}_i f_{d,c_y}(\psi)]}{\partial \zeta_i} = \frac{\partial}{\partial z} \left[D_y \frac{\partial f_{d,c_y}(\psi)}{\partial z} \right] + \frac{Q_y^{in} f_y^{in}}{A_c \bar{v}_{in}} (d, c_y; t) \delta(z - z_y) + R\{\psi\} \quad (7)$$

In this equation $\psi = [d \ c_y \ z \ t]$ is a vector, whose components are: the droplet internal coordinates (diameter and solute concentration), the external coordinate is z (column height), and t is time. The velocity vector along the internal coordinates is given by $\dot{\zeta} = [\dot{d} \ \dot{c}_y]$. The source term $R\{\psi\}$ represents the net number of droplets produced by breakage and coalescence per unit volume and unit time in the coordinate's range $[\zeta, \zeta + \partial\zeta]$ (McGraw, 1997; Attarakih et al., 2004b). The left-hand side is the continuity operator in both the external and internal coordinates, while the first part on the right-hand side is the droplet axial dispersion characterized by the dispersion coefficient, D_y . The second term on the right-hand side is the rate at which the droplets enter the liquid-liquid extraction column with volumetric flow rate, Q_y^{in} , that is perpendicular to the column cross-sectional area, A_c , at a location z_y with an inlet number density, f_y^{in} . The form of the source term $R\{\psi\}$ depends on the specific processes by which particles appear and disappear from the system (particle breakage, aggregation and growth). Generally $R\{\psi\}$ is an integral expression and is given below:

$$\Upsilon = B^b(d, c_d; t, x) - D^b(d, c_d; t, x) + B^c(d, c_d; t, x) - D^c(d, c_d; t, x) \quad (8)$$

In the above equation, B^b and B^c are the rate of droplets birth due to droplet breakage and coalescence respectively, whereas D^b and D^c are the rates of droplet death due to droplet breakage and coalescence respectively. However, the breakage and coalescence source terms are written as follows (Ramkrishna, 2000):

Birth by breakage:

$$\int_d^{d_{\max}} \int_0^{c_{y,\max}} \Gamma(d', \phi_y, \mathbf{P}) \beta_n(d | d') f_{d,c_y}(d', c'_y; t, z) \delta(c'_y - c_y) \partial d' \partial c'_y \quad (9)$$

Birth by coalescence:

$$\frac{1}{2} \int_0^d \int_{c'_{y,\min}}^{c'_{y,\max}} \omega(d', \eta, \phi_y, \mathbf{P}) \left(\frac{d}{\eta} \right)^5 f_{d,c_y}(d', c'_y; t, z) f_{d,c_y}(\eta, c''_y; t, z) \partial d' \partial c'_y \quad (10)$$

$$\eta = (d^3 - d'^3)^{1/3}, \quad c''_y = \frac{c_y v(d) - c'_y v(d')}{v(d) - v(d')}$$

$$c'_{y,\min} = \max \left(0, c_{y,\max} \left(1 - \frac{v(d)}{v(d')} \left(1 - \frac{c_y}{c_{y,\max}} \right) \right) \right), \quad c'_{y,\max} = \min \left(c_{y,\max}, \left(\frac{v(d)}{v(d')} \right) c_y \right)$$

Death by breakage:

$$-\Gamma(d, \phi_y, \mathbf{P}) f_{d,c_y}(d, c_y; t, z) \quad (11)$$

Death by coalescence:

$$f_{d,c_y}(d, c_y; t, z) \int_0^{(d_{\max}^3 - d^3)^{1/3}} \int_0^{c_{y,\max}} \omega(d, d', \phi_y, \mathbf{P}) f_{d,c_y}(d', c'_y; t, z) \partial d' \partial c'_y \quad (12)$$

2.4. Population balance equation solution methods

The PBE proves to be the natural transport equation for modelling many discrete systems such as liquid-liquid, aerosols dynamics, crystallization, precipitation, gas-liquid and combustion processes (Ramkrishna, 2000; Attarakih et al., 2006a); [I-X, Jaradat et al., 2012a, 2012b, 2012c, 2012d, 2011a, 2011b, 2011c, 2011d, 2010a, 2010b]. These transport equations range from integro-partial differential to integro-differential equations. These equations comprise both the external (time and location) coordinate and the internal (any entity property) coordinates, whereas the source term usually associate with single or multi-integrals. Hence, the resulting model is very complex with no general analytical solutions; therefore, there is an unavoidable need for numerical techniques in most practical applications. Such techniques should be accurate with a moderate computational cost. Numerous numerical solution approaches have been proposed to satisfy the accuracy and acceptable calculation speeds along with the ease of implementation.

An accurate solution with moderate computational time of the population balance is a challenging task. This task has motivated many researchers to develop several numerical methods for solving population balance equations (for example, see Ramkrishna, 1985; Nicmanis and Hounslow, 1998; Ramkrishna, 2000, Attarakih et al., 2004a; Cameron et al., 2005). These methods can be categorised into: the method of moments, the method of characteristics, the method of weighted residuals/orthogonal collocation, Monte Carlo simulation, and finite difference methods/discretized population balances. Ramkrishna (1985, 2000); Cameron et al., 2005; Attarakih et al., (2004a, 2006b) have provide intensive review of the available numerical methods.

The general solution of the population balance equation does not exist and hence numerical approximations are resorted to in general. Accordingly, there exist in the literature many numerical methods as attempts to solve certain type of the (PBE). An intensive review for the numerical methods is given in (Ramkrishna, 2000; Cameron et al., 2005; Attarakih et al., 2004a, 2006a). Several numerical methods have been developed to achieve the accuracy requirements, among which are the classes' method (CM) (Kumar and Ramkrishna, 1996a,b; Vanni, 2000), the Monte Carlo method (MCM) (Smith and Matsoukas, 1998; Tandon and Rosner, 1999; Goodson and Kraft, 2004; Goodson, 2007) and the method of moment (MOM) (McGraw, 1997; Fan et al., 2004) and the Quadrature Method Of Moments (Attarakih et al., 2006a). In the CM, the continuous size range of the internal coordinate is partitioned into a finite series of contiguous subintervals or classes. Good accuracy can be achieved if a large number of classes is used, but at the expense of high computational time due to increased number of equations to be solved. The MCM is based on the solution of the PBE in terms of its stochastic equivalent. A population of particles undergoes "real" physical processes, and events occur according to appropriate probabilities. In order to reduce the statistical error, a very large number of particles must be used (Smith and Matsoukas, 1998). Due to limitations on the computational resources, the full incorporation of the MCM into CFD codes is still intractable (Fan et al., 2004). In the MOM, the particle size distribution (PSD) is not tracked directly but through its moments, which are integrated over the internal coordinates. This approach has many advantages such as low CPU time and relatively high accuracy. The standard method of moment (SMM) needs to be closed, which limits its practical application. The quadrature method of moments (QMOM) (McGraw, 1997) comes to solve this problem. This method is developed to solve the PBE with pure growth and is found very efficient from accuracy and computational point of view. Unlike the sectional methods, the QMOM has a drawback of destroying the shape of the distribution by representing the distribution function only through its moments. QMOM has been widely used for PBE in recent years (Marchisio et al., 2003a, 2003b; Wang et al., 2005a; 2005b), and has been extended to bivariate PBE applications (Wright et al., 2001; Yoon and McGraw, 2004a, 2004b). However, this approach is difficult to handle systems where there is a strong dependence of the dispersed-phase velocity on internal coordinates (e.g. fluidized bed and bubble column), and can become quite complex in the case of bivariate PBE (Marchisio and Fox, 2005). Rong et al., (2004) has proposed the direct quadrature method of moments (DQMOM), which can be extended to multi-variable application in a straightforward manner (Rong et al., 2004) where different characteristic lengths with different velocities have considered. Because DQMOM uses different phases to distinguish characteristic lengths, hence is more time-consuming than QMOM when coupled with CFD. Sectional methods are used to solve the PBE (Kumar and Ramkrishna, 1996a, b), (Vanni, 2000). These methods range from simple finite difference schemes (FDS) or sectional methods using linear grids to Galerkin and orthogonal collocations methods on finite elements (Attarakih et al., 2009a). On the other hand, the limitation of the FDS is their inability to predict accurately integral quantities (low-order moments as an especial case) associated with populations of sharp shapes (Ramkrishna, 2000). A recent advance in the numerical methods for solving the PBE is the Sectional Quadrature Method Of Moments (SQMOM), which

combines the advantages of the FDS and the QMOM (Attarakih et al., 2009a, c). In [IV, Jaradat et al., 2012d] the MPOSPM is developed for steady state and in [I; II, Jaradat et al., 2012a, 2012b] for transient simulation of stirred extraction columns. In [XIV, Attarakih et al., 2010a] developed also the Cumulative Quadrature Method of Moments (CQMOM) and in [XIII, Attarakih et al., 2011] the integral formulation of CQMOM.

In this work different methods were used in the numerical solution of the population balance equation, namely, the fixed-pivot technique (Kumar and Ramkrishna, 1996) that is extended to take into account solute transfer and external coordinate (column height) (Attarakih et al., 2006a, 2008a), the OPOSPM [XVI; XVII; XVIII, Attarakih et al., 2009b, 2009c, 2008b], the MPOSPM [I; II; IV; X, Jaradat et al., 2012a, 2012b, 2012d, 2010b], the BVSQMOM [XV, Attarakih et al., 2010b], the CQMOM [XIV, Attarakih et al., 2010a] and the integral form of CQMOM [XIII, Attarakih et al., 2011].

2.4.1. Monte Carlo simulations

Monte Carlo methods are a class of computational algorithms that rely on repeated random sampling to compute their results. These methods are most suited to calculation and tend to be used when it is infeasible to compute an exact result with a deterministic algorithm.

Monte Carlo (MC) is considered as an important numerical method for the solution of the population balance equation, especially for multivariate and multidimensional application. Recently, considerable applications of MC to population balances have appeared, including agglomeration (Matsoukas and Friedlander, 1991), fractal aggregation (Lattuada et al., 2003), bipolar charging (Maisels et al., 2004), coalescence (Gillespie, 1972, 1975), coating (Kruis et al., 2000), chemical reaction (Gillespie, 1976), crystallization (Gooch and Hounslow, 1996), higher-dimensionality problems (Rosner et al., 2003), multi-component aerosols (Efendiev and Zachariah, 2002), restructuring (Tandon and Rosner, 1999; Rosner and Yu, 2001) and wet scavenging (Zhao and Zheng, 2006). In MC-based methods, discretization of the size distribution is not required.

According to the treatment of the time step, MC methods can be classified into two subdivisions, namely, “time-driven” and “event-driven” MC. In time-driven simulations the simulation implements all possible events within a specified time step (Liffman, 1992). In event-driven, the simulations start by event implementation, then the time is advanced by an appropriate amount (Garcia et al., 1987). According to the total number of simulation particles the Monte Carlo methods can be further classified to constant number MC and variable number MC (Liffman, 1992; Garcia et al., 1987; Smith and Matsoukas, 1998; Kruis et al., 2000).

The constant number MC is an event-driven method, where the number of particles remains constant and equal to a constant value that is already specified at the beginning of the simulation (Smith and Matsoukas, 1998; Lee and Matsoukas, 2000; Lin et al., 2002). The stepwise constant-volume MC, is event-driven method also that regulates the number of particles frequently to maintain this number within the bounds of the simulation box (Maisels et al., 2004; Zhao and Zheng, 2006). Liffman, (1992) developed the direct simulation Monte Carlo (noted as time-driven DSMC). This is a time-driven simulation with periodic regulation of the number of particles. However, the Multi-Monte Carlo is time-driven method and combines elements of

constant-number and constant-volume Monte Carlo (Zhao and Zheng, 2006; Zhao et al., 2005a, 2005b, 2005c).

2.4.2. Moment Methods

Hulburt and Katz, (1964) has been first who proposed the Moment Methods (MMs) for the solution of the population balance equation. In their work they emphasize the promising possibilities of the method but also with strong limitations. The solution of the population balance equation using the Moment Methods is accomplished through the moments of the droplet size distribution. Thus, if $f(v; x, t)$ is the droplet size distribution in terms of the particle volume v , the r^{th} moments of the distribution is defined as follows:

$$m_r(x, t) = \int_0^{+\infty} f(L; x, t) v^r dv \quad (13)$$

This method affords the main advantage of defining the droplet size distribution only by tracking a few lower-order moments. However, for modelling size-dependent molecular growth, and size-dependent breakage and coalescence this method is not valid.

Diemer, (2002) present an extensive discussion for different methods that have been proposed in order to solve the closure problem of MMs. The QMOM that was first proposed by McGraw (1997) is considered as one of the most promising method for studying aerosol evolution. In this method the solution of the integrals involving the distribution is evaluated through a quadrature approximation:

$$m_r(x, t) = \int_0^{+\infty} f(L; x, t) v^r dv \approx \sum_{i=1}^{N_q} w_i v_i^r \quad (14)$$

The Product-Difference (PD) algorithm (Gordon, 1968) was used to calculate the abscissas v_i and weights w_i from the lower-order moments. However, for a larger number of moments, the PD algorithm is sensitive to small errors (e.g., Gautschi, 1994). Therefore, in order to compute the quadrature points from the moments of the droplet size distribution the PD algorithm is not always the optimal approach (e.g., Lambin and Gaspard, 1982). Accordingly, the applicability of QMOM is limited to no more than six quadrature points or even fewer for more complex cases such as diffusion-controlled growth with secondary nucleation (McGraw, 1997).

2.4.3. Quadrature Method of Moments

McGraw (1997) proposed the so-called quadrature method of moments (QMOM) which is considered as attractive and very efficient from accuracy and computational cost point of view method for solving the population balance equation for studying size-dependent growth in aerosols applications. The QMOM has been extended and applied into aggregation, aggregation, and breakage systems by Barrett and Webb, 1998; Wright et al., 2001; Rosner and Pyykonen, 2002; Fan et al., 2004 and Marchisio et al. (2003a, 2003c).

However, the QMOM has a drawback of destroying the shape of the distribution which is contradictory to the sectional (finite difference) methods, where the moments of the distribution are used to retain the required information about the distribution itself. The r^{th} moment is defined

by integrating the population number density function with respect to certain population property (e.g. droplet sizes) weighted with this property raised to its r^{th} power. The r^{th} moment is given by:

$$m_r(x, t) = \int_0^{\infty} f(v, x, t) v^r dv, \quad (15)$$

where v is the droplet size. The total number of particles per unit volume (zero moment) is calculated by restricting r equals zero. However, when r equals three the third moment represents the volume fraction (volume concentration) of the particles. The QMOM tracks the population moments (e.g. the zero and third moments) rather than its size and hence it does not depend on the minimum and maximum particle sizes. The QMOM is based on the Product-Difference algorithm to find weights and abscissas from the moments, which requires the solution of an eigenvalue problem in terms of the population low order moments.

2.4.4. The Direct Quadrature Method of Moments

The PD algorithm is a numerical ill-conditioned method for computing the Gauss quadrature rule (e.g. Lambin and Gaspard, 1982). Computation the quadrature rule based on the density function power moments is quite sensitive to small errors as the number of moments used becomes large (e.g. Golub and Welsh, 1969; Gautschi, 1994). As an alternative to the PD algorithm, McGraw and Wright, (2002) proposed the Jacobian matrix transformation (JMT) as a new moment closure method. Marchisio et al., (2004) extended the QMOM method to the direct quadrature method of moments (DQMOM) for multifluid applications. In the DQMOM and QMOM only a few abscissas are necessary to describe a particles distribution due to using the numerical quadrature approximation closure. In DQMOM the solution of population balance equation is accomplished using the weights and abscissas directly. The difference between the QMOM and the DQMOM is how to compute the nodes and weights of the quadrature formula. In the QMOM the moments tracked by integrating their transport equations and back-calculates nodes and weights. However, the DQMOM tracks directly the nodes and weights, solving transport equations that govern their evolution. Fan et al., (2004) argue that some shortcomings of the PD-QMOM are avoided by solving the weights and abscissas directly especially when concerning a CFD-PBM problem. However, the DQMOM has some drawbacks, namely, the numerical accuracy or computational expense that is depends strongly on relative magnitude of the moments, for long period of simulations time (physical time) the associated numerical errors tend to accumulate and even escalate to an unacceptable level and the numerical accuracy is highly sensitive to physical parameters.

2.4.5. Classes Method

Numerous numbers of Classes Methods (CMs) have been proposed for simultaneous modelling of breakage, coalescence, nucleation and growth. Hounslow et al. (1988); Litster et al., (1995) and Kumar & Ramkrishna, (1996a) developed the widely applied schemes for the method of classes, which include both coalescence and breakage. A reasonably up to date comparison of various classes methods is presented by Vanni, (2000). Based on a geometrical grid with a factor equals 2, thus $\left(\frac{v_i}{v_{i-1}} = 2 \right)$, Hounslow et al., (1988) proposed a conservative discretisation

technique that conserves droplet number and volume during coalescence and growth. Lister et al., (1995) improved the work of Hounslow et al. (1988) by introducing an adjustable geometric factor instead of the constant one (2) for droplet coalescence and growth. In the CM the particle population is subdivided into a finite number of intervals that are used to track the population density directly. Kumar & Ramkrishna, (1996a) proposed the so-called fixed pivot technique, in this method; the size domain is discretized into contiguous intervals, with the particles in each interval being concentrated at a representative size (the pivot). If the size of a particle formed by coalescence does not have a representative size, the new particle is assigned to the two neighbour pivots. This method was extended into the moving pivot technique (Kumar & Ramkrishna, 1996b). Through varying the pivot size for each interval to adapt the prevailing non-uniformity of the number density in the interval. This method formulates macroscopic balances of populations of the evolving non-uniformity of the size distribution in each size interval as a result of breakage and aggregation events.

In terms of volume fraction the PBE could be written for droplet size i :

$$\frac{\partial}{\partial t}(\alpha_i) + \nabla \cdot (u_d \alpha_i) = v_i \Upsilon_i \quad (16)$$

In the above equation, the volume fraction α_i of particle size v_i is defined as:

$$\alpha_i = N_i v_i = v_i \int_{v_i}^{v_{i+1}} f(v, t) dv \quad (17)$$

Whereas N_i is the number of droplets in the class i .

The moving pivot technique by Kumar & Ramkrishna, (1996b) is extended by Attarakih et al., (2004b) to continuous flow systems. This method is adopted to describe the hydrodynamics and mass transfer of liquid-liquid extraction columns. The extended scheme is called the generalized fixed-pivot (GFP) technique and is found sufficiently fast to simulate the hydrodynamic and mass transfer behaviour of the aforementioned LLEC. The GFP was utilized to develop the so-called LLECMOD and applied in the publications [III; V; VI; VII; VIII; IX; XX, Jaradat et al., 2012c, 2011a, 2011b, 2011c, 2011d, 2010a, Bart et al., 2011].

2.4.6. Sectional Quadrature Method of Moments

Based on the concept of primary and secondary particles Attarakih et al, (2009a) invented the so-called Sectional Quadrature Method of Moments (SQMOM); this method combines the advantages of classes method and the method of moments. In the SQMOM the primary particles are responsible for the distribution reconstruction (classes), while the secondary ones (method of moments) are responsible for breakage and coalescence events and carry detailed information about the distribution. In the SQMOM the population density function is categorized into contiguous sections and in each section the QMOM is applied. In each section, the primary particles represent the population density function by carrying sufficient information about the shape of the original distribution. Through the so-called secondary particles the population in a given partition is allowed to interact with that in the others.

The SQMOM has the advantage of self-distribution reconstruction, moderate computational time, track accurately any set of low-order moments and by considering small number of secondary particles (small size eigenvalue problem) the difficulty encountered in solving the ill-conditioned eigenvalue problem associated with the QMOM is avoided at the expense of increasing the number of primary particles (increasing the number of sections). The SQMOM avoided the major problems that are encountered in the QMOM and classes methods, namely, the inversion of the moment problem using the product difference algorithm or the direct QMOM by deriving analytically the two equal weights and abscissas, ill-conditioning problem by restricting the number of abscissas to two and convergence of the solution by increasing the number of primary particles (sections).

2.4.6.1. The SQMOM: Primary and Secondary Particles Concept

In the finite difference methods the particle size is discretized into a finite number of sections N_{pp} , where the population in each section is considered to behave like a single particle. In the Primary and Secondary Particles Concept (PSPM) framework of discretization, this single particle will be called the primary particle and it will be responsible for the reconstruction of the distribution. The interaction between the primary particles in different sections, due to breakage and coalescence events, results in a new primary particle with no representative size due to the discrete approximation of the distribution. Because the newly-birthed particle could not conserve any of its low order moments but one, the rest of the low-order moments are predicted with low accuracy and hence the associated integral quantities. To overcome this fundamental problem of the sectional methods, N_{sp} secondary particles in the PSPM are generated in each section i with positions $d_j^{<i>}$ and weights $w_j^{<i>}$ where $i = 1, 2, \dots, N_{pp}$, $j = 1, 2, \dots, N_{sp}$ (Attarakih et al., 2009a). The secondary particles are exactly equivalent to the number of quadrature points in Gauss-like quadratures or the QMOM (McGraw, 1997). Accordingly, each secondary particle could conserve or reproduce two low-order moments and in general $2N_{sp}$ moments in each section.

The way in which the PSPM works is started by envisaging the dispersed phase as contiguous N_{pp} primary particles. Each primary is associated with the desired number of secondary particles which carry detailed information about the distribution. The active particle mechanisms such as breakage and coalescence occur through interactions between the secondary particles. It is obvious now that $N_{sp} \times N_{pp}$ particles are contributing in the breakage and coalescence events.

Due to the increase of the number of interacting particles, more information is gathered about the distribution itself. This distribution could be reconstructed from the secondary particles by averaging the total weights of the secondary particles with respect to the smallest domain containing these particles associated with the i^{th} primary particle and locating them at the mean size of the secondary particles. In pure mathematical sense, the above presentation is equivalent to applying the QMOM to each size partition of an arbitrary width: $[d_{i-1/2}, d_{i+1/2}]$: $i = 1, 2, \dots, N_{pp}$ resulting in a set of low order moments

$\mu_r^{<i>}$: $r = 0, 2, \dots, 2N_{sp} - 1$. Due to the computational load when applying the full SQMOM to the spatially distributed population balance equations, we used only one secondary particle which explained in the following sections.

2.4.6.2. The One Primary and One Secondary Particle Methods (OPSPM)

Despite the accuracy of the SQMOM it still has the disadvantage of increased computational load. Many engineering problems required only moderate accuracy and fast efficient solutions. So, the objective of this work is to develop a discrete population balance model conserving the most important properties of the discrete system (the total number and volume concentrations) and yet retaining all the features of the PBE. The model should be extendable in such a way that its accuracy is increased as required and at the same time can reconstruct the shape of the distribution. This is could be achieved by collapsing the whole population density per a given section to a one particle characterized by its mean position and its total number and volume concentrations. In terms of the SQMOM (Attarakih et al., 2009a), the population is represented by different number of primary particles (depending on the required accuracy) and one secondary particles and hence the name of the method: the Multi-Primary One Secondary Particle Method (MPOSPM). The method retains the simplicity in structure, ease of explanation and efficient in coding and analysing multiphase flow problems without losing the essential information furnished by the continuous PBE [XVI, Attarakih et al., 2009b].

By restricting the number of primary and secondary particle to one the simplest case of the SQMOM is obtained, The One Primary and Secondary Particle Method (OPOSPM) [XVI; XVII; XVIII, Attarakih et al., 2009b, 2009c, 2008b]. In this case the primary and secondary particles coincide with each other. So, the population density is represented by a single particle whose position (size) is set according to the variation of the population density and is given by:

$$d_{30} = \sqrt[3]{\frac{\pi\alpha}{6N}} \quad (18)$$

where N and α are the total number and volume concentrations of the population of real particles. The transport equations for the integral quantities N and α are solved in the method. By assigning two distinct integral properties to the secondary particle, it is equivalent to a one-point Gauss-like quadrature according to the QMOM framework (McGraw, 1997). So, the population balance equation is represented by a couple of transport equations conserving both the total number and volume concentrations of the whole population. The OPOSPM is equivalent to taking one secondary and one primary particle using the SQMOM.

2.4.6.3. The Multi Primary and One Secondary Particle Methods (MPSPM)

The MPSPM is another form of the SQMOM, in this method the number of secondary particle is restricted to one and the number primary particle is variable. The greater the number of primary particles (N_{pp}), the more accurate is the reconstruction of the distribution [IV, Jaradat et al., 2012d]. Unfortunately, large number of primary particles in the classical sectional methods is required, not only to reconstruct the shape of the distribution, but also to estimate the desired integral quantities associated with the distribution (such as the total number of particles and the mean particle size).

The Multi-Primary one Secondary Particle Method (MPOSPM) is a special case of the Sectional Quadrature Method of Moments (SQMOM). The underlying idea behind the multi-primary method is that the particle population is categorized into a finite number of particles N_{pp} in which each particle is characterized by its number, volume and solute concentrations as well as its mean diameter. In this framework, each single particle will be called the primary particle and it will be responsible for the distribution reconstruction. The primary particle is allowed to conserve (selectively) its sectional number N_i , volume $\alpha_{y,i}$ and mean solute concentrations \bar{c}_y by tracking them directly through a set of transport equations. The number and volume concentration equations are coupled through the particle mean mass-number diameter that is given by:

$$d_{30,i} = \sqrt[3]{\frac{6}{\pi} \frac{\alpha_{y,i}}{N_i}}, i = 1, 2, \dots, N_{pp} \quad (19)$$

By increasing the number of interacting particles (the number of primary particles), more information is gathered about the distribution itself. This distribution could be reconstructed from the primary particles by averaging the number concentration of each primary particle with respect to the smallest domain containing it. The location of these particles along the size coordinate is given by Eq.(19).

The MPOSPM provides a compromise between ease of implementation, less computational time and the order of accuracy. Despite the simplicity of these equations, they capture all the relevant features of the continuous population balance equation. The advantage of this formulation is the disappearance of the convective terms along the particle property coordinates and hence eliminating the difficulties arising from numerical treatment of these terms (Ramkrishna, 2000). Hence, the MPOSPM is an efficient tool for modelling and simulation of liquid-liquid extraction columns. The MPOSPM is derived and applied to study the steady state [IV; X, Jaradat et al., 2012d, 2010b] and transient [I; II, Jaradat et al., 2012a, 2012b] behaviour of the coupled hydrodynamics and mass transfer in stirred liquid-liquid extraction column.

2.4.7. A Multivariate Sectional Quadrature Method Of Moments for the solution of the population balance equation (BVSQMOM)

In [XV, Attarakih et al., 2010b] extended the SQMOM to the BVSQMOM, which is a bivariate numerical framework to solve the population balance equation. This framework utilizes the secondary and primary layers concept that contains secondary and primary particles respectively. The particle interactions such as aggregation events are reflected through the so called secondary particles. However, the multivariate distribution is reconstructed through using the filtered data passed from the secondary layer to primary particles. This method solved the tedious problem and dependant procedures to find the optimal moment set for quadrature nodes and weights approximation using the standard QMOM or DQMOM. The presence of the primary layer enables this method to provide a natural distribution reconstruction and predict low-order moments other than those included in the integration quadrature itself. In the SQMOM there is no need for solving large eigenvalue problems (the product-difference algorithm) or inverting ill-

conditioned linear systems, which is in contrast to the existing quadrature methods (e.g. quadrature method of moments (QMOM) and the direct quadrature method of moments (DQMOM)).

2.4.8. Solution of the population balance equation using the Cumulative Quadrature Method of Moments (CQMOM)

The population balance equation (PBE) considered as the core stone in modelling of many applications with mono and multivariate number density functions. However, coupling of the PBE to computational fluid dynamics (CFD) in such applications is required. The contemporary quadrature methods (QMOM and DQMOM) have a drawback of destroying the shape of the distribution itself. However, distribution reconstruction from the moments of the distribution function results in an ill-posed problem, which is still unresolved. To resolve and overcome this shortage, [XIV, Attarakih et al., 2010a] presents the Cumulative Quadrature Methods Of Moments (CQMOM). The CQMOM is derived in terms of the monotone increasing the number density function cumulative low-order moments results in a complete distribution reconstruction, which in contrast to the QMOM. The CQMOM has the advantage of conservative numerical scheme with a smooth solution.

This method utilizes the cumulative Gauss-Christoffel quadrature to close the moments closure problem, in which the weight function is the unknown number density function. Consequently, the Product Difference Algorithm (Gordon, 1968) is extended to solve the closure problem and to accommodate the low-order cumulative moments. In this contribution, the analytical derivation of a two-equal and unequal weight cumulative quadratures are presented as a special case. Applying the finite difference or finite volume schemes to PBEs with particle growth usually associated with numerical diffusion, however, the CQMOM eliminates this error.

In [XIV, Attarakih et al., 2010a] the CQMOM is analysed numerically, which reveal the distinguish advantage of the CQMOM, namely, its considered as a mesh-free method, moreover, just only the cumulative nodes and weights of quadrature determine the accuracy of the low-order cumulative moments.

2.4.9. Integral Formulation of the Population Balance Equation using the Cumulative Quadrature Method of Moments (CQMOM)

In [XIII, Attarakih et al., 2011] the integral formulation of the population balance equation using the CQMOM is presented. The presented method considered a novel and hierarchical method to couple the QMOM and the physically evolving particle size distribution. This method is able to reconstruct the cumulative number density function and the low-order moments. In [XIII, Attarakih et al., 2011] the numerical analysis shows that the method is a free-mesh method and the accuracy of the intended low-order cumulative moments depends on the nodes and weights of the cumulative Gauss-Christoffel quadrature. However, this accuracy does not depend on sampling the continuous low-order cumulative moments. Therefore, the CQMOM is a general integral formulation of the population balance equation and is an effective numerical scheme in which the QMOM is imbedded as a limiting case. In this method the r th (with respect to any particle entity space) cumulative distribution is reconstructed at given arbitrary grid points. Here,

the r th cumulative moment is function of the particle internal property and evolves in time and physical space.

The number and structure of the grid points are not affecting the accuracy of the cumulative integration quadrature, since the r th cumulative moment at any grid point along the particle property space is not affecting the global moments. In this method the continuous Gauss-Christoffel quadrature is utilized, also the equal and unequal weights two-node quadrature is derived analytically. For the n th-node quadrature, the standard Product Difference Algorithm (PDA) is used (McGraw, 1997). This method combines the cumulative (rather than global moments) moments with the QMOM so this method called CQMOM.

3. MATHEMATICAL MODELLING

3.1. Introduction

Modelling of liquid-liquid extraction columns aid to develop a computer simulation program that is capable to simulate the coupled hydrodynamic and mass transfer behaviour of the dispersed phase in extraction columns in order to avoid long and expensive pilot tests. Several attempts have been done to develop models for proper and reliable design of liquid-liquid extraction columns and predict the influence of various operational and process parameters on the performance of such types of equipment without the need for a pilot plant study (Grinbaum, 2006; Blass and Zimmerman, 1982).

The influences of droplet movement, droplet interaction (breakage and coalescence), energy input (stirrer, pulsation) and mass transfer cannot be described satisfactorily under the frame work of the simplified models. In order to tackle this problem, population balance models were proposed by various authors Garg and Pratt, 1984; Casamatta & Vogelpohl, 1985; Al Khani et al., 1989; Xiaojin, et al., 2005. Recently much work has been done in the population balance modelling in extraction columns (Gourdon, et al., 1994; Kronberger, et al., 1995; Attarakih, et al., 2004a, 2004b, 2008a); [XVI, Attarakih et al., 2009b]. In this work, [III; V; VI; VII; VIII; IX, Jaradat et al., 2012c, 2011a, 2011b, 2011c, 2011d, 2010a] the generalized fixed (Attarakih et al., 2004b) is utilized to develop a population balance model for the dynamic and steady state behaviour of pulsed (packed (see Fig. III.12) and sieve plate (see Fig. III.13)) extraction columns. However, in [I; II; IV, X; XVI; XVII; XVIII, Jaradat et al., 2012a, 2012b, 2012d, 2010b, Attarakih et al., 2009b, 2009c, 2008b] the PSPM is utilized to develop the OPOSPM and the MPOSPM for the dynamic and steady state behaviour of stirred (RDC (see Fig. III.10) and Kühni (see Fig. III.11)) extraction columns.

3.1.1. The Population Balance Equation (PBE)

The PBE proves to be the natural transport equation for modelling many discrete systems such as liquid-liquid, aerosols dynamics, crystallization, precipitation, gas-liquid and combustion processes (Ramkrishna, 2000; Attarakih et al., 2006a), [I-XXIV, Jaradat et al., 2012a, 2012b, 2012c, 2012d, 2011a, 2011b, 2011c, 2011d, 2010a, 2010b, Attarakih et al., 2008b, 2008c, 2009a, 2009b, 2009c, 2010a, 2010b, 2010c, 2011]. These transport equations range from integro-partial differential to integro-differential equations with no general analytical solutions.

The dispersed phase velocity, u_y (see Eq.(7)), relative to the walls of the column is determined in terms of the relative (slip) velocity with respect to the continuous phase and the continuous phase velocity, u_x , with respect to the walls of the column as follows:

$$u_y = u_s - u_x \quad (20)$$

The slip velocity, u_s , appearing in the above equation can be related to the single droplet terminal velocity, u_t , to take into account droplet swarm (the effect of the dispersed phase hold up, ϕ_y) and the flow conditions in specific equipment:

$$u_s = K_v(1 - \phi_y)^m u_t(d, P) \quad (21)$$

The exponent m is called the velocity exponent and is a function of the droplet's Reynolds number (Gerstlauer, 1999; Garthe, 2006). The elements of the vector P consists of the system physical properties $[\mu \rho \sigma]$, and K_v is a slowing factor to take into account the effect of the column internal geometry on the droplet terminal velocity ($0 < K_v \leq 1$) (Modes et al., 1999; Steinmetz et al., 2005; Garthe, 2006). A useful guide for selecting the suitable droplet terminal velocity based on the shape of the droplet (rigid, oscillating or circulating), and hence on the system physical properties, can be found in Gourdon et al., (1994).

3.1.2. Continuous and dispersed phase's solute balance

Conducting a component solute balance on the continuous phase lead to the solute concentration in the continuous phase c_x equation (Attarakih et al., 2006b), [V, Jaradat et al., 2011a]:

$$\frac{\partial(\phi_x c_x)}{\partial t} - \frac{\partial}{\partial z} \left(u_x \phi_x c_x + D_x \frac{\partial(\phi_x c_x)}{\partial z} \right) = \frac{Q_x^{in} c_x^{in}}{A_c} \delta(z - z_y) - \int_0^\infty \int_0^{c_{y,max}} \dot{c}_y v(d) f_{d,c_y}(\psi) \partial d \partial c_y \quad (22)$$

Note that the volume fraction of the continuous phase, ϕ_x , satisfies the physical constraint: $\phi_x + \phi_y = 1$. The left hand side of Eq.(22) as well as the first term on the right hand side have the same interpretations as those given in Eq.(7); however, with respect the continuous phase. The last term appearing in Eq.(22) is the total rate of solute transferred from the continuous to the dispersed phase, where the liquid droplets are treated as point sources. Note that Eq.(7) is coupled to the solute balance in the continuous phase given by Eqs.(22&23) through the convective and the source terms.

By multiplying both sides of Eq.(7) by $v(d) c_y$, and integrating with respect to c_y from zero to $c_{y,max}$ and with respect to d from d_{min} to d_{max} one can get the mean solute concentration in the dispersed phase (Attarakih et al., 2006b), [V, Jaradat et al., 2011a]:

$$\frac{\partial(\phi_y \bar{c}_y)}{\partial t} + \frac{\partial}{\partial z} \left(u_y \phi_y \bar{c}_y - D_y \frac{\partial(\phi_y \bar{c}_y)}{\partial z} \right) = \frac{Q_y^{in} \bar{c}_y^{in}}{A_c} \delta(z - z_y) + \int_0^\infty \int_0^{c_{y,max}} \dot{c}_y v(d) f_{d,c_y}(\psi) \partial d \partial c_y \quad (23)$$

In this equation, ϕ_y is the holdup of the dispersed phase, c_y is the solute concentration in the dispersed phase. The first term on the right hand side is the rate at which the droplets entering the LLEC with volumetric flow rate, Q_y^{in} , that is perpendicular to the column cross-sectional area, A_c , at a location z_d with an initial solute concentration, \bar{c}_y^{in} , and is treated as a point source in space. The last term appearing in Eq.(23) is the total rate of solute transferred from the continuous to the dispersed phase, where the liquid droplets are treated as point sources.

3.2. The multi primary one secondary particle model (MPOSPM)

The state of any primary particle formed by dispersing the light phase is represented by a bivariate density function $f_{d,c_y}(d, c_y; t, z)$ accounting for the number of droplets having sizes and solute concentration in the ranges $[d, d + \partial d]$ & $[c_y, c_y + \partial c_y]$ per unit volume of the contactor.

This allows the discontinuous macroscopic (breakage and coalescence) and the continuous microscopic (interphase mass transfer) events to be coupled in a single spatially distributed population balance equation as given by Eq.(7). To derive the MPOSPM model equations, the bivariate density function in the PBE in each section is considered as a Dirac delta function having weight N_i and centred at $d_{30,i}$ and \bar{c}_y . This can be represented mathematically by (Attarakih et al., 2009a), and for MPOSPM by [IV, Jaradat et al., 2012d]:

$$f^{(i)}(d, c_y, t) = N_i \delta(d - d_{30,i}) \delta(c_y - \bar{c}_y) \quad (24)$$

The model equation, which describes the number concentration N and volume fraction α are derived by substituting the above expression in Eq.(7) and integrating both sides with respect to particle size over the section $[d_{i-1/2}, d_{i+1/2}]$ and solute concentration from zero to infinity.

The particle weight and volume fractions are tracked directly through a set of transport equations for the conservative quantities N and α , which are coupled through the mean droplet diameter. In this formulation, the population density is represented by a single particle with a spherical shape and whose position (size) is given by the mean mass diameter given by Eq.(19). N and α are the total number and volume concentrations that are related by the zero (m_0) and third (m_3) moments of the distribution.

3.2.1. Number balance

By restricting the number of secondary particles to one, the transport equations for the integral quantities: N and α are obtained from Eq.(25) and (29) by first multiplying Eq.(7) by v^m , $m = 0, 1$ followed by the integration with respect to d from $(d_{i-1/2})$ to $(d_{i+1/2})$. By doing this, the following set of transport equations (number balance) is derived for the MPOSPM by [IV, Jaradat et al., 2012d]:

$$\frac{\partial}{\partial t} N_i + \frac{\partial}{\partial z} u_{y,i} N_i = \frac{N_i^{in}}{v^{in}} \frac{Q_y^{in}}{A_c} \delta(z - z_y) + \pi_{0,i} \quad (25)$$

The above equation represents the number concentration equation; where N_i is the number of droplet in the i^{th} section, $u_{y,i}$ is the droplet velocity of the dispersed phase, v^{in} is the inlet droplet volume and z is the column height. The first term on the right hand side is the rate at which the droplets entering the extraction column with volumetric flow rate, Q_y^{in} , that is perpendicular to the column cross-sectional area, A_c , at a location z_y with an inlet number, N_i^{in} , and is treated as a point source in space. Whereas $\pi_{0,i}$ is the source term that accounts for the net number of drops per unit volume, which generated by breakage and coalescence in the i th section of particle size. This is due to interactions among the droplets themselves and the turbulent continuous phase. This source term consists of four sub-terms: birth and death due to droplet coalescence and breakage respectively. The source term for the number concentration balance (zero moment) is given by:

$$\pi_{0,i} = \pi_{0,i}^b + \pi_{0,i}^c \quad (26)$$

where the droplet breakage and coalescence source terms are given for the MPOSPM by Eqs.(27 and 28) respectively by [IV, Jaradat et al., 2012d]:

$$\pi_{0,i}^b = -\Gamma_i N_i + \sum_{m=i}^{N_{pp}} \Gamma_m N_m \int_{d_{i-\frac{1}{2}}}^{\min\left(\bar{d}_m, d_{i-\frac{1}{2}}\right)} \beta_n(d|\bar{d}_m) \partial d \quad (27)$$

$$\pi_{0,i}^c = \sum_{m=1}^i \sum_{k=m}^i \left(1 - \frac{1}{2} \delta_{k,m}\right) \omega(v_m, v_k) N_m N_k - N_i \sum_{j=1}^{N_{pp}} \omega(v_j, v_i) N_j \quad (28)$$

Note that in Eq.(27), the first term is the rate loss of particles with breakage frequency Γ , while the second term is the rate of formation of particles in the i th section of particle size d_i per unit volume of the dispersion. The mean number of daughter droplets is determined by integrating the daughter droplet distribution function $\beta(d|\bar{d}_m)$ with respect to d . This distribution is determined using single droplet experiments in small scale devices (Schmidt et al., 2006). The second term in Eq.(28) represents the death of droplets due to coalescence of two droplets of sizes (d_i and d_j) with coalescence frequency $\omega(v_m, v_k)$. The first term in the above equation represents the formation of new droplets due to coalescence between two droplets of sizes (d_k and d_m) with coalescence frequency $\omega(d, d')$.

3.2.2. Volume balance

The transport equation for volume concentration α is derived by multiplying Eq.(7) by $v(d)$, substituting Eq.(24) in Eq.(7) followed by the integration with respect to d from ($d_{i-1/2}$) to ($d_{i+1/2}$). By doing this, the following set of transport equations (volume balance) is derived for the MPOSPM by [IV, Jaradat et al., 2012d]:

$$\frac{\partial}{\partial t} \alpha_{y,i} + \frac{\partial}{\partial z} u_{y,i} \alpha_{y,i} = \frac{\alpha_{y,i}^{in} Q_y^{in}}{v^{in} A_c} \delta(z - z_y) + \pi_{3,i} \quad (29)$$

In the above equation, $\alpha_{y,i}^{in}$ is the inlet volume concentration. The source term of the volume concentration equation (third moment) is given by:

$$\pi_{3,i} = \pi_{3,i}^b + \pi_{3,i}^c \quad (30)$$

where the breakage and coalescence source terms are given for the MPOSPM by Eqs.(31 and 32) respectively by [IV, Jaradat et al., 2012d]:

$$\pi_{3,i}^b = -\alpha_i \Gamma_i + \sum_{m=i}^{N_{pp}} \Gamma_m \alpha_m \int_{d_{i-\frac{1}{2}}}^{\min\left(d_{i+\frac{1}{2}}, \bar{d}_m\right)} \left(\frac{v(d)}{v(\bar{d}_m)} \right) \beta(d|\bar{d}_m) \partial d \quad (31)$$

$$\pi_{3,i}^c = \sum_{m=1}^i \sum_{k=m}^i \left(1 - \frac{1}{2} \delta_{k,m}\right) \omega(v_m, v_k) N_m N_k [v_k + v_m] - \alpha_i \sum_{j=1}^{N_{pp}} \omega(v_i, v_j) N_j \quad (32)$$

where N_i and $\alpha_{y,i}$ are the total number and volume concentrations of the population of real particles in the i th section. By assigning two distinct integral properties N_i & α_i , $i = 1, 2 \dots N_{pp}$ to each particle, the secondary particles are exactly equivalent to a one-point Gauss-like quadrature according to the QMOM framework (McGraw, 1997).

The breakage and coalescence kernels are functions of droplet size, system physical properties (such as viscosity and surface tension) and the turbulence energy (Schmidt et al., 2006; Garthe, 2006; Zacccone et al., 2007). Note that the above transport equations for number and volume concentrations (Eqs.(25) and (29)) are coupled through the secondary particle size given by Eq.(19). So, the population balance equation is now selectively represented by a couple of transport equations, which conserve both the total number and volume (mass) concentrations of the whole population.

3.2.3. The Momentum Balance Equation

The classical liquid extraction models use the algebraic slip velocity model to predict the velocity of rising droplets (primary particles) by assuming that the droplet reaches instantaneously its terminal velocity. The terminal velocity by itself is predicted using many (and often conflicting) correlations from the literature (Attarakih et al., 2004b; Bart et al., 2008; Drumm et al., 2010). In this model the particle velocity is predicted using a modified momentum balance to take into account the droplet swarm and the column internal geometry. The derived model is shown to be equivalent to the algebraic slip velocity model at steady state [XVII, Attarakih et al., 2009c]. In this way by solving the momentum balance equation, the use of the algebraic velocity models can be avoided. The droplet velocity, u_y , relative to the walls of the column is determined in terms of the slip velocity $u_{0,i}$ with respect to the continuous phase as a result of momentum balance on the rising droplet of mean diameter $d_{30,i}$, the modified momentum balance is derived for OPOSPM in [XVII, Attarakih et al., 2009c] and is extended for MPOSPM in [IV, Jaradat et al., 2012d]:

$$\frac{\partial(\alpha_{y,i}u_{y,i})}{\partial t} + \frac{\partial(\alpha_{y,i}u_{y,i}^2)}{\partial z} + \frac{\alpha_{y,i}u_{y,i}}{\tau_{p,i}} = \frac{(u_{r,i} - u_x)\alpha_{y,i}}{\tau_{p,i}} + \frac{\alpha_{y,i}^{in}}{v^{in}} \left(\frac{Q_y^{in}}{Ac} \right)^2 \delta(z - z_y) \quad (33)$$

where the droplet velocity is given by:

$$u_{y,i} = [k_v f(\alpha_y)] u_{r,i} - u_x \quad (34)$$

In the above equation, the function k_v takes into account the slowing of droplet motion due to column internals and is a function of the mean droplet diameter and the column internal geometry (Schmidt et al., 2006). The function $f(\alpha_y)$ is used to account for the hindering effect due to the presence of other droplets in the dispersion (swarm effect). The simplest form of this function is given by:

$$f(\alpha) = (1 - \alpha_y)^n \quad (35)$$

where the exponent n is function of the droplet Reynolds number (Richardson and Zaki, 1954; Garthe, 2006; Attarakih et al., 2006c). This function is similar to that introduced by Ishii and

Mishima, (1984) to compensate for the increase of the drag coefficient due to the surrounding droplets. The droplet relaxation time τ_p is derived for OPOSPM in [XVII, Attarakih et al., 2009c] and is extended for MPOSPM in [IV, Jaradat et al., 2012d]:

$$\tau_{p,i} = \frac{d_{30,i}^2 \bar{\rho}_y}{18\mu_x} \left(\frac{24}{C_{D,i} Re_i} \right) \quad (36)$$

where the drag coefficient C_D can be estimated from the correlation of Schiller and Nauman (Clift et al., 1978). Note that the relaxation time is explicit (independent of droplet velocity) in the viscous region where Stokes's law applies. The initial velocity of the primary particles is estimated from the peak terminal velocity equation for droplets formed at tip of nozzles immersed in the continuous phase [XVII, Attarakih et al., 2009c]; (Drumm et al., 2010). Note that the source term in Eq.(33) could become negative due to high continuous phase velocity u_x or an increase of the dispersed phase holdup. In this way, small particles will be dragged by the continuous phase resulting in what is known as entrainment in the operation of liquid extraction columns (Lo et al., 1983).

3.2.4. Continuous and dispersed phase's solute balance

The continuous and dispersed phases solute material balances (by considering the rising droplets as point sources) are given by Eqs.(37 and 38) below. The transport equation for solute concentration \bar{c}_y is derived by multiplying Eq.(7) by $c_y v(d)$, substituting Eq.(24) in Eq.(7) and integrating from 0 to ∞ and 0 to c_y^* with respect to d and c_y respectively to get the mean solute concentration in the dispersed phase [I; II; IV, Jaradat et al., 2012a, 2012b, 2012d]:

$$\frac{\partial Y}{\partial t} + \frac{\partial u_{y,avg} Y}{\partial z} - \frac{\partial}{\partial z} \left(D_y \frac{\partial Y}{\partial z} \right) = \frac{Q_y^{in} C_y^{in}}{A_c} \delta(z - z_y) + 6 \sum_{i=1}^{N_{pp}} \frac{K_{oy,i}}{d_{30,i}} (m'X - Y) \quad (37)$$

In the above equation: Y is the total solute concentration in the dispersed phase, K_{oy} is the overall mass transfer coefficient, D_y is the axial dispersion coefficient that takes into account the back-mixing of the dispersed phase, z_y is the position of the dispersed phase inlet, while the source term accounts for the mass conservation during solute transfer. The first term on the right hand side is the rate at which the droplets entering the column with volumetric flow rate, Q_y^{in} , that is perpendicular to the column cross-sectional area, A_c , at a location z_y with an initial solute concentration, c_y^{in} , and is treated as a point source in space. The last term appearing in Eq.(37) is the total rate of solute transferred from the continuous to the dispersed phase, where the liquid droplets are treated as point sources.

The solute balance in the continuous phase is given for MPOSPM by [I; II; IV, Jaradat et al., 2012a, 2012b, 2012d] as:

$$\frac{\partial X}{\partial t} + \frac{\partial}{\partial z} \left[-u_x X - D_x \frac{\partial X}{\partial z} \right] = \frac{Q_x^{in}}{A_c} C_x^{in} \delta(z - z_x) - 6 \sum_{i=1}^{N_{pp}} \frac{K_{oy,i}}{d_{30,i}} (m'X - Y) \quad (38)$$

In the above equation, the left hand side of Eq.(38) as well as the first term on the right hand side have the same interpretations as those given in Eq.(37); however, with respect the continuous phase. The last term appearing in Eq.(38) is the total rate of solute transferred from the continuous to the dispersed phase, where the liquid droplets are treated as point sources. The variables X and Y are defined as: ($X = \alpha_x c_x$, $Y = c_y \sum_i^{N_{pp}} \alpha_{y,i}$ and $m' = m \sum_i^{N_{pp}} \alpha_{y,i} / \alpha_x$), and the average droplet velocity is given by: ($u_{y,avg,s} = \sum_{i=1}^{N_{pp}} \alpha_{y,i,s} u_{y,i,s} / \sum_{i=1}^{N_{pp}} \alpha_{y,i,s}$). After the estimation of the individual mass transfer coefficients, the rate of change of solute concentration in the liquid droplet (\dot{c}_y) is determined in terms of the droplet volume average concentration and the overall mass transfer coefficient, K_{oy} .

3.3.Numerical solution of the MPOSPM

The present mathematical model, which is given by system of partial differential equations and the associated algebraic closure equations is coupled through the convective and source terms and is dominated by macro convection transport with discontinuous breakage and coalescence events. The time scale of these events is considered too small compared to that of convection and diffusional transport mechanisms.

The MPOSPM model consists of a system of conservation laws that are dominated by convection since the axial dispersion coefficients are relatively small ($D_x = 1.152 \times 10^{-9}$ and $D_y = 2.788 \times 10^{-9} \text{ m}^2/\text{sec}$). This calls for special discretization technique, which one usually used to solve nonlinear hyperbolic conservation laws. For this reason, a finite volume method based on the first order upwind scheme is used as a spatial solver (Leveque, 2004; Attarakih et al., 2008a). The major difficulty lies in the convective terms where special discretization techniques are required when nonsmooth profiles are expected to appear along the spatial domain. One of the popular methods of discretization is the finite volume methods, which makes use of the conservation nature of the partial differential equations. This allows the method to handle discontinuous profiles successfully (although with front smearing). To solve the above system of equations, the first order upwind scheme with Flux Vector Splitting (FVS) is chosen. The name upwind comes from the fact that discretization is performed using grid points on the side from which information flows. The time variable is discretized using semi-implicit first order Euler method with constant time step. The magnitude of time step is taken as 0.25 sec and the number of spatial cells is 200. The numerical solutions of the model's equations are given in a matrix form as:

$$A_i^n X_i^{n+1} = R_i^n \quad (39)$$

In the above equations n is the time index, i is number of variable index, A_i^n is the coefficients matrix, X_i^{n+1} is the unknown vector, R_i^n is the right hand side vector, m_i are the elements of the main diagonal, r_i are the elements of the upper diagonal and l_i are the elements of the lower diagonal. The discretized mathematical model is programed in MATLAB.

3.4. Population balance submodels

The spatially distributed population balance equation (SDBPBE) is general for any type of liquid-liquid extraction column. However, what makes the equation specific is the internal geometry of the column as reflected by the required correlations for hydrodynamics and mass transfer. Experimental correlations are used for the estimation of the turbulent energy dissipation and the slip velocities of the moving droplets along with interaction frequencies of breakage and coalescence. These correlations and models were found the best for the simulation of pulsed (packed and sieve plate) and stirred (RDC and Kühni) extraction columns (see Table 1). These models and correlations cover a wide range of operating conditions and physical properties of test system varies from the low interfacial tension test systems to the high interfacial tension test systems. However, the other correlations given in literature are very limited to special cases of operating conditions and the physical properties.

3.4.1. Daughter droplet distribution and mean number of daughter droplets

In addition to the breakage frequency $\Gamma(d)$ for describing the breakage source term in the population balance equation, it is necessary to specify the daughter droplet distribution $\beta(d, d')$. The distribution of the daughter droplets can be described by a beta distribution function (Bahmanyar et al., 1991) as given by (Eq.(40) below). The beta distribution function is characterized by the mean number of daughter droplets ϑ , caused by the breakup of a parent droplet of diameter d_m :

$$\beta(d, \bar{d}_m) = 3\vartheta(\vartheta - 1) \left[1 - \left(\frac{d}{\bar{d}_m} \right)^3 \right]^{(\vartheta-2)} \frac{d^5}{\bar{d}_m^6} \quad (40)$$

In general, droplet breakage is a function of the chemical system, the energy input (stirrer or pulsation). Schmidt, (2006) has developed a correlation to predict the average number of daughter droplets taking into account stirrer geometry and the chemical system physical properties. The mean number of daughter droplets in RDC and Kühni extraction columns is estimated using the following set of correlations respectively (Schmidt, 2006):

$$\vartheta = 2 + 0.95 \left[\left(\frac{d'}{d_{crit}} \right) - 1 \right]^{-0.75} \left(\frac{H_C}{D_R} \right)^{2.5} \left(\frac{p}{1-p} \right) \quad (41)$$

$$\vartheta = 2 + 2.48 \left[\left(\frac{d'}{d_{crit}} \right) - 1 \right]^{-0.92} \left(\frac{H_C}{D_R} \right)^{2.5} \left(\frac{p}{1-p} \right) \quad (42)$$

In the above equation, d_{crit} is the droplet critical diameter, H_C is the compartment height, D_R rotor diameter and p is the droplet breakage probability.

For pulsed packed extraction column the average number of daughter droplets per breakage that is given by:

$$\nu = 2 + 0.34 \left(\left(\frac{d'}{d_{stab}} \right) - 1 \right)^{1.96} \quad (43)$$

Here, d_{stab} is the stable droplet diameter, below which no more breakage takes place, the values of d_{stab} used in the simulation of this work is given in [V, Jaradat et al., 2011a].

For pulsed sieve plate extraction column, according to Henschke, 2004, the mean number of daughter droplet is given by:

$$\bar{n}_z = 2.0 + \xi_3 \left[\left(\frac{d'}{d_{stab}} \right)^{\xi_4} - 1 \right] \left(\frac{af}{\varphi_{st} v_t} + 1 \right)^{\xi_5} \quad (44)$$

where af is the pulsation intensity, φ_{st} is the relative free cross-sectional area of a sieve tray, v_t is the terminal droplet velocity, and ξ_i are adjustable parameters. Here, d_{stab} is the stable droplet diameter, below which no further droplet breakage takes place, the values of the constants used in the simulation of this work are given in [V, Jaradat et al., 2011a].

For pulsed sieve plate extraction column, the daughter droplet size distribution n_z after Henschke, (2004) is given by:

$$n_z = \left(\bar{n}_z - \left(\frac{0.2}{\bar{n}_z - 1.8} \right) \right) (1 + (1 - \sqrt{S})) \quad (45)$$

where S is random number that is generated randomly using a normalized distribution function.

3.4.2. Breakage frequency

The breakage source term in the population balance model is characterized by the breakage frequency $\Gamma(d, \phi_d)$ and the daughter droplet distribution function $\beta(d, d')$. The droplet breakage frequency and the daughter droplet distribution are correlated based on single droplet experiments. Different available correlations are used to calculate the droplet breakage frequency. The breakage frequency in droplet population balance model (DPBM) is calculated by following Gourdon et al., (1994) using the breakage probability $p(d)$ and the time required by the liquid droplet to cross a stirred cell of height H_c :

$$\Gamma(d, \phi_d) = p(d) \frac{u_d(d, \phi_d)}{H_c} \quad (46)$$

In this equation, $u_d(d, \phi_d)$ is the dispersed phase velocity relative to the column walls. The breakage probability in stirred (Kühni and RDC) extraction columns is given by (Schmidt, 2006):

$$\frac{p}{1-p} = C_1 \left[\frac{We_{mod}}{1 + C_3 \mu_y [We_{mod} / (\sigma d \rho_y)]^{0.5}} \right]^{c_2} \quad (47)$$

The modified Weber number We_{mod} is given by:

$$We_{mod} = \frac{\rho_x^{0.8} \mu_x^{0.2} d D_R^{1.6} \left((2\pi N)^{1.8} - (2\pi N_{crit.})^{1.8} \right)}{\sigma} \quad (48)$$

The dimensionless constants C_1 , C_2 and C_3 are dependent on the stirrer geometry and are fitted using steady state experimental data in small scale devices, the values of the constants used in the simulation of this work are given in [IV, Jaradat et al., 2012d].

The critical rotor speed N_{krit} in RDC and Kühni columns is predicted using a correlation after Schmidt, (2006):

$$N_{crit} = C_4 \frac{D_R^{-2/3} \mu_y d^{-4/3}}{2(\rho_x \rho_y)^{0.5}} + \left[\left(C_4 \frac{D_R^{-2/3} \mu_y d^{-4/3}}{2(\rho_x \rho_y)^{1/2}} \right)^2 + C_5 \frac{\sigma}{\rho_x D_R^{4/3} d^{5/3}} \right]^{0.5} \quad (49)$$

The constants C_4 and C_5 in Eq.(49) are determined experimentally at the critical rotor speeds, the values of the constants used in the simulation of this work are given in [IV, Jaradat et al., 2012d]. The critical rotor speed in turn is determined experimentally from the extrapolation of the breakage probability curves for a given mother droplet to a zero breakage probability (Gourdon, et al., 1994). In the above equation N is the stirrer speed and D_R is the stirrer diameter.

Garthe, (2006) droplet breakage probability is used in the simulation of pulsed (sieve plate and packed) extraction column (see Fig.III.7) that is given by:

$$P_B(d) = C_1 \pi_{af}^{C_2} \left(\left(\frac{(d - d_{stab})}{(d_{100} - d_{stab})} \right)^{C_3} / C_4 + \left(\frac{(d - d_{stab})}{(d_{100} - d_{stab})} \right)^{C_3} \right) \quad (50)$$

where C_i are adjustable parameters for the breakage probability, d_{100} is the characteristic droplet diameter due to a breakage probability of 100 %, the values of the constants used in the simulation of this work are given in [V, Jaradat et al., 2011a]. π_{af} is a dimensionless number taking into account the influence of the pulsation intensity on the breakage probability, and is given by Garthe, (2006) as:

$$\pi_{af} = af \left(\frac{\rho_c^2}{\mu_c \Delta \rho g} \right)^{1/3} \quad (51)$$

In this equation ρ_c is the density of the continuous phase, μ_c the viscosity of the continuous phase, g is the gravity acceleration constant and $\Delta \rho$ is the density difference. This breakage frequency describes the breakage in pulsed packed and sieve plate columns with only one set of constant parameters for a given liquid-liquid-system.

3.4.3. Droplet coalescence frequency

In addition to modelling droplet motion and breakage, droplet coalescence is of crucial importance in the modelling and simulation of extraction columns. The physicochemical properties of the continuous phase, the direction of solute transfer and the turbulent fluctuations play an important role in droplet coalescence. It is believed that droplet coalescence occurs if the contact time between any two randomly coalescing droplets exceeds the time required for the complete intervening film drainage and rupture. Coalescence rate analysis and modelling has been paid greater attention. Many authors proposed phenomenological models based on the concept of collision frequency and coalescence efficiency, where the latter assumed to be a

function of the two coalesce droplets, an intensive review on the coalescence models is provided by Liao and Lucas, 2010 which support this assumption.

Thus, the coalescence model after Henschke, (2004) is modified [V, Jaradat et al., 2011a] to take into account the size of the two coalesce droplets (see Fig.III.8). In this work, the modified coalescence model is used in the simulation of both pulsed (packed and sieve plate) columns:

$$\omega(d, d') = c \left(v(d)^n + v(d')^n \right) \frac{\phi_y \sigma^{1/3} H_{cd}^{1/6} (\Delta \rho g)^{1/2}}{\xi_8 \mu_c d^{1/3}} \quad (52)$$

In this modified coalescence frequency $\omega(d, d')$, d, d' is the droplet diameter, v is the droplet volume, ϕ_y is the dispersed phase holdup, σ is the mixture interfacial tension and H_{cd} is the Hamaker constant, the value used in the simulation is $10e-20$. The adjustable parameter ξ_8 was fitted to experimental data for the two standard EFCE test systems: water-acetone (solute)-toluene and water-acetone (solute)-butyl acetate and is given by Henschke, 2004. The values for this parameter are 2500 and 1500 for the first and second system respectively. The values of the constants used in the simulation of this work are given in [V, Jaradat et al., 2011a].

The popular phenomenological model of Coulaloglou and Tavlarides, (1977) is used in the simulation of the stirred (RDC and Kühni) columns. In this model, the coalescence frequency $\omega(d, d')$ is represented as a product of the collision rate $h(d, d', \phi)$ and the Coalescence efficiency $\lambda(d, d', \phi)$ as given by Eqs.(53) and (54) respectively:

$$h(d, d', \phi) = C_1 \frac{\varepsilon^{1/3}}{1 + \phi} (d + d')^2 \left(d^{1/3} + d'^{1/3} \right)^{1/2} \quad (53)$$

$$\lambda(d, d', \phi) = \exp \left[-C_2 \frac{\mu_x \rho_x \varepsilon}{\sigma^2} \left(\frac{dd'}{d+d'} \right)^4 \right] \quad (54)$$

The parameters C_1 and C_2 in the above equations represent specific coalescence model parameters, which need to be determined experimentally for each chemical system; the values of the constants used in the simulation of this work are given in [IV, Jaradat et al., 2012d].

3.4.4. The Terminal Droplet Velocity

The hydrodynamic behaviour of droplets during the movement in a surrounding continuous phase depends on the droplet diameter. On this account, four different droplet velocity boundaries can be distinguished. The first one of droplet diameters identifies small droplets with rigid phase boundaries, which have no internal circulation. These droplets are moving as rigid spheres. For larger diameter there is shear forces at the droplet surface, so that an internal circulation begins to occur. Due to the circulation of the droplets they move faster than rigid spheres. For even larger diameter droplets they lose their spherical shape, at the same time the droplets begin to oscillate. With further increasing of the droplet diameter, the droplet deforms and finally breaks up. The velocity of the droplets decreases as a result of the increasing flow resistance (Clift et al., 1978; Wesselingh and Bollen, 1999; Henschke, 2004).

In LLECMOD several correlations for terminal droplet velocity has been implemented that can be chosen by the user. These velocity correlations are: Klee and Treybal, (1956); Vignes, (1965);

Grace, (1976); Henschke, (2004), and the rigid sphere law interpolated between the viscous and inertial regimes as given by Wesselingh and Bollen, (1999). If the user does not choose any of these correlations, LLECMOD automatically chooses the suitable velocity correlation by default, based on the selection chart described in detail by Godfrey and Slater, (1994).

Recently, Henschke, (2004) proposed a terminal velocity model utilizing different droplet velocity models based on their droplet diameter (see Fig.III.9). In his model the spherical, oscillating and deformed droplets velocity models are combined into a single model utilizing a crossover function, which is applicable over the entire diameter range. The resulting droplet velocity model is given by (Henschke, 2004):

$$v_t = \frac{v_{oscillating \text{ or } deformed} v_{spherical}}{(v_{oscillating \text{ or } deformed}^{a_{16}} + v_{spherical}^{a_{16}})^{1/a_{16}}} \quad (55)$$

where $v_{oscillating \text{ or } deformed}$ is a smooth transition from oscillating to deformed droplets, $v_{spherical}$ is the velocity model for spherical droplets (Henschke, 2004). The exponent a_{15} , a_{16} describe the sharpness of the transition between sub-models, where the parameter a_{15} , a_{16} is adjusted to measured values that are given in [V, Jaradat et al., 2011a]. The parameters in this velocity model can be fitted to the experimental data for certain test system based on single droplet experiments (Henschke, 2004).

3.4.5. Effect of internal column geometry on rising droplet velocity

The slowing factor K_v takes into account the effect of the column internal geometry and energy input (agitation or pulsation) on the droplet terminal velocity, the value of K_v vary in the range between 0 and 1 (Modes et. al., 1999). The slowing factor K_v is dependent on the droplet size, agitation intensity, internal geometry and the flow structure of the continuous phase. This factor is the ratio of the measured relative droplet velocity to the terminal rising velocity in the column without internals. Based on Modes' correlation, Garthe (2006) developed a correlation for K_v in RDC extraction columns:

$$K_v = 1 + 0.512 N_P^{0.362} - 0.507 \left(\frac{d}{d_s - d_A} \right)^{1.035} - 0.341 \left(\frac{h_c}{D_C} \right)^{-0.565} \quad (56)$$

The dimensionless power number N_P is given by Kumar and Hartland (1996):

$$N_P = \frac{109.36}{Re_R} + 0.74 \left(\frac{1000 + 1.2 Re_R^{0.72}}{1000 + 3.2 Re_R^{0.72}} \right)^{3.3} \quad (57)$$

and the rotor Reynolds number is given by:

$$Re_R = \frac{n_R d_A^2 \rho_C}{\mu_c} \quad (58)$$

Based on works of Modes, Garthe (2006) developed a correlation for K_v in Kühni extraction columns as:

$$K_v = 1 - 1.669 N_P^{-3.945} - 2.807 \left(\frac{d}{D_C - d_A} \right)^{1.336} - 1.159 \left(\frac{h_c}{D_C} \right)^{2.049} + 2.1 \varphi_s^{1.032} \quad (59)$$

The dimensionless power number N_P is given by Kumar and Hartland, (1996):

$$N_P = 1.08 + \frac{10.94}{Re_R^{0.5}} + \frac{257.37}{Re_R^{1.5}} \quad (60)$$

and the rotor Reynolds number is given by:

$$Re_R = \frac{n_R d_A^2 \rho_C}{\mu_C} \quad (61)$$

In the above equations D_C is the column diameter, d_A is the shaft diameter, h_C is the compartment height, φ_s is the relative free cross-sectional area of a stator and n_R is the rotor speed.

For the description of the droplet motion in the pulsed structured packing column a correlations for the slowing factor developed by Garthe, (2006) is applied, which is given by:

$$k_v = 0.077 \pi_{H_{pk}}^{0.138} \pi_{a_{pk}}^{-0.566} \pi_d^{-0.769} \pi_\sigma^{0.184} (1 + \pi_{af})^{0.08} \quad (62)$$

In the above equation $\pi_\sigma = \sigma (\rho_c^2 / \mu_c^4 \Delta \rho g)^{1/3}$ is the dimensionless interfacial tension, $\pi_{h_p} = h_p (\rho_c \Delta \rho g / \mu_c^2)^{1/3}$ is the dimensionless height of a packing, $\pi_{a_p} = a_p (\mu_c^2 / \rho_c \Delta \rho g)^{1/3}$ is the dimensionless volumetric surface area of a packing and $\pi_d = d (\rho_c \Delta \rho g / \mu_c^2)^{1/3}$ is the dimensionless droplet diameter.

Based on the analysis of experimental results, Garthe, (2006) developed a new correlation for slowing factor in pulsed sieve plate column:

$$k_v = 1.406 \varphi_{st}^{0.145} \pi_\sigma^{-0.028} \exp \left(-0.129 (d/d_h)^{1.134} (1 - \varphi_{st})^{-2.161} \right) \quad (63)$$

where d_h is the diameter of sieve plates' holes.

3.4.6. Continuous phase velocity models

To close the model, there is an obvious need for expression for the continuous phase velocity u_x .

The continuous phase velocity models are required to calculate the dispersed phase velocity u_y from the momentum balance equation, for this, there are three available models: The oscillatory model, which shows an oscillatory behaviour in the dispersed phase hold-up as reported both experimentally by Hufnagl et al., (1991) and theoretically by Weinstein et al., (1998) and Attarakih et al., (2004a). The second velocity model is the non-oscillatory model, which is given by Attarakih et al., (2004b, 2006a). The third velocity model is the steady state velocity model and, hence, it is not applicable for transient simulations, which is given by Kronberger et al., (1994):

$$u_x = \Delta_x \frac{Q_{x,in}}{A_c (1 - \phi)} + \frac{D_x}{1 - \phi} \frac{\partial \phi}{\partial z} \quad (64)$$

The non-oscillatory velocity model, which is given by Attarakih et al., (2004):

$$u_x = \alpha_y(z, t)u_s(d, \bar{c}_y, z) - \alpha_y(H, t)u_s(d, \bar{c}_y, H) + \Delta_x(z)\frac{Q_x^{in}}{Ac} + \Delta_y(z)\frac{Q_y^{in}}{Ac} \quad (65)$$

where: $\Delta_x = \begin{cases} 1, & z \leq Z_x \\ 0, & \text{otherwise} \end{cases}$, $\Delta_y = \begin{cases} 1, & z < Z_y \\ 0, & \text{otherwise} \end{cases}$, D_x is the axial dispersion coefficient and H is the height at the exit of the dispersed phase from the top of the column (see Fig.1).

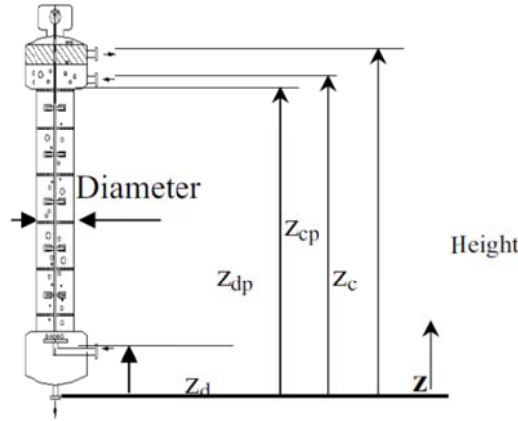


Fig.1. RDC column geometry

The discontinuity appearing in the continuous phase velocity u_x is due to the presence of the step function Δ_x & Δ_y and is physically understood by referring to the column geometry shown in Fig.1. The lower and upper settling zones are designed to separate the heavy and light phases at the bottom and top of the column respectively. So, the velocity of the continuous phase is zero in the upper settling zone to allow the coalescence of the light phase droplets to disengage from the column.

3.4.7. Mass Transfer Models

Mass transfer models depend generally on droplet internal state, where droplet circulation and oscillation can occur affecting the mass transfer performance. Thus, the mass transfer coefficients are drop-size dependent to take into account inner circulation, presence of surfactants and the rising velocity. The mass transfer coefficient of the dispersed or continuous phase is one of the fundamental and essential parameters in extraction column design. Several models have been proposed for the estimation of the mass transfer coefficient of the dispersed phase. Kumar and Hartland, (1999) showed that the dispersed phase individual mass transfer coefficient is dependent on the behaviour of the single droplet in the sense whether it is circulating or oscillating. The mass transfer fluxes in the simulation programs are calculated based on the two-film theory. The two individual mass transfer coefficients (k_x & k_y) are defined separately for the continuous and the dispersed phases. The mass transfer model used in the simulation of the pulsed (packed and sieve plate columns) is taken from the work of Henschke, 2004. In this model, the author followed the idea of Handlos and Baron, (1957) to develop a semi-empirical model, which describes the mass transfer inside a droplet based on the diffusion and mass-transfer-induced turbulence. Their assumption used in this model is that mass transfer induces the

interfacial vortices. They define a transport coefficient, which is added to the molecular diffusion coefficient. It contains the so-called instability coefficient C_{IP} as system-specific parameter and is based on the Handlos and Baron, (1957) equation. Many available phenomenological and experimentally correlated mass transfer models are programmed and available (Newman, 1931; Kronig and Brink, 1950; Handlos and Baron, 1957; Wolschner, 1980; Korschinsky and Young, 1989; Slater, 1995; Kumar and Hartland, 1999; Henschkae, 2004). Accordingly, the suitable combination of these individual mass transfer coefficients results in the overall mass transfer coefficient, K_{oy} , which is used to predict the rate of change of solute concentration in the liquid droplet. In the present version of LLECMOD, the direction of mass transfer (from continuous to dispersed phase or vice versa) can be easily chosen. Moreover, the type of phase to be dispersed is also allowed to be specified by the user. This provides great flexibility in investigating the performance of liquid extraction columns.

Kumar and Hartland (1999) proposed a new equation for calculating the overall dispersed phase mass transfer coefficients for circulating and oscillating drops in extraction columns. In the present work, the correlation of Kumar and Hartland, (1999) is used the simulation for RDC and Kühni liquid-liquid extraction columns. After the estimation of the individual mass transfer coefficients, the rate of change of solute concentration in the liquid droplet (\dot{c}_y) is determined in terms of the droplet volume average concentration and the overall mass transfer coefficient, K_{oy} :

$$\frac{\partial c_y(z, t)}{\partial t} = \frac{6K_{oy}}{d} (c_y^*(c_x) - c_y(z, t)) \quad (66)$$

Note that K_{oy} may be the function of the droplet diameter, d , and time depending on the internal state of the droplet; that is, whether it is circulating or oscillating. The overall mass transfer coefficient is usually expressed using the two-resistance theory in terms of the individual mass transfer coefficients for the continuous and the dispersed phases (Ribeiro et al., 1996) and $c_y^* = (\partial c_y / \partial c_x) c_x$.

3.4.8. Axial dispersion coefficients

The axial dispersion coefficients (\bar{D}_x & \bar{D}_y) for the dispersed and continuous phases are defined in the user input module as functions. These coefficients are allowed to vary with the column height in the present version of LLECMOD. Typical published axial dispersion correlations for pulsed and stirred extraction columns used in the LLECMOD program are listed in (Attarakih et al., 2008a).

3.5.LLECMOD program (retrofitting, development and modification)

The model equations are solved using an optimized and efficient numerical algorithm developed by Attarakih et al., (2006) based on the generalized fixed-pivot technique (Attarakih et al., 2003) and a first-order upwind scheme based on the finite volume method. This utilized successfully for the simulation of coupled hydrodynamics and mass transfer for general liquid-liquid extraction columns with reasonable CPU time requirements. However, using the available commercial software, hydrodynamics simulations the order of magnitude is in minutes, but mass transfer simulations is in the order of hours. The complete mathematical model described above is

programmed using Visual Digital FORTRAN with optimized and efficient numerical algorithms and integrated with whole existing program. To facilitate the data input and output, a graphical user interface was designed. The graphical interface of the LLECMOD (Liquid-Liquid Extraction Column Module) program contains the main input window and sub-windows for parameters and correlations input. The main window contains all correlations and operating conditions that can be selected using drop down menus. The basic feature of this program (Attarakih et al., 2008a) is to provide an easy tool for the simulation of coupled hydrodynamics and mass transfer in liquid-liquid extraction columns based on the population balance approach for both transient and steady states conditions through an interactive windows input dialog. Note that LLECMOD is not restricted to a certain type of liquid-liquid extraction column since it is built in the most general form that allows the user to input the various droplet interaction functions. These functions include droplet terminal velocity (taking into account the swarm effect) and the slowing factor due to column geometry, the breakage frequency and daughter droplet distribution, the coalescence frequency and the axial dispersion coefficients. The correlation parameters that are obtained based on single droplet and droplet swarm experiments, are considered in a modularized structure for the simulation program. Using LLECMOD, simulations can now be carried out successfully for different types of extraction columns including agitated (RDC and Kühni) and pulsed (sieve plate and packed) columns.

Table 1. Available hydrodynamics and mass transfer correlations implemented in LLECMOD

Hydrodynamics			Mass Transfer
Breakage	Coalescence	Droplet Velocity	
- Laso et. al., 1987	- Laso et. al., 1987	- Klee and Treybal, 1956	- Newman, 1931
- Coulaloglou & Tavlarides, 1977	- Coulaloglou & Tavlarides, 1977	- Vignes, 1965	- Kronig & Brink, 1950
- Narsimhan et. al., 1984	- Sovova, 1981	- Rigid sphere (Bauer, 1976)	- Handlos & Baron, 1957
- Schmidt et. al., 2006	- Tsouris & Tavalarides, 1994	- Grace, 1976	- Korschinsky and Khatayloo, 1976
- Garthe, 2006	- Garthe, 2006	- Godfrey & Slater, 1994	- Wolschner, 1980
- Henschke, 2004	- Henschke, 2004	- Henschke, 2004	- Kumar & Hartland, 1988
			- Slater, 1994, 1995
			- Henschke, 2004
			- User defined-Model

Part of this doctoral thesis work was emerged on retrofitting, modification and further development of LLECMOD program. However, new features were added, namely, the choice of mass transfer direction (continuous to dispersed or vice versa) and the choice of dispersion type (heavy or light) [IX, Jaradat et al., 2010a], moreover several new correlations were implemented and validated under the LLECMOD program (see Table 1), and finally two modules were developed for pulsed (packed (see Fig.III.12) and sieve plate (see Fig.III.13)) columns [III; V; VI; VII; VIII; IX, Jaradat et al., 2012c, 2011a, 2011b, 2011c, 2011d, 2010a] the developed

modules are integrated in the whole LLECMOD program. Moreover, the LLECMOD program is modified to take into account the exponential step change in the dynamic analysis of extraction columns (see Fig.III.4).

4. STEADY STATE MODELLING AND SIMULATION OF EXTRACTION COLUMNS

4.1. Stirred extraction columns

The mechanical agitation helps improve the formation of droplets and increase the interfacial area, resulting in greater efficiency, hence, improves the overall performance of extraction columns. Examples of agitated extraction columns include: Scheibel columns, Oldshue-Rushton Columns, Kühni columns, Rotating Disk Contactor (RDC), etc. In the latter the agitating elements are planar disks that are mounted on a centrally supported shaft. Mounted on the column wall and offset against the agitator disks are the stator rings, whose aperture is greater than the agitator disk diameter. The Kühni extractor operates on a quite different principle to the RDC, where the stator disks are made of perforated plates and the rotor is a turbine impeller. The variable hole arrangement of this column promotes flexibility of design for different column applications. Stirred liquid-liquid extraction columns are widely applied in many process industries for many years and their performance is relatively good. However, still there is deficiency of reliable design and scale-up of these columns. The design of such type of extraction column is not a straightforward process. In practice, the design of extraction columns based on a theoretical basis and pilot experimental study (see Fig.III.3). Great efforts have been done during the last decades to develop predictive methods based on the population balance modelling, which is capable to provide detailed information of the hydrodynamic and mass transfer behaviour [I-X, Jaradat et al., 2012a, 2012b, 2012c, 2012d, 2011a, 2011b, 2011c, 2011d, 2010a, 2010b].

4.1.1. RDC and Kühni columns

In real extraction columns where droplet breakage and coalescence are encountered and the dispersed phase undergoes continuous changes, the back-mixing or dispersion model (pseudo-homogeneous treatment of the dispersed phase) breaks down, and hence the population balance model should be applied (Attarakih et al., 2006a, 2008a); [XVI, Attarakih et al., 2009b]. Here a differential balance is formulated for the number of drops in the dispersed phase, taking into account birth and death rates due to breakage, coalescence, and convective transport. Hence, the modelling and research in the field of liquid-liquid extraction focuses on the Population Balance Equation (PBE) (Ramkrishna, 2000; Attarakih et al., 2004b; Drumm et al., 2010); [I; II; IV; X; XVI; XVII; XVIII, Jaradat et al., 2012a, 2012b, 2012d, 2010b, Attarakih et al., 2009b, 2009c, 2008b]. Droplet breakage and coalescence are considered in the PBE in order to describe part of the real droplet behaviour in a stirred liquid-liquid extraction column (Drumm et al., 2010). This allows the model to take into account the transport of solutes from or to the liquid droplet by diffusion on one hand, and the transport of droplets by convection on the other hand. Due to the interactions between the droplets themselves and the surrounding turbulent continuous phase, a hydrodynamic equilibrium is established between droplet breakage and coalescence. This in general leads to a multivariate distribution evolving in time and space with different time scales leading to a multi-scale problem [I; II; IV; XVII, Jaradat et al., 2012a, 2012b, 2012d, Attarakih et

al., 2009c]. To take this into account, the multivariate population balance equation is used as a general transport equation of modelling.

In this model, the micro- and macro transport phenomena prevailing in the dispersion (diffusive and convective transport) are coupled through a set of integro-partial and ordinary differential equations in Eulerian frame of reference. Unfortunately, the resulting multidimensional population balance equation could not be fully resolved numerically within a reasonable time, which is necessary for the steady state or dynamic simulations, particularly when embedded in complex chemical process flow-sheets (Attarakih et al., 2008c); [XVIII, Attarakih et al., 2008b]. For this reason, there is an obvious need for a reduced liquid extraction model that captures all the essential physical phenomena and still tractable from computational point of view. Hence, the present mathematical model (based on the multivariate population balance equation) is reduced using the primary and secondary particle concept developed for solving the Population Balance Equation [I; II; IV; X; XVII, Jaradat et al., 2012a, 2012b, 2012d, Attarakih et al., 2009c].

Table 2: RDC column geometry

	Garthe, 2006	Schmidt et al., 2006
Column diameter	0.080 m	0.15 m
Stator diameter	0.050 m	0.105 m
Rotor diameter	0.045 m	0.090 m
Compartment height	0.050 m	0.030 m
Column height	4.400 m	2.50 m
Dispersed phase inlet	0.850 m	0.25 m
Continuous phase inlet	3.80 m	2.25 m

This model utilizes the concept of the multi-primary particle method to represent the droplet internal properties (droplet size and concentration), which undergoes changes due to different transport mechanisms [XVI, Attarakih et al., 2009b]. The developed model is capable to conserve the most important integral properties of the distribution; namely: the total number, solute and volume concentrations. The particle internal properties are tracked directly and coupled through the mean positions of the particle along the size and solute concentration coordinates. The primary particles can be viewed as fluid particle carrying information about the distribution as it evolves in space and time. In this way the entrainment of the dispersed phase can be easily detected.

Table 3: Physical properties of the test systems (Garthe, 2006)

physical property	unit	<i>w-a-t</i>	<i>w-a-b</i>
density ρ_c	[kg.m ⁻³]	992.0	990.9
density ρ_d	[kg.m ⁻³]	863.3	877.5
viscosity μ_c	[10 ⁻³ Pa s]	1.134	1.163
viscosity μ_d	[10 ⁻³ Pa s]	0.566	0.709
interfacial tension σ	[10 ⁻³ N m]	24.41	10.96
distribution coefficient m	[kg.kg ⁻¹]	0.843	0.933
diffusion coefficient of acetone in aqueous phase D_c	[10 ⁻⁹ m ² .s ⁻¹]	1.152	1.092
diffusion coefficient of acetone in organic phase D_d	[10 ⁻⁹ m ² .s ⁻¹]	2.788	2.199

In this work, an RDC pilot plant liquid-liquid extraction column is used. The technical specifications of this column are given in Table 2. For all numerical simulations, the inlet feed distribution is normally distributed with mean droplet diameter of 2.7 mm and standard deviation of 0.25 mm . The minimum and maximum droplet diameters for the inlet feed distribution are $d_{min} = 0.01 \text{ mm}$ and $d_{max} = 8 \text{ mm}$ such that a negligible number of droplets exists outside this range. The chemical test system water-acetone (solute)-toluene is used, which is recommended by the EFCE. The physical properties of this system are given in Table 3. The inlet solute concentrations in the continuous and dispersed phases are taken as 5.68 and 0.1% respectively, the rotor speed is 200 rpm and the total flow rate of the disperse phase is $(48) \text{ l/h}$, and for the aqueous phase is $(40) \text{ l/h}$. The direction of mass transfer is from the continuous to the dispersed phase.

In this section, we present first the use of the momentum balance equation (Eq.(33)) to estimate the primary particles' velocity causes a jump in the number and volume concentrations at the dispersed phase inlet. This is a physical jump due to the acceleration of the particles (droplets) at the entrance of the column. The algebraic velocity (empirical) model used to calculate the droplet velocity cannot capture this jump. To prove this, the number balance equation (Eq.(25)) without source term is solved analytically at steady state using only one primary particle. The analytical (steady state) solution for the number balance is given by:

$$N = c = \frac{Q_y^{in}}{A_c v_m u} \quad (67)$$

Now, the particle velocity u is obtained by solving the momentum balance numerically. Fig.2 shows the particle velocity profile in the first part of the column ($0 < z < 0.3 \text{ m}$) where 0.3 m distance is found enough for the liquid droplet to reach steady state velocity. Now, using this velocity profile, Eq.(67) is used to calculate the number concentration profile. The result is depicted Fig.2 (left panel) where the jump in the number concentration is now clear. However, the algebraic slip velocity model cannot capture this phenomenon as can be seen from Fig.3, the algebraic slip velocity model used here is after Wesselingh and Bollen, (1999).

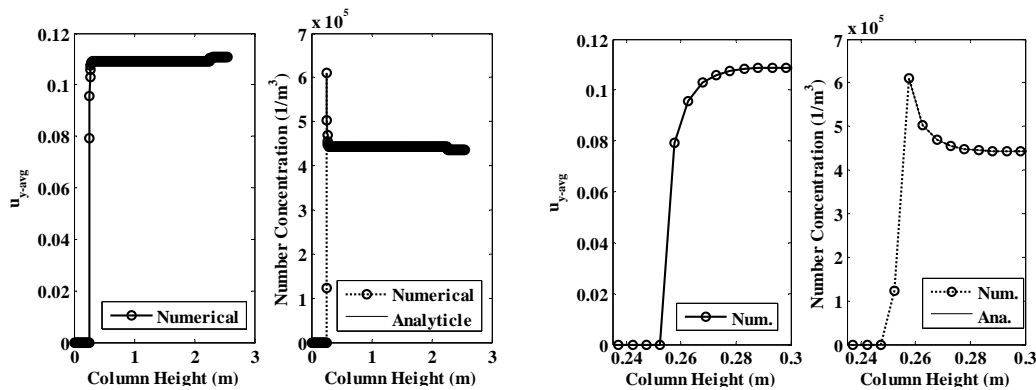


Fig.2. Effect of the rising droplet velocity as predicted from the momentum balance equation on the number concentration profile at steady state. The right part of this figure is zoomed to justify the jump in the number concentration profile.

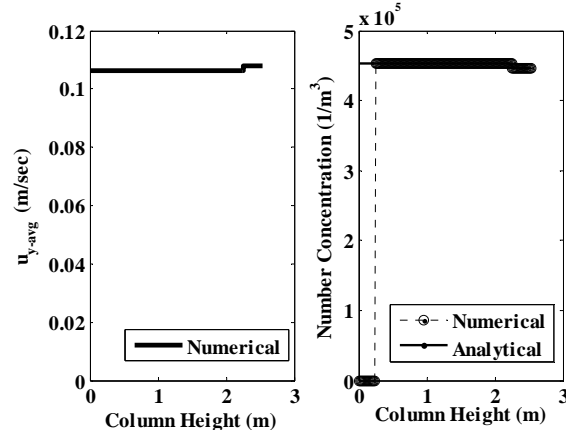


Fig.3. Analytical and numerical number concentration profiles using the algebraic slip velocity model.

This jump is not reported in the experimental literature because all the experimental measurements start from the first compartment of the column, and does not take into account the distributor zone in which the particle accelerate to their steady state velocity. In the existing models, the distributor zone is not included and hence this model comes to fill this gap and provides modelling for the full column simulation including the distributor zone. As a result, neither the steady-state relationships (algebraic models) nor the exciting models could capture this physical jump.

Fig.4 shows the convergence of the number concentration profiles along the column height using different number of primary particles. It is clear that both profiles converge as the number of primary particles is increased. Fig. 5 depicts the simulated holdup profiles using different number of primary particles where the simulated profiles are compared to the experimental data of Garthe (2006).

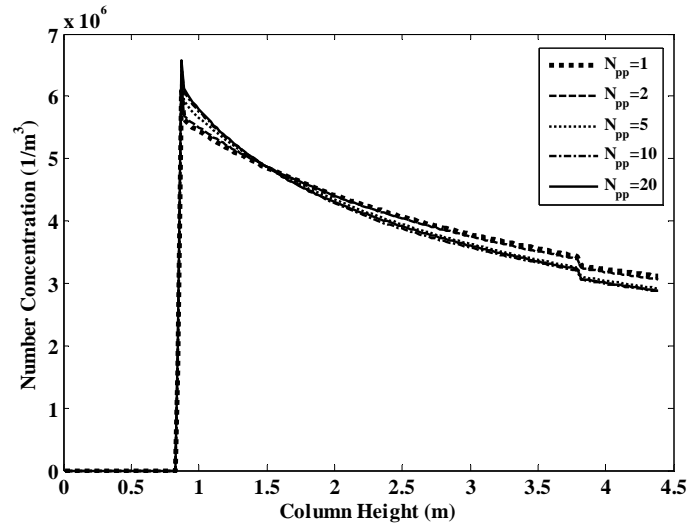


Fig.4. Effect of number of primary particles on the number concentration profile along the column height.

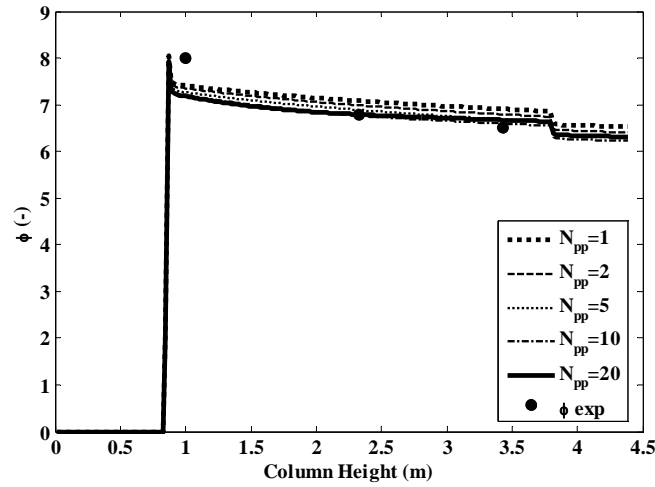


Fig.5. Simulated holdup profiles along the column height compared to the experimental data (Garthe, 2006).

Fig. 6 shows a comparison between the simulated and measured (Garthe, 2006) mean droplet diameter using different number of primary particles. It is clear that the simulated results are in good agreement with the experimental data. The mean droplet diameter appears to be insensitive to the number of primary particles since it is proportional to the cubic root of the volume to the number concentration. This result is also reported in the case of the homogenous population balance [XVII, Attarakih et al., 2009c].

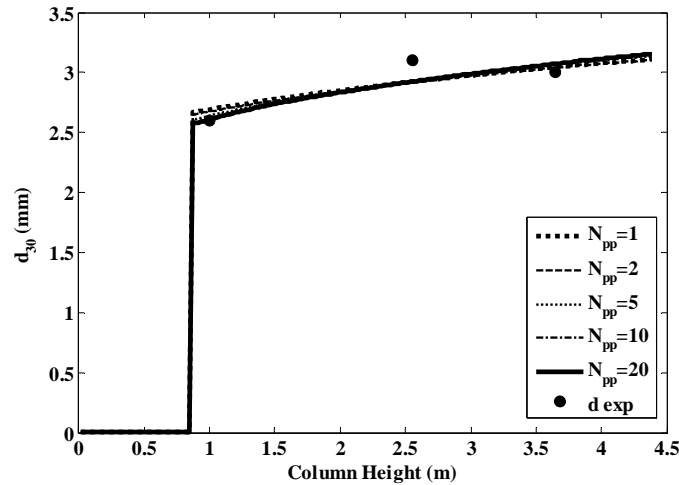


Fig.6. Simulated mean droplet diameter (d_{30}) along the column height compared to the experimental data (Garthe, 2006).

Fig.7 elucidates the convergence of the mean dispersed phase velocity along the column height. This figure shows how the average dispersed phase velocity is so sensitive to the number of primary particles. This justifies the sensitivity of the number and volume concentration profiles to the number of primary particles as shown in Figs.4 and 5. This is because the number and volume concentration profiles reflect the droplet residence time inside the column, which are inversely proportional to the droplet velocity. As a special case Drumm et al., (2010) showed that the coupling of the present population balance model with detailed CFD solvers is very efficient for the case where $N_{pp}=1$.

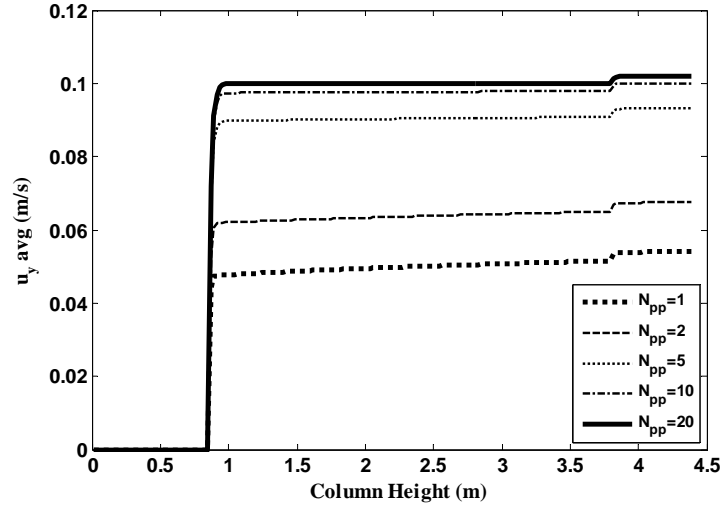


Fig.7. Effect of number of primary particles on the convergence of the mean dispersed phase velocity along the column height.

Fig.8 shows the convergence of the number distribution at a given height along the RDC column. It is clear that the number distribution converges very quickly to the reference solution ($N_{pp} = 50$) at all given locations along the column height. This result is expected since the SQMOM (the MPOSPM is a special case) converges quadratically with respect to the number of primary particles as reported in [XVII, Attarakih et al., 2009c].

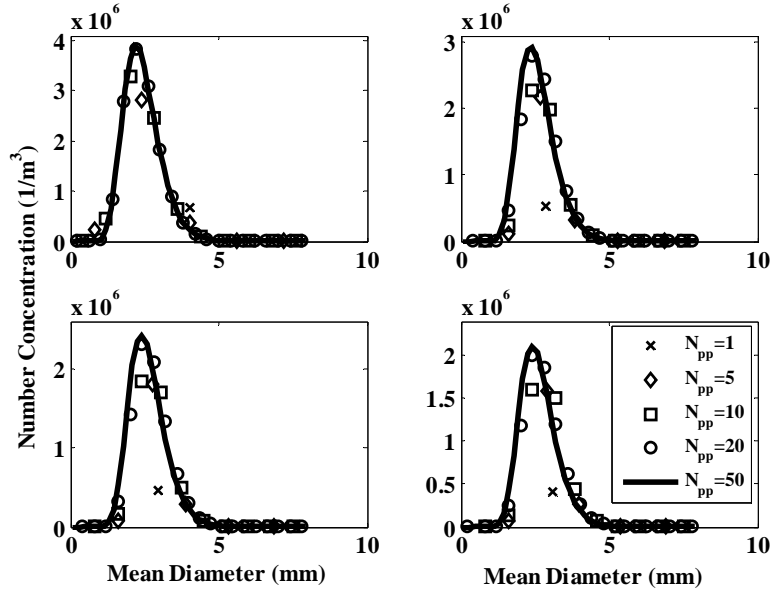


Fig.8. Convergence of the number distribution at different height of the column by increasing the number of primary particles.

Finally, the solute concentration profiles (here acetone) are depicted in Fig.9 along the column height. The jump in the concentration profile at the inlet of the dispersed phase is one of the characteristic of the axial dispersion model (Seader, 2005) and is almost negligible. Like the mean droplet diameter, the profiles are found quite insensitive to the number of primary particles.

However there is a deviation between the experimental and the simulation results, the deviation could be due to experimental error as well as computational errors; since the correlation used to predict the mass transfer coefficient are based on experiential work; again the experimental error comes into the picture.

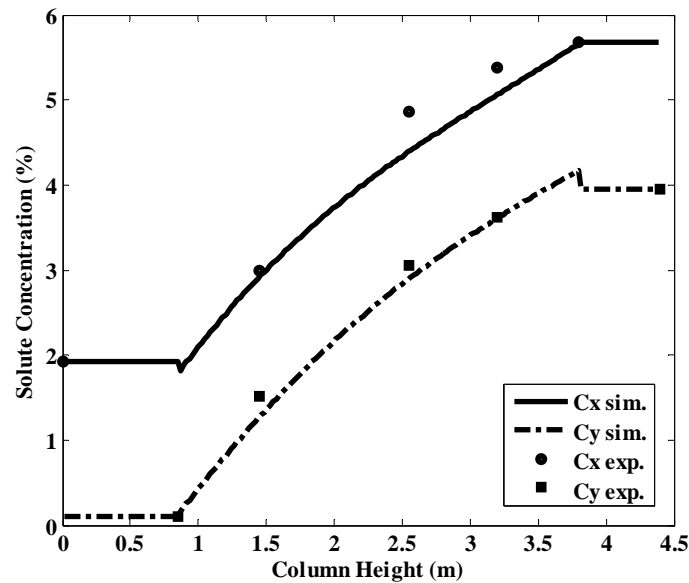


Fig.9. Variation of solute concentration profiles in both phases along the column height for both dispersed and continuous phases.

4.2.Pulsed extraction columns

Liquid-liquid extraction is an important separation processes encountered in many chemical process industries (Lo et al., 1983; Bart, 2001), biochemical and petroleum industries (Mostaedi et al., 2010). The generally poor performance of non-agitated spray columns can be improved by introducing column internals such as packings or sieve plates to create new droplets and appropriate interfacial area (Kumar and Hartland, 1986, 1994; Lorenz et al., 1990; Bart and Stevens, 2004). Internal column geometry (packing/ sieve plates) reduces axial mixing, increases droplet coalescence and breakage rates resulting in increased mass transfer rates, and affects the mean residence time of the dispersed phase which allows the handling of large loads especially with small differences of interfacial tension and density (Pérez et al., 2005). They improve the hydrodynamic performance of the column and subsequently the mass transfer performance (extraction efficiency) with chemical system where stirred columns are difficult to apply (Bateyand Thornton, 1989; Sattler and Feindt, 1995; Cavatorta et al., 1999; Igarashi et al., 2004; Kelishami et al., 2009; Azizi et al., 2010; Mostaedi et al., 2010; Rahbar et al., 2010). In sieve plate columns, the dispersed phase is redistributed over the column cross section at every tray. However, the columns with structured packing the dispersed phase is redistributed over the column cross-section at certain position along the column using liquid distributors if necessary.

The performance of these columns can be enhanced by mechanical pulsation of one or both phases. This is a result of an increase in shear forces and consequent reduction in the size of dispersed droplets. This in turn increases the interfacial area and thence the mass transfer rate (Pratt and Stevens, 1992). Van Dijk, (1935) devised the use of external energy in the form of pulsing in sieve plate columns that had found wide applications in the processing of nuclear fuel. Since the pulsing unit can be remote from the pulsed column, the pulsed columns are recommended for processing the corrosive or radioactive solutions (Mostaedi et al., 2010) and nuclear fuel reprocessing (Smoot et al., 1959; Jahya et al., 2005; Yadav and Patwardhan, 2008). These columns have a clear advantage over other mechanical contactors when processing corrosive or radioactive solutions. Pulsed columns are one of the most important liquid-liquid extraction equipment (Rahbar et al., 2010). Pulsed columns have distinct advantages practically the capability of high flow capacities (high throughputs) (Gottlieb et al., 2000; Wang et al., 2006), simple operation, extraction efficiencies, considerable flexibility (Mafield and Church, 1952; Haverland et al., 1987; Lorenz et al., 1990), small footprint for multistage extraction systems (Lo et al., 1983), reduction in organic losses and organic inventory (Fox et al., 1998) and insensitivity towards contamination of the interface. Such type of extraction column has been used successfully in a great variety of extraction processes (Lo et al., 1983; Godfrey and Slater, 1994; Bhawsar et al., 1994), pharmaceutical and hydrometallurgical industries as well in the original Redox and Purex processes (Galla et al., 1990) in atomic energy industry (Sege and Woodfield, 1954). However, pulsed columns are relatively trouble-free, have a reasonably small residence time, good extraction efficiency, better capacity-efficiency relation with minimum HTU occurring at close to flooding, less power requirement and suitability for heterogeneous phase contacting using small size particles with large holdup (Prabhakar et al., 1988).

4.2.1. Sieve plate and Packed columns

Till now, the design of liquid-liquid extraction columns based on a combination of pilot plant tests, designer's prior experience and empirical correlations (Grinbaum, 2006; Bart et al., 2008). Better understanding of the hydrodynamics and mass transfer behaviour of liquid-liquid extraction columns can ingeniously be used to increase the reliability in the design of extraction columns (Oliveira et al., 2008; Attarakih et al., 2008a); [III; V; VI; VII; VIII; IX, Jaradat et al., 2012c, 2011a, 2011b, 2011c, 2011d, 2010a]. For this reason, there is an obvious need to include droplet interactions (breakage, coalescence and droplet interface mass transfer) on the basis of a population balance equation (PBE).

The main objective of this work is to develop a PBE based model that is capable to describe the dynamic and steady state behaviour of pulsed (packed and sieve tray) extraction columns. The models of both columns are integrated into the existing program: LLECMOD (Attarakih et al., 2008a); [III; V; VI; VII; VIII; IX, Jaradat et al., 2012c, 2011a, 2011b, 2011c, 2011d, 2010a], which already can simulate agitated extraction columns (RDC and Kühni). LLECMOD can simulate the steady state and dynamic behaviour of extraction columns taking into account the effect of dispersed phase inlet (light or heavy phase is dispersed) and the direction of mass transfer (from continuous to dispersed phase and vice versa) [III, Jaradat et al., 2012c]. The

model predictions are extensively compared to the experimental data of Garthe, (2006) with two EFCE test systems (water-acetone (solute)-toluene and water-acetone (solute)-butyl acetate) for extraction under varying operating conditions [V; VI; VII; VIII; IX, Jaradat et al., 2012c, 2011a, 2011b, 2011c, 2011d, 2010a].

Table 4: Pulsed (sieve plate and packed) column geometry (Garthe, 2006)

Dimension	Value
Height of the column (H)	4.40 (m)
Inlet for the continuous phase (Z_c)	3.80 (m)
Inlet for the dispersed phase (Z_d)	0.85 (m)
Column diameter (d_c)	0.08 (m)
Dimension	Value
Height of the column (H)	4.40 (m)

In this section, a sample problem is considered to illustrate the basic features of LLECMOD. For this purpose, a pilot plant scale pulsed column is considered. The dimensions of this column are given in Table 4. Two internal types are installed inside the active part of the column: sieve tray and packing's (Montz-Pak B1-350), the geometrical data of these internals are given in Table 5.

Table 5: Geometrical data of column internals (Garthe, 2006)

Sieve tray	Packing (Montz-Pak B1-350)
diameter of sieve tray $D_{st} = 79$ (mm)	diameter of a packing $D_P = 79$ (mm)
diameter of holes $d_h = 2$ (mm)	volumetric surface area $a_P = 350$ ($m^2.m^{-3}$)
rel. free cross-sectional area $\phi_{st} = 0.20$ ($m^2.m^{-2}$)	void fraction $\phi_P = 0.97$ ($m^3.m^{-3}$)
height of compartment $h_{st} = 100$ (mm)	height of a packing $h_P = 100$ (mm)

The test systems published by the EFCE: water-acetone (solute)-butyl acetate and water-acetone (solute)-toluene are used in the simulations (see Table 3). These systems have wide range of physical properties and thence they permit the prediction of extraction columns for other systems. To completely specify the model, the inlet feed is normally distributed where the mean and standard deviation are dependent upon the test system used in the simulation and on the operating conditions (volumetric flow rate and pulsation intensity).

Table 6: Operating conditions for (w-a-t) chemical test system

Column type	Exp. set	\underline{Q}_c ($l.h^{-1}$)	\underline{Q}_d ($l.h^{-1}$)	$C_{x,in}$ (%)	$C_{y,in}$ (%)	af ($cm.s^{-1}$)
sieve-tray	\underline{Q}_1	40.0	48.0	5.44	0.36	1
	\underline{Q}_3	61.3	74.1	5.52	0.15	
	\underline{Q}_1	40.0	48.0	5.35	0.40	2
	\underline{Q}_3	61.3	74.1	5.45	0.41	
packed	\underline{Q}_1	40.0	48.0	5.73	0.00	1
	\underline{Q}_3	61.3	74.5	5.69	0.00	
	\underline{Q}_1	40.0	48.0	5.84	0.61	2
	\underline{Q}_3	61.3	74.5	5.89	0.60	

The direction of mass transfer is from the continuous to the dispersed phase. The inlet solute concentrations in the continuous and dispersed phases are taken for the water-acetone (solute)-

toluene test system and shown in Table 6, and for the water-acetone (solute)-butyl acetate test system as in Table 7. The pulsation intensities and the volumetric flow rates used in the simulations are given in Tables 6 and 7.

Table 7: Operating conditions for (w-a-b) chemical test system

Column type	Exp. set	$Q_c (l.h^{-1})$	$Q_d (l.h^{-1})$	$C_{x,in} (\%)$	$C_{y,in} (\%)$	$af (cm.s^{-1})$
sieve-tray	Q_1	40.0	48.0	5.17	0.16	1
	Q_2	60.0	72.0	5.46	0.00	
	Q_1	40.0	48.0	5.35	0.00	2
	Q_2	60.0	72.0	5.15	0.00	
packed	Q_1	40.0	48.0	5.22	0.00	1
	Q_2	60.0	72.0	5.1	0.00	
	Q_1	40.0	48.0	5.61	0.00	2
	Q_2	60.0	72.0	5.21	0.00	

The influence of pulsation intensity and volumetric flow rates on the performance of pulsed (sieve plate and packed) extraction columns were investigated.

4.2.1.1. Steady state column hydrodynamics: pulsed sieve plate column

Fig.10 shows the variation of the mean droplet diameter along the pulsed sieve plate column height compared to the experimental data for the chemical system (water-acetone (solute)-toluene) using two different volumetric flow rates as a function of pulsation intensities. In the left panel, the set Q_1 is used, and Q_3 is used in the right panel (see Table 6), from this figure, it is clear that the higher the pulsation intensity the smaller is the droplet diameter. A good agreement between the experimental and simulated profiles is achieved for both cases.

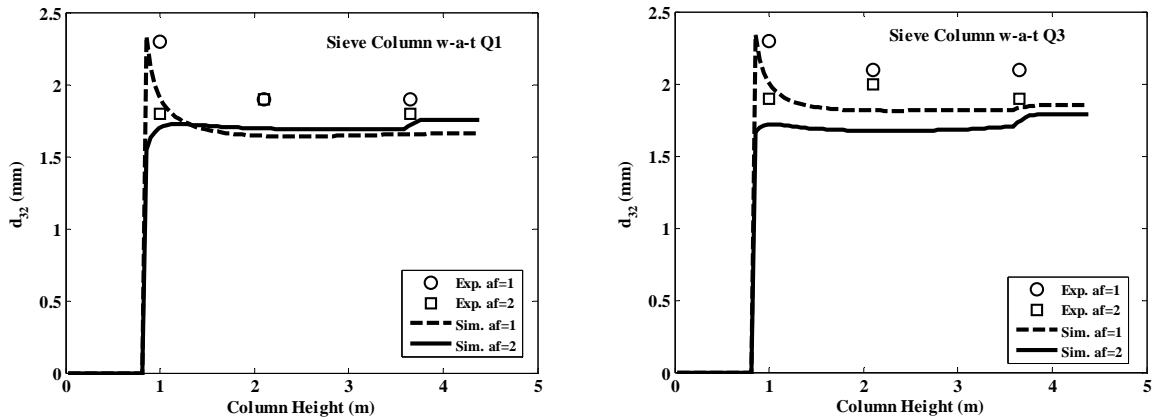


Fig.10. Simulated mean droplet diameter along the pulsed sieve plate column height as a function of pulsation intensity compared to the experimental data (Garthe, 2006) using the test system (w-a-t): in the left panel the volumetric flow rate is Q_1 and Q_3 in the right panel (see Table 6).

According to the definition of the dispersed phase holdup, when the dispersed phase flow rate and the number of dispersed phase droplets increase, the value of holdup will increase. By increasing the continuous phase flow rate, the drag force between the dispersed droplets and continuous phase increases, so the droplets movement will be limited and the residence time and consequently the holdup will increase. Fig.11 depicts the variation of the dispersed phase hold up along the pulsed sieve plate column height and compared to the experimental data of Garthe,

(2006) for the test system water-acetone (solute)-toluene, where by increasing the pulsation intensity the holdup increased. In this figure, the effect of pulsation intensity on the holdup is investigated, where two different flow rates are used in the simulation, Q_1 in the left panel and Q_3 in the right panel. From this figure, the effect of pulsation intensity at higher volumetric flow (Q_3) is less profound than at lower volumetric flow rates (Q_1).

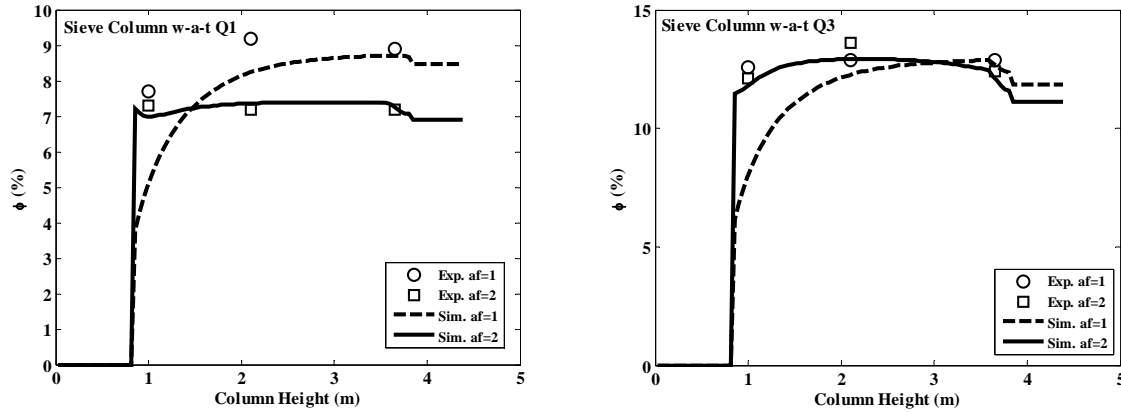


Fig.11. Simulated holdup profiles along the pulsed sieve plate column height as a function of pulsation intensity compared to the experimental data (Garthe, 2006) using the test system (w-a-t): in the left panel the volumetric flow rate is Q_1 and Q_3 in the right panel (see Table 6).

The effect of the dispersed phase flow rate on the performance of the extraction column is found to be not appreciable as shown in Fig.12 (the right panel). Since the pulsation intensities are reasonably high, the effects of flow rates of the two phases on the performance of the extraction column had minor contribution. A comparison between the simulated mean droplet diameter along the pulsed sieve plate column height and the experimental data (Garthe, 2006) is shown in Fig.12. The test system used here is water-acetone (solute)-toluene to show the effect of the volumetric flow rates of both phases under two different pulsation intensities, $af = 1 \text{ cm.s}^{-1}$ in the left panel and $af = 2 \text{ cm.s}^{-1}$ in the right panel. Again, a good agreement is achieved.

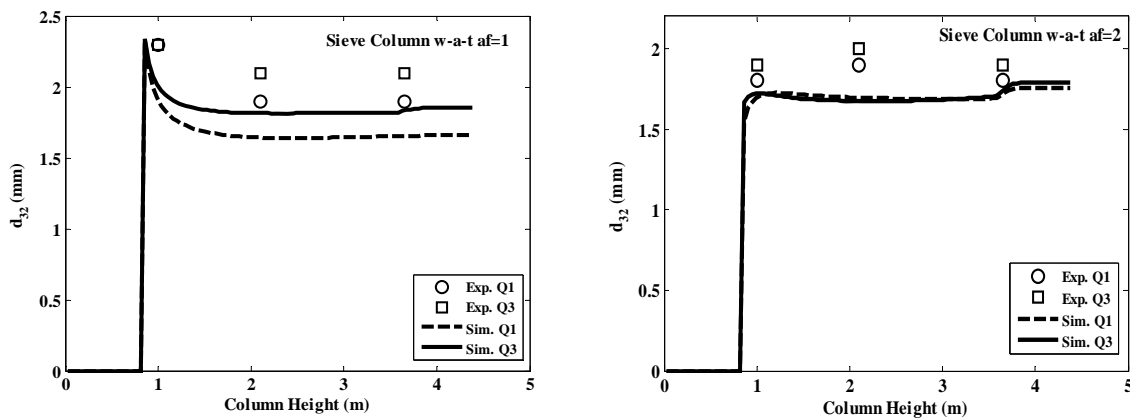


Fig.12. Simulated mean droplet diameter along the pulsed sieve plate column height as a function of volumetric flow rate compared to the experimental data (Garthe, 2006) using the test system (w-a-t): in the left panel the pulsation intensity is 1 and 2 in the right panel (see Table 7).

Fig.13 shows the effect of changing the flow rates on the holdup profiles along the pulsed sieve plate column for the test system water-acetone (solute)-toluene, the simulation are conducting

using two different pulsation intensities: 1 and 2 $cm.s^{-1}$ in the left and right panels respectively. However, a comparison between the experimental and simulated results reveals a good agreement.

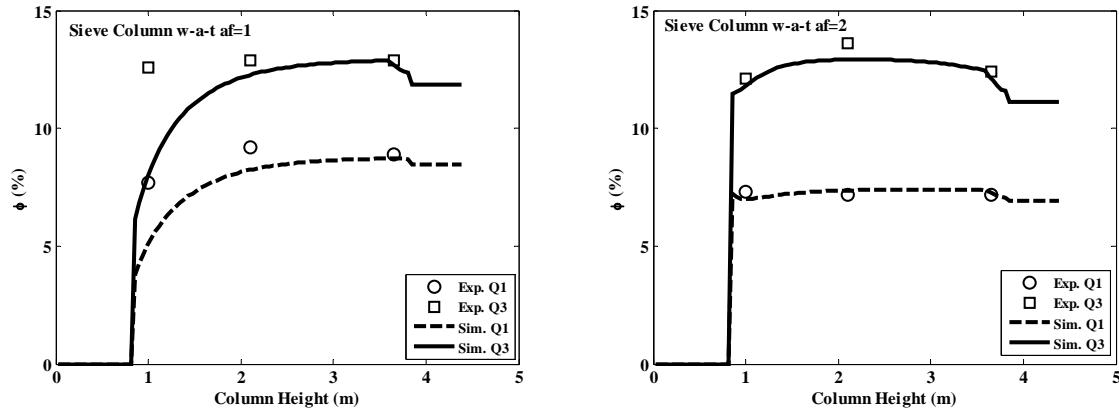


Fig.13. Simulated holdup profiles along the pulsed sieve plate column height as a function of volumetric flow rate compared to the experimental data (Garthe, 2006) using the test system (w-a-t): in the left panel the pulsation intensity is 1 and 2 in the right panel (see Table 7).

4.2.1.2. Steady state column hydrodynamics: pulsed packed column

Fig.14 depicts the variation of the mean droplet diameter along the pulsed packed column height to show the effect of pulsation intensity on the performance of the pulsed packed extraction columns using two different volumetric flow rates. In this figure, the volumetric flow rate used in the left panel is Q_1 , while Q_2 used in the simulation of the right panel (see Table 7). The chemical test system used in the simulation is water-acetone (solute)-butyl acetate; the effect of volumetric flow rates on the variation of mean droplet diameter is minor especially at relative high pulsation intensities. It is clear that the higher pulsation intensity results in smaller droplet diameter.

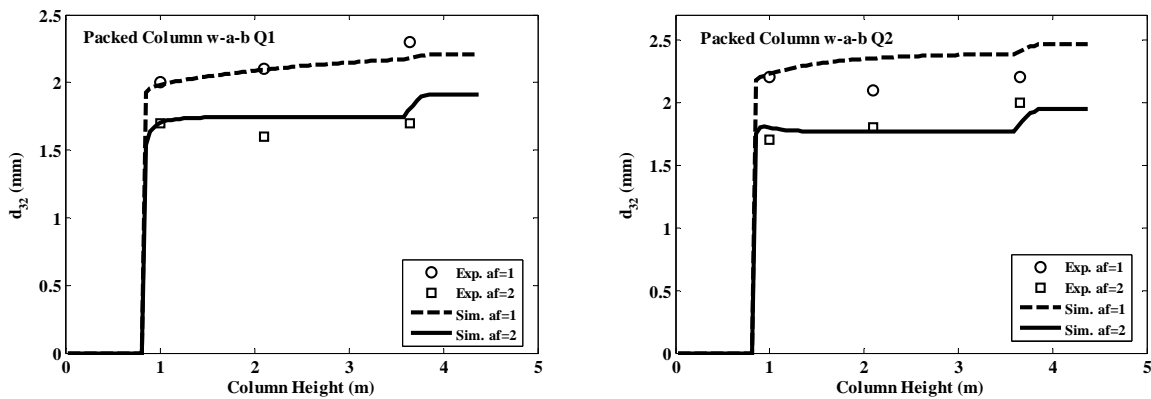


Fig.14. Simulated mean droplet diameter along the pulsed packed column height as a function of pulsation intensity compared to the experimental data (Garthe, 2006) using the test system (w-a-b): in the left panel the volumetric flow rate is Q_1 and Q_2 in the right panel (see Table 7).

As mentioned early, according to the definition of the dispersed phase holdup, when the dispersed phase flow rate and the number of dispersed phase droplets increase, the value of the holdup will increase. By increasing the continuous phase flow rate, the drag force between the dispersed droplets and continuous phase increases, so the droplets movement will be limited and

the residence time and consequently the holdup will increase. Fig.15 depicts the variation of dispersed phase hold up along the pulsed packed column height as compared to the experimental data (Garthe, 2006) for the test system water-acetone (solute)-butyl acetate, where a very good agreement is achieved. This figure shows the effect of pulsation intensity on the holdup, the results for two different flow rates, Q_1 in the left panel and Q_2 in the right panel. From the two panels, as the pulsation intensity increased the droplet diameter decreased and therefore the holdup increased.

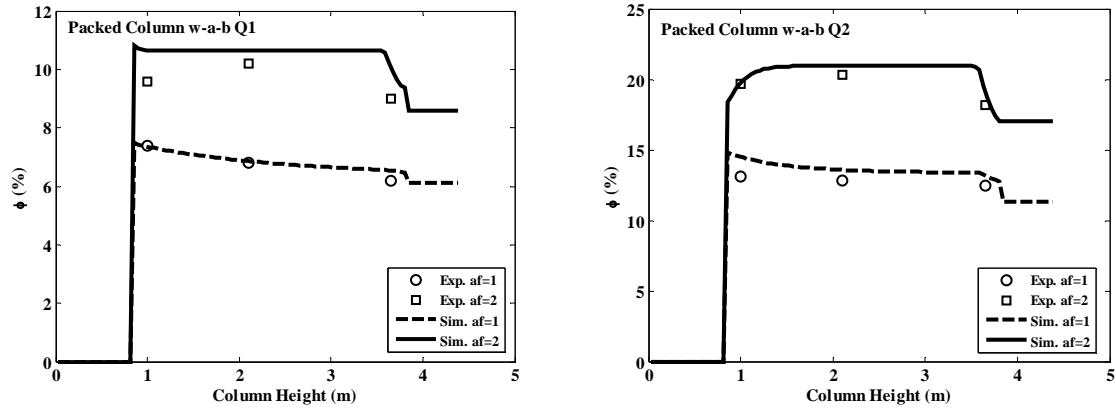


Fig.15. Simulated holdup profiles along the pulsed packed column height as a function of pulsation intensity compared to the experimental data (Garthe, 2006) using the test system (w-a-b): in the left panel the volumetric flow rate is Q_1 and Q_2 in the right panel (see Table 7).

The performance of extraction columns are expected to vary with interfacial tension. To show the effect of interfacial tension on the performance of extraction columns, the test system with low interfacial tension (water-acetone (solute)-butyl acetate) is used in the simulations. It is known that, for higher interfacial tension test systems, the size of droplets is larger than the droplet size in the lower interfacial tension test systems, this results in a decrease in their residence time in the column. Finally, the slip velocities increase and consequently the value of dispersed phase holdup will decrease and the column operates in a more stable manner.

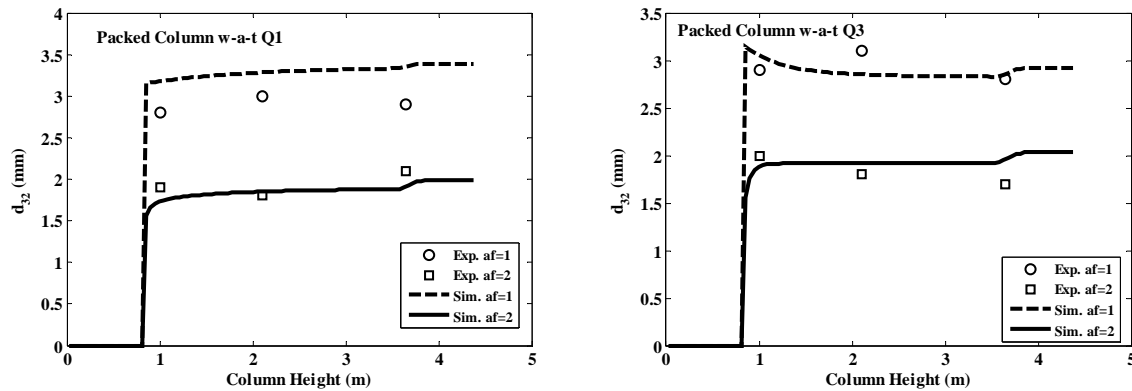


Fig.16. Simulated mean droplet diameter along the pulsed packed column height as a function of pulsation intensity compared to the experimental data (Garthe, 2006) using the test system (w-a-t): in the left panel the volumetric flow rate is Q_1 and Q_3 in the right panel (see Table 6).

According to Figs.14 and 16, it can be concluded that the mean droplet diameter of the water-acetone (solute)-butyl acetate (low interfacial tension) system is smaller than that of the water-acetone (solute)-toluene (high interfacial tension) system due to the interfacial tension effect. At low pulsation intensity, the break-up of droplets is controlled by the ratio of buoyancy and interfacial tension forces (Soltanali and Ziaie-Shirkolaei, 2008; Yadav and Patwardhan, 2008). As can be seen from Figs.14 and 15 compared to Figs.16 and 17 the smaller the droplet diameter the higher is the holdup. Figs.15 and 17 show the variation of the dispersed phase holdup along the pulsed packed column height. Fig.15 shows the simulation for the test system water-acetone (solute)-butyl acetate. In the meanwhile, Fig.17 shows the simulation for the test system water-acetone (solute)-toluene. These figures show the effect of pulsation intensity on the holdup profiles. Two different test systems with different interfacial tensions are used to show the effect of the interfacial tension on the performance of pulsed extraction column.

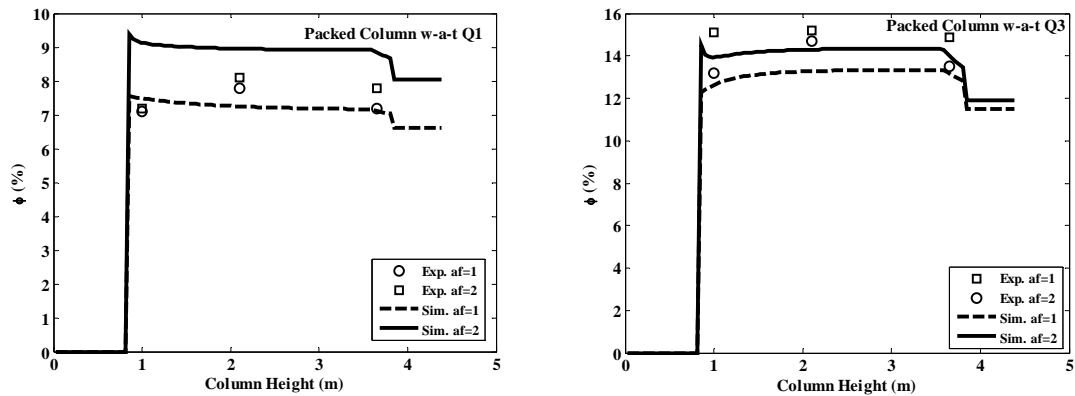


Fig.17. Simulated holdup profiles along the pulsed packed column height as a function of pulsation intensity compared to the experimental data (Garthe, 2006) using the test system (w-a-t): in the left panel the volumetric flow rate is Q_1 and Q_3 in the right panel (see Table 6).

Fig.14 shows the effect of pulsation intensity on the mean droplet diameter along the packed extraction column for the test system water-acetone (solute)-butyl acetate as a function of volumetric flow rates, and to show the effect of interfacial tension. Fig.16 depicts the effect of pulsation intensity on mean droplet diameter along the packed column height for the test system water-acetone (solute)-toluene. A comparison of Figs.14 and 16, reveals that the pulsation intensity has more profound effect on the test system of higher interfacial tension. The effect of pulsation intensity on the Sauter mean diameter is shown in Figs.14 and 16. As it can be seen, the Sauter mean diameter decreases with an increase in the pulsation intensity in the two chemical systems studied. As a conclusion, it is apparent from the simulation results plotted in Figs.14 and 16 that the droplet size decreases with pulsation intensity as well as along the column height.

Fig.18 depicts the variation of mean droplet diameter along the packed column height to show the effect of the volumetric flow rates on the performance of the pulsed extraction columns. In this figure, the test system used in the left panel is water-acetone (solute)-butyl acetate, while the test system water-acetone (solute)-toluene used in the simulation of right panel. From this figure and for both test systems, the effect of volumetric flow rates on the variation of mean droplet diameter is minor especially at relative high pulsation intensities. In conclusion, it is apparent

from the data plotted in Figs.12 and 18 that the changes in feed rates have less effect on the mean droplet diameter, and accordingly on the performance of extraction columns when pulsation is used than with the usual column operation.

Fig.19 shows the variation of holdup profiles along the pulsed packed column height, in left panel of this figure, the simulated and experimental holdup results are compared for the test system water-acetone (solute)-butyl acetate, in the meanwhile the right panel shows the comparison for the test system water-acetone (solute)-toluene, in both cases an excellent agreement are achieved. A comparison between the two panels reveals that, the variation of volumetric flow rates shows more profound effect on the test system with low interfacial tension, where the higher interfacial tension test system is more affected by the pulsation intensity.

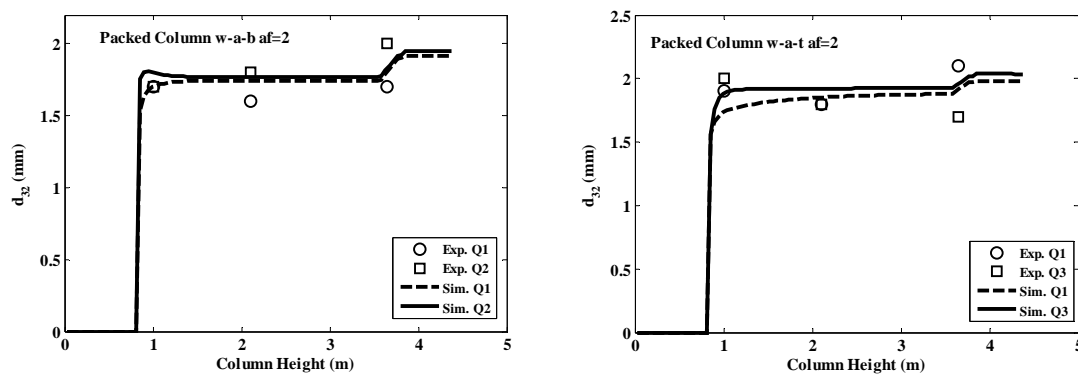


Fig.18. Simulated mean droplet diameter along the pulsed packed column height as a function of volumetric flow rate compared to the experimental data (Garthe, 2006) using different chemical test systems and the same pulsation intensity (see Tables 6 & 7).

The pulsed (packed and sieve plate) columns hydrodynamics (holdup and droplet diameter) is affected by the pulsation intensity and by changing in the flow rates as well. The hydrodynamics behaviour of the dispersed phase against the pulsation intensity is shown in Figs. 11, 15 and 17 (holdup), Figs.10, 14 and 16 (mean droplet diameter). According to this figures, it can be found that droplet mean diameter decreased by increasing the pulsation intensity, and hence the holdup increased. The rise of the pulsation intensity leads to higher shear stress and to intense droplet breaking (smaller droplet). It appears that the number of droplets in the column increases and consequently the values of holdup will increase. The droplet size and the degree of turbulence are dependent on the pulsation intensity, however high pulsation intensities can increase axial mixing and reduce the extraction efficiency. Thus, the pulsation intensity can be used to control the droplet size, dispersed phase holdup and consequently the performance of the extraction columns. The hydrodynamics behaviour of the dispersed phase is varying with interfacial tension. Figs.15 and 17 show the effect of interfacial tension on the dispersed phase holdup, in the meanwhile Figs.14 and 16 show the effect of interfacial tension on the droplet diameter. It is known that, for higher interfacial tension, the size of droplets is larger, thus their residence time in the column will decrease. Finally, the slip velocities increasing and consequently the value of dispersed phase holdup will be decreased and the column operates in a more stable manner. According to Figs.18 and 19, it can be concluded that the holdup of the water-acetone (solute)-toluene system (large droplet size) is lower than the holdup of the water-acetone (solute)-butyl acetate system (small

droplet size) due to interfacial tension. Figs.10, 12, 14, 16 and 18 show the mean droplet diameter profiles at different pulsation intensity, Figs.11, 13, 15, 17 and 19 show the holdup profiles of dispersed phase at different pulsation intensity. The free opening area and flow paths through the plates affect the dependency and magnitude of holdups on pulsation intensity. However, the minimum holdup exists at a certain pulsation intensity that is sometimes called transition frequency at the corresponding amplitude, which is reached faster for perforated plates of small free opening area. Comparing Figs.10, 11, 14, 15, 16 and 17 with Figs.12, 13, 18 and 19 reveals that the effect of changing the two phases flow rates on hydrodynamics behaviour (mean droplet diameter and holdup) is larger than that of changing the pulsation intensities. The hydrodynamics behaviour as a function of the volumetric flow rate is shown in Figs.12, 13, 18 and 19. However, the effect of pulsation intensity on hydrodynamics behaviour is given in Figs.10, 11, 14, 15, 16 and 17.

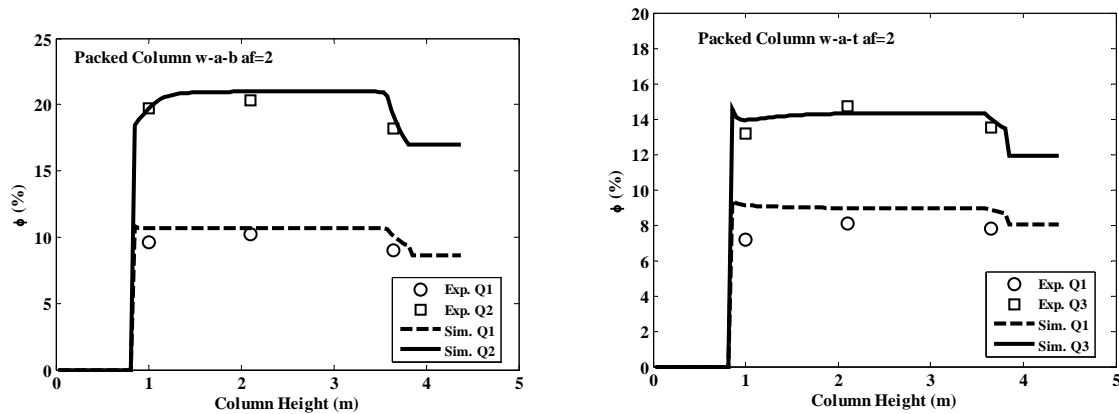


Fig.19. Simulated holdup profiles along the pulsed packed column height as a function of volumetric flow rate compared to the experimental data (Garthe, 2006) using different chemical test systems and the same pulsation intensity (see Tables 6 & 7).

In conclusion, it is apparent from the above results, the test systems with high interfacial tension (water-acetone (solute)-toluene) presented the most significant changes in column performance with the variation of pulsation intensity. In contrast to this, the chemical test system water-acetone (solute)-butyl acetate presented the most significant changes in column performance with the variation of volumetric flow rates.

4.2.1.3. Steady state mass transfer profiles: pulsed (packed and sieve plate) columns

The rate of mass transfer of a solute from one phase to the other in extraction columns depends mainly on the interfacial area between the two phases, the difference in the solute concentration in the two phases, the mass transfer coefficient and the physical properties of the test system.

A series of simulation runs were conducted to determine the best operating conditions and attainable efficiencies for a pulsed extraction column. All the simulation in this work were carried out with mass transfer direction from the continuous phase to the dispersed phase. When the direction of mass transfer is from the continuous phase to the dispersed phase, the solute concentration in the wake of the droplet is larger than that at the top of the droplets; the consequence of the resulting interfacial tension gradient is that the interface moves opposite to

the direction of the inner circulation generated inside the droplet. Therefore, it is expected that the interface deformations due to this mass transfer direction enhance the droplet deformation, that is, the break-up process (Godfrey and Slater, 1994; Bahmanyar et al., 2007). Moreover, during solute transfer from the continuous phase to the dispersed phase, solute equilibrium is quickly established between the droplets and the continuous phase, whereas solute transfer continues over the rest of the droplet surface. This creates an interfacial tension gradient, which opposes the forces causing drainage in the film, thus reducing coalescence. Consequently, the droplet size becomes smaller than that in the case of no mass transfer and the values of holdup become higher and the column operates in a more unstable manner.

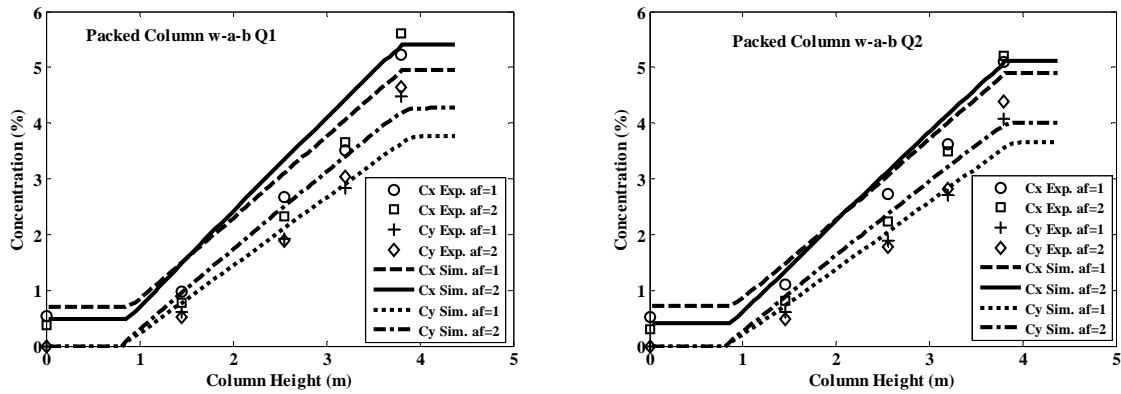


Fig.20. Simulated solute concentration profiles in both phases along the pulsed packed column height as a function of pulsation intensity compared to the experimental data (Garthe, 2006) using the test system (w-a-b): in the left panel the volumetric flow rate is Q_1 and Q_2 in the right panel (see Table 7).

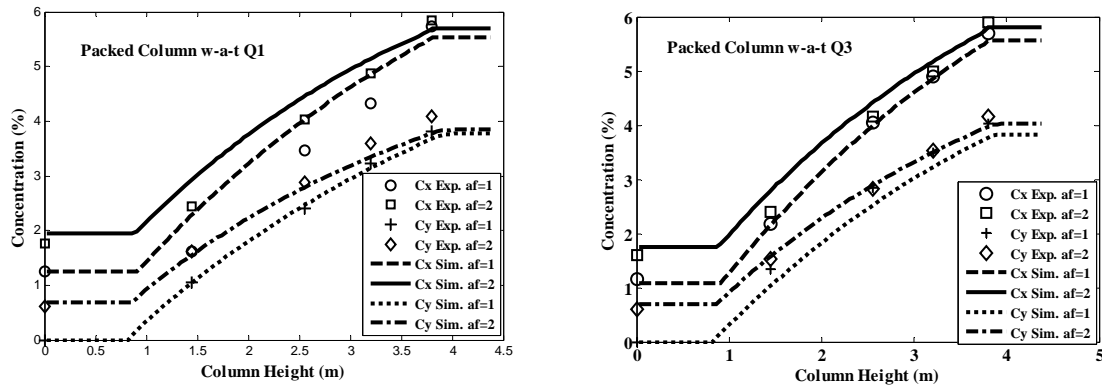


Fig.21. Simulated solute concentration profiles in both phases along the pulsed packed column height as a function of pulsation intensity compared to the experimental data (Garthe, 2006) using the test system (w-a-t): in the left panel the volumetric flow rate is Q_1 and Q_3 in the right panel (see Table 6).

Figs.20 and 21 depict the effect of pulsation intensity on the mass transfer rate. The rise of the pulsation intensity results in intense droplet breaking and consequently the Sauter mean droplet diameter will decrease. A decrease of relative velocity between the dispersed phase and continuous phase results in an increase of the droplets number in the column and consequently the values of holdup will also increase. Therefore, it can be concluded that the value of interfacial area (and consequently mass transfer rate) increases with both effects (Torab-Mostaedi and Safdari, 2009). Both the simulation and experimental data from both systems (especially water-

acetone (solute)-butyl acetate) shows that at high pulsation intensity, increased entrainment and poor extraction efficiency is observed, with the production of fine dispersed droplets. Figs.20 and 21 show the simulated and experimental solute concentration profiles as function of pulsed packed column height in both phases. The simulations are carried out at two different sets of volumetric flow rates.

The effect of pulsation intensity on the mass transfer rate of the water-acetone (solute)-toluene system (high interfacial tension) is larger than that of water-acetone (solute)-butyl acetate (lower interfacial tension), because breakup of the dispersed phase droplets into smaller ones is limited for the latter system due to its lower interfacial tension. Fig.22 shows the simulated and experimental solute concentration profiles as function of the pulsed packed column height in both phases. This figure shows the effect of changing the volumetric flow rates on the mass transfer profiles. The agreement between the simulation and experiment is excellent for both test systems. Fig.23 depicts the simulated and experimental solute concentration profiles in both phases along the pulsed sieve plate column height. This figure shows the effect of changing the volumetric flow rates on the mass transfer profiles. The agreement between the simulation and experiment is good for both test systems.

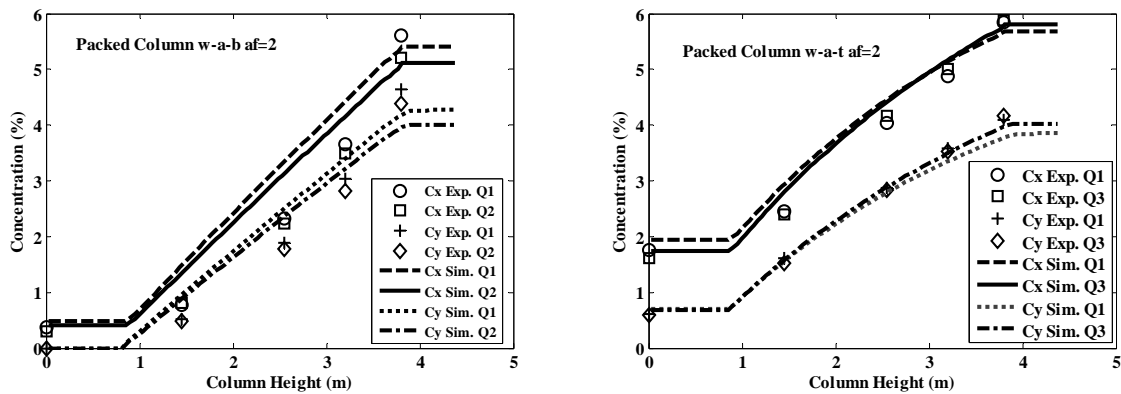


Fig.22. Simulated solute concentration profiles in both phases along the pulsed packed column height as a function of volumetric flow rates compared to the experimental data (Garthe, 2006) using different chemical test systems and the same pulsation intensity (see Tables 6 & 7).

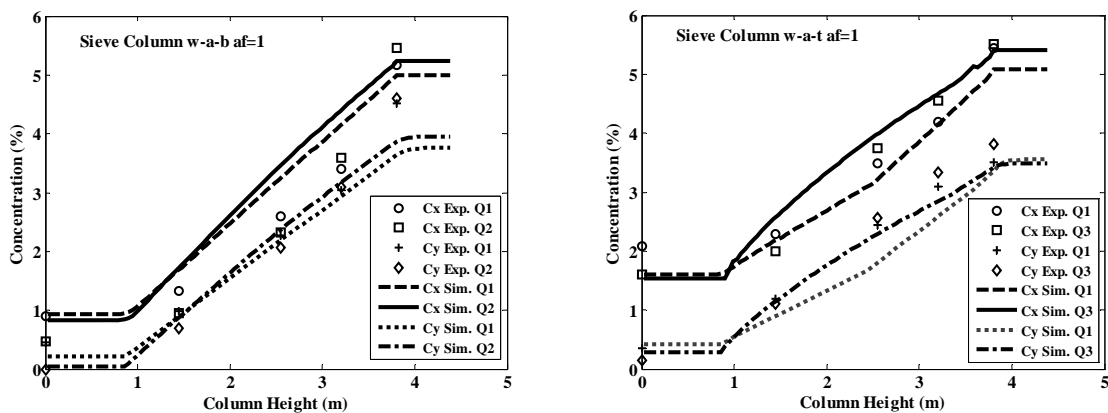


Fig.23. Simulated solute concentration profiles in both phases along the sieve plate column height as a function of volumetric flow rates compared to the experimental data (Garthe, 2006) using different chemical test systems and the same pulsation intensity (see Tables 6 & 7).

In conclusion, there is an optimum pulsation intensity to obtain the best efficiency improvement. These results lead to the conclusion that the best operation of a pulsed (sieve plate and packed) columns is obtained with a combination of high holdup and sufficient turbulence (Chantry et al., 1955; Sanvordenker, 1960). Plates with smaller holes appear best for both effects. Sufficient pulsation intensity must be supplied for turbulence and feed rates must be maintained at a high enough level for sufficient holdup. The column must be operated near the flooding point to have a coalesced dispersed phase layer at each plate.

4.3. Effect of phase dispersion and mass transfer direction

In liquid-liquid contacting equipment, consisting of completely mixed or differential stages (Lo et al., 1983; Godfrey and Slater, 1994; Gerstlauer, 1999; Modes et al., 1999; Attarakih et al., 2008), droplet population balance based-modelling is now being used to describe complex interactions of coupled hydrodynamics and mass transfer. This is due to the nature of the macroscopic dispersed phase interactions (breakage & coalescence) coupled with microscopic ones (diffusional solute transfer) in a continuous turbulent flow field, which result in a population of droplets. This population is distributed not only in the spatial domain of the contacting equipment, but also randomly distributed with respect to the droplet state (properties) such as size, concentration and age (Gerstlauer, 1999; Modes et al., 1999; Attarakih et al., 2008a). In such equipment, the dynamically changing behaviour of the dispersed phase droplets makes it necessary to consider a detailed mathematical rather than lumped modelling approach. In this connection, the population balance equation can be used to improve the column simulation by taking these details into account. The population of droplets constituting the dispersed phase is modelled in terms of a multivariate population balance equation in which the evolution processes such as breakage, coalescence and growth are taken into account. Actually, accurate prediction of the evolved dispersed phase properties depends strongly in proper modelling of these coupled processes. Consequently, the coupled hydrodynamics and mass transfer in agitated liquid-liquid extraction columns are mainly determined by the interactions between the dispersed phase constituents and the continuous phase. For realistic performance predictions, not only the dispersed phase mean properties such as holdup and droplet mean diameter are to be taken into consideration but also the evolution of the droplet size distribution along the column height.

The performance of liquid-liquid extraction columns is well known to be dependent on the mass transfer direction and on the choice of the dispersed phase (light or heavy phase is dispersed). This is one of the most important factors influencing the global efficiency of solvent extraction columns (Saboni et al., 1999). This can be attributed to Marangoni effects caused by surface tension gradients along a droplet surface due to mass transfer (Godfrey and Slater, 1991). The available interfacial area resulting from competition between droplet breakage and inter-droplet coalescence is sensitive to the mass transfer direction and intensity, even in the case of dilute solutions. This is illustrated, for instance, by the profiles of the Sauter mean droplet diameter (d_{32}) along the height of the extraction column (Gourdon, 1989; Gourdon and Casamatta, 1991). It is also known that mass transfer and its direction have a significant effect on the size of droplet swarms. This is attributed to the fact that coalescence and breakage of droplets are markedly affected by the transfer of solute (Johnson and Bliss, 1946; Logsdail and Thornton, 1957;

Groothuis and Zuiderweg, 1960; Madden and Damerell, 1962; Prabhakar et al., 1988; Weiss et al., 1995; Cauwenberg et al., 1997a, 1997b; Garthe, 2006; Schmidt, et al., 2006). Thornton, (1957) and Tung and Luecke, (1986) indicated that the values of the characteristic velocity (when the mass transfer direction is from the dispersed to the continuous phase) were higher, and of course the holdup is lower, than those without mass transfer. This is because the direction of mass transfer affects the droplet size via its droplet coalescence behaviour (Kleczek et al., 1989). As compared with a pure two component system, the mean droplet size increases when the mass transfer direction is from the dispersed to the continuous phase, and it is reduced in the case of reversing the mass transfer direction (Komasawa and Ingham, 1978), indicating that droplet coalescence is dominant in this case. In the case of mass transfer from the continuous to the dispersed phase, coalescence is hindered since film drainage between the droplets is retarded and the mean droplet size is always smaller than that without solute transfer (Marangoni, 1871, 1878; Bapat and Tavlarides, 1985; Bensalem, 1985; Prabhakar et al., 1988; Gourdon, et al., 1994; Cauwenberg et al., 1997a, 1997b).

Kleczek et al., 1989 confirmed that the presence of a solute in the two phase liquid system tends to lower the interfacial tension between the two immiscible liquids, and hence has a profound effect on droplet coalescence. When mass transfer occurs from the continuous to the dispersed phase, the concentration in the draining film between two approaching droplets is lower than that in the surrounding continuous phase. The resulting interfacial tension gradients retard film drainage (and hence coalescence) when the solute transfer is from the continuous to the dispersed phase; while film drainage is enhanced for the case of solute transfer from the dispersed to the continuous phase.

Concerning mass transfer rates, higher values of the mass transfer coefficients were observed during mass transfer from the dispersed to the continuous phase. This is due to the oscillations created by coalescence between interacting droplets, which is enhanced by the Marangoni effect. Huang and Lu, (1999) reported that when the resistance to mass transfer is in the continuous phase, a decrease in inter-droplet distance causes a decrease of the mass transfer coefficient. Whereas, when the resistance to mass transfer is on the dispersed phase, no much variation of the mass transfer coefficient versus inter-droplet distances was found. Kumar and Hartland, (1988) showed that the mass transfer coefficients depend on the mass transfer direction (this is in turn affected by the inter-droplet coalescence), which for a given system is only dependent on the interfacial conditions and agitation intensity.

To investigate the effect of the dispersed phase inlet and the direction of mass transfer on the performance of an RDC extraction column, LLECMOD was used to perform this task. In this version of LLECMOD the options for changing the inlet of dispersed phase and the direction of mass transfer were added [IX, Jaradat et al., 2010a]. Three chemical systems are used in the present work: The first one is a mixture of n-heptane plus benzene (light phase) and sulpholane (heavy phase) whose physical properties are shown in Table 8. The second and third ones are the standard test systems, water-acetone (solute)-toluene and water-acetone (solute)-butyl acetate. The column operating conditions are shown in Table 9 and the external and internal column geometries are shown in Fig.1. LLECMOD was extensively used to simulate the coupled

hydrodynamics and mass transfer using different types of agitated columns (Steinmetz et al., 2005; Schmidt et al., 2006; Attarakih et al., 2008a); [IX, Jaradat et al., 2010a]. Based on single droplet and small laboratory experiments, droplet breakage and coalescence functions were obtained from the experimental data using different column geometries. The predictions of the program were found satisfactory in most of the simulated cases. In this section, LLECMOD is further validated against available experimental data (Wolschner, 1980; Garthe, 2006) with respect to the effect of mass transfer direction and dispersion type [IX, Jaradat et al., 2010a]. The RDC column diameter used for this validation is 0.1 m with a total height of 1.3 m. The dispersed and continuous phase's inlets are 0.2 and 1.2 m respectively. The column operating conditions for both mass transfer directions are shown in Table 10. It is worthwhile to mention here that the equilibrium surface tension of the chemical system (water-acetone (solute)-toluene) is available in LLECMOD as an empirical correlation (Gerstlauer, 1999). With this the effect of interfacial tension on droplet breakage probability can be taken into account, which is profoundly affected by the mass transfer direction (Schmidt et al., 2006).

Table 8: Physical and chemical properties of the chemical systems used in simulation.

Physical property	Unit	Test system					
		n-Heptane + Benzene mixture	Sulpholane	Toluene	Water	Butyl Acetate	Water
Density	kg/m^3	800	1266	863.3	992.0	877.5	990.9
Viscosity	$10^{-3} kg/m.s$	0.8	6.0	0.566	1.134	0.709	1.163
Interfacial tension	N/m	0.033		0.02441		0.01096	

All the simulations using LLECMOD were run until steady state conditions (with respect to mass transfer) were reached. First, the effect of the dispersed phase inlet (which phase to be dispersed: light or heavy phase) on the column hydrodynamics (flow variables) is investigated. Fig.24 shows the effect of the dispersed phase inlet on the mean droplet size and the average dispersed phase holdup along the column height (the phases inlets are clear from the jump discontinuities in these profiles).

Table 9: Typical operating conditions of an RDC extraction column.

RDC	Continuous top	Dispersed top
Continuous phase volumetric flow rate	100 l/h	25 l/h
Dispersed phase volumetric flow rate	25 l/h	100 l/h
Mass transfer direction	c \rightarrow d	d \rightarrow c
Solute concentration in the continuous phase	100 kg/m^3	0 kg/m^3
Solute concentration in the dispersed phase	0 kg/m^3	100 kg/m^3

First, the effect of dispersed phase inlet is studied by neglecting droplet breakage and coalescence. It is well known that the droplet terminal velocity is inversely proportional to the

continuous phase density and viscosity (Godfrey and Slater, 1994). It seems that the droplet terminal velocity is more affected by the continuous phase viscosity when compared to the dispersion of the light phase, which results in a lower terminal droplet velocity. However, the holdup is slightly higher than that when the light phase is dispersed (see Fig.25). This is because the flow rate of the dispersed phase (heavy phase) is four times larger than that of the continuous phase (see Table 9).

Since droplet breakage and coalescence are neglected, the mean droplet diameter is approximately independent of the dispersed phase inlet because the inlet feed distribution is the same in both cases. When droplet breakage and coalescence are taken into account the predicted mean droplet diameters are slightly higher in the case of dispersing the light phase (dispersed phase inlet is at the bottom) as can be seen from Figs.24 and 25. This can be explained by referring to the breakage probability function given by Eqs.(46-49). It is clear that the breakage probability is proportional to the continuous phase density. This results in more droplet breakage by the heavy continuous phase, which results in a slightly higher dispersed phase holdup as can be seen from Fig.25. By referring to Figs.24 and 25, the effect of mass transfer direction on the column hydrodynamics is negligible. This is because the interfacial tension (which is a critical physical property effecting droplet breakage as indicated by Eq.(46-49)) was assumed constant due to the lack of experimental data. On the other hand, the effect of the dispersed phase (type) inlet on the solute concentration profiles is found quite significant as can be seen from Fig.26.

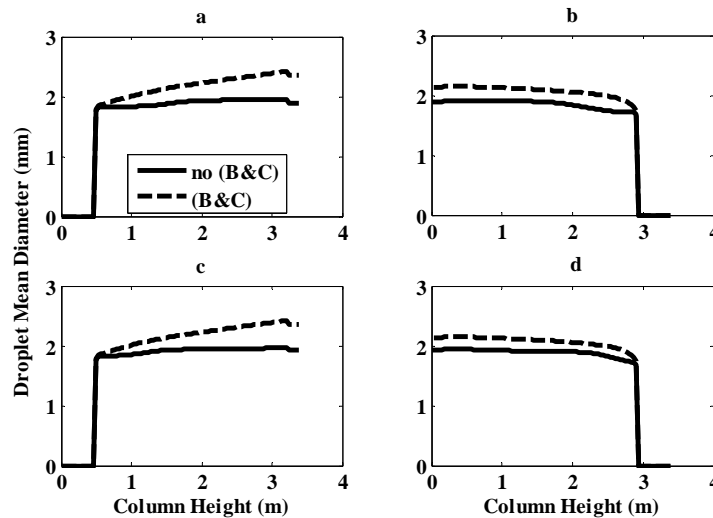


Fig.24. Droplet mean diameter along column height without and with droplet breakage and coalescence (B&C). Mass transfer direction: a- From heavy to light (dispersed). b- From heavy (dispersed) to light. c- From light (dispersed) to heavy. d- From light to heavy (dispersed) phase.

By considering the direction of mass transfer from the continuous phase to the dispersed phase, the effect of the dispersed phase inlet (at top or bottom of the column) on the solute concentration profiles is investigated as can be seen in Fig.26a and Fig.26d. It is evident that when the heavy phase is dispersed, the steady state solute removal from the heavy phase is improved when the mass transfer direction is from the continuous phase to the dispersed phase. This is clear by the reduction of the column height required for solute removal (Fig.26d) due to the decrease in the

mean droplet diameter as can be seen in Fig.24d when compared to Fig.24a. Since the mass transfer flux is inversely proportional to the mean droplet diameter, this increase in the extractor performance is expected. However, when the direction of mass transfer is from the dispersed phase to the continuous phase, the performance of the extraction column is improved by dispersing the heavy phase (see Fig.26b & Fig.26c). This is in fact agrees with the reduced mean droplet diameter as can be seen by comparing Fig.24b & Fig.24c. It is worthwhile to stress again that the Marangoni effects were not modelled in this example since the interfacial tension was kept constant. So, further discussion on the effect of mass transfer direction as reported by many researchers (Shen et al., 1985; Venkatanarasaiah and Varma, 1988; Weiss et al., 1995) could not be considered in this case.

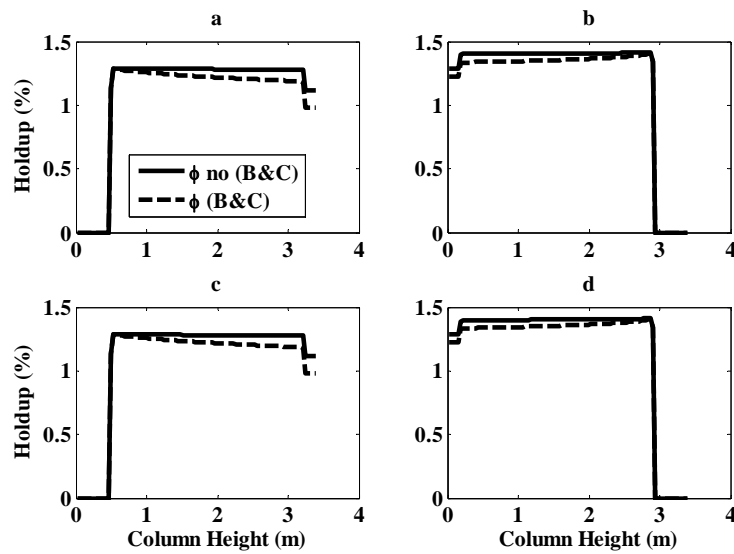


Fig.25. Dispersed phase hold up with and without droplet breakage and coalescence (B&C): a to d are the same as those in Fig.24.

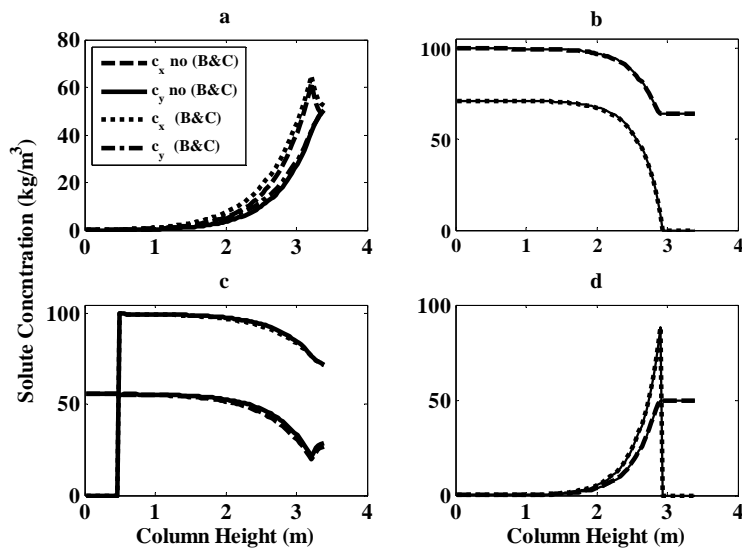


Fig.26. Solute concentrations in the light and heavy phases with and without droplet breakage and coalescence (B&C): a to d are the same as those in Fig.24.

To clarify the effect of the interfacial tension on the column performance (due to the dependency of droplet breakage and coalescence on interfacial tension), two chemical systems: water-acetone (solute)-toluene (high interfacial tension) and water-acetone (solute)-butyl acetate (low interfacial tension) are chosen for which the equilibrium interfacial tension are available as a function of solute concentration (Misek, 1978, 1985; Gerstlauer, 1999). The other physical properties of this system are shown in Table 9. The LLECMOD program predicts the effect of mass transfer direction on the column hydrodynamics by providing an interfacial tension correlation as function of solute concentration along the column height (Schmidt et al., 2006) as shown in Figs.27 and 28 (a & b).

Fig.27 shows the effect of the mass transfer direction on the simulated holdup profiles along the column height when the light phase is dispersed. In this figure two aforementioned chemical systems with low (water-acetone (solute)-butyl acetate) and high (water-acetone (solute)-toluene) interfacial tension are simulated. The results show that mean dispersed phase holdup is higher when the direction of mass transfer is from the continuous phase to the dispersed phase. This is due to the droplet breakage probability given by Eq.(46-49), which increases by a decreasing the system interfacial tension resulting in higher breakage probability. This fact is reflected by the decrease of the mean droplet diameter (especially along the upper part of the column where the rate of mass transfer is high) as can be seen in Fig.28. Actually, this result agrees qualitatively with the experimental findings of Komasaawa and Ingham, (1978); and Weiss et al., (1995). It should be noticed in this example that droplet coalescence is dominant at this low rotational speed (100 rpm).

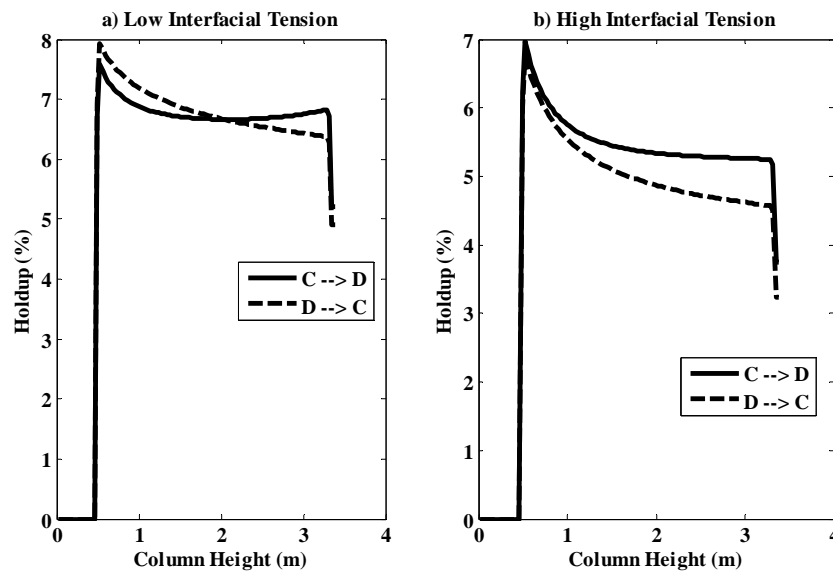


Fig.27. Influence of mass transfer direction on the dispersed phase holdup. The continuous and dispersed phase flow rates are 200 and 100 l/h respectively and the rotor speed is 100 rpm. a: the chemical test system is water-acetone-butyl acetate (low interfacial tension). b: the chemical test system is water-acetone-toluene (high interfacial tension).

The simulation results shown in Figs.27 & 28 (a & b) are carried out when the interfacial tension of both chemical systems (water-acetone (solute)-toluene and water-acetone (solute)-butyl acetate) is function of solute concentration. The models for droplet breakage probability and

coalescence frequency are given by Eqs.(47) and (53) respectively. The continuous and dispersed phase flow rates are 200 and 100 l/h respectively and the rotor speed is 100 rpm.

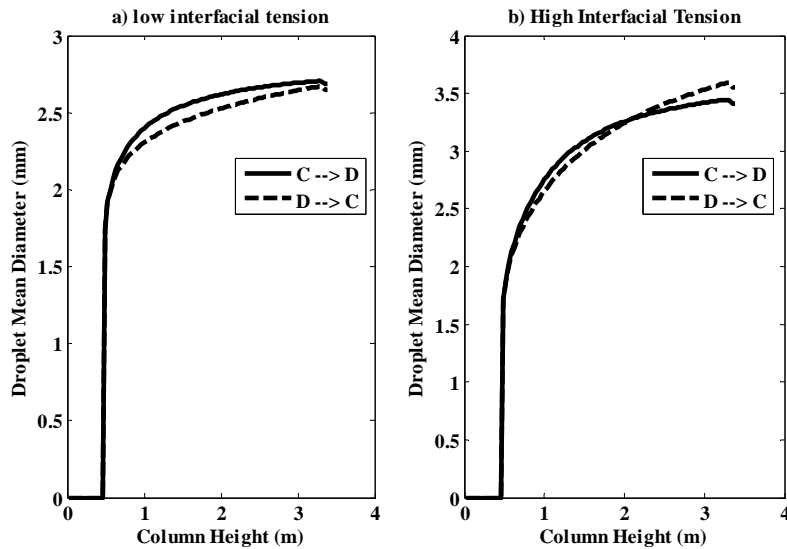


Fig.28. Influence of mass transfer direction on droplet diameter. The continuous and dispersed phase flow rates are 200 and 100 l/h respectively and the rotor speed is 100 rpm. a: the chemical test system is water-acetone-butyl acetate (low interfacial tension). b: the chemical test system is water-acetone-toluene (high interfacial tension).

To validate the population balance model for an RDC column, steady state experimental data were compiled from the literature (Wolschner, 1980; Garthe, 2006). Fig.29 compares the simulated dispersed phase (toluene) holdup to the experimental data when the direction of mass transfer is from the continuous to the dispersed phase, while Fig.30 shows the effect of droplet breakage and coalescence on the simulated mean droplet diameter. It is clear that the error increases by neglecting droplet breakage and coalescence. The relative error was less than 15% which is a good achievement when compared to the many and often conflicting correlations in the literature (Kumar and Hartland, 1986, 1988, 1994).

Table 10: Column operating conditions used to compare the experimental and simulated results taking into account different mass transfer directions (Garthe, 2006; Wolschner, 1980).

RDC 100 mm	d → c, exp.	c → d, exp.
Continuous phase volumetric flow rate	50 l/h	60 l/h
Dispersed phase volumetric flow rate	25 l/hr	60 l/h
Dispersion coefficient in the continuous phase	0.000155 m/sec ²	0.000155 m/sec ²
Dispersion coefficient in the dispersed phase	0.0006520 m/sec ²	0.0006520 m/sec ²
Solute concentration in the continuous phase	0.0 %	6.0 %
Solute concentration in the dispersed phase	5.5 %	0.0 %
Rotor speed	17 l/sec	11 l/sec

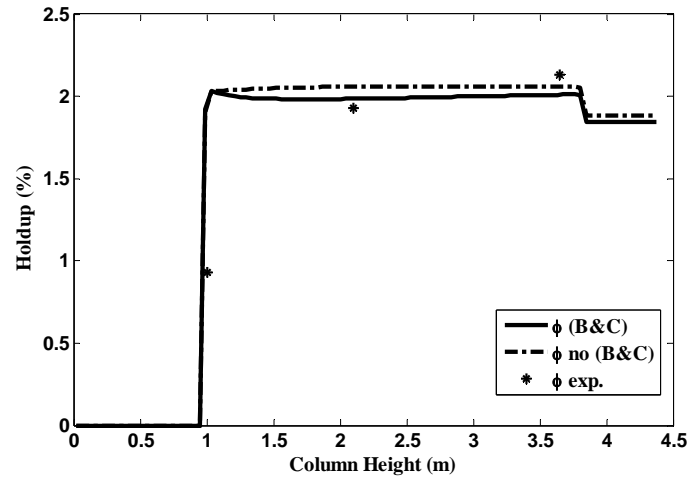


Fig.29. Simulated and experimental (Garthe, 2006) dispersed phase hold up as function of column height. Mass transfer direction from continuous to dispersed.

The effect of mass transfer direction on the simulated and experimental solute concentration profiles is depicted in Figs.31 and 32. As can be seen from Fig.31, LLECMOD predictions of the solute profiles is in good agreement with experimental data when the mass transfer direction is from the dispersed to the continuous phase (Wolschner, 1980). Similarly, the experimental data of Garthe, (2006) were compared to LLECMOD simulations when the mass transfer direction is from the continuous to the dispersed phases as depicted in Fig.32. Note that the mean properties of the dispersed phase are always less accurate than that of the continuous one as observed by Attarakih et al., (2008) and Schmidt et al., (2006). This may be attributed to the difficulty in measurement of the dispersed phase properties. Anyhow, the error in the predicted solute concentration profiles is less than 10 percent. It should be mentioned at this point that the column performance is better when the mass transfer direction is from the continuous to the dispersed phase. This is in agreement to the published literature since droplet breakage is enhanced leading to an increase in the interfacial area available for mass transfer (Groothuis and Zuiderweg, 1960).

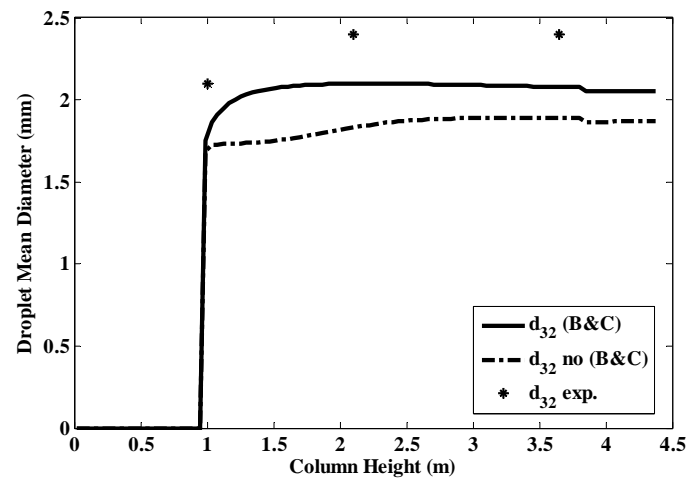


Fig.30. Simulated and experimental (Garthe, 2006) mean droplet diameter as function of column height. Mass transfer from continuous to dispersed.

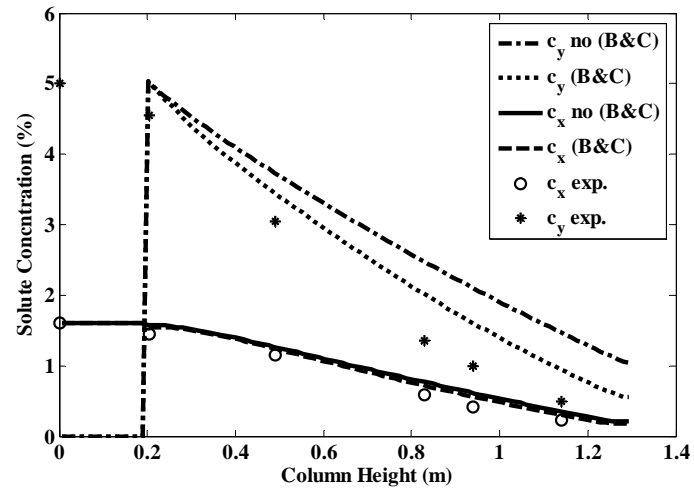


Fig.31. Simulated and experimental (Wolschner, 1980) solute concentration profiles as function of the column height. Mass transfer from dispersed to continuous.

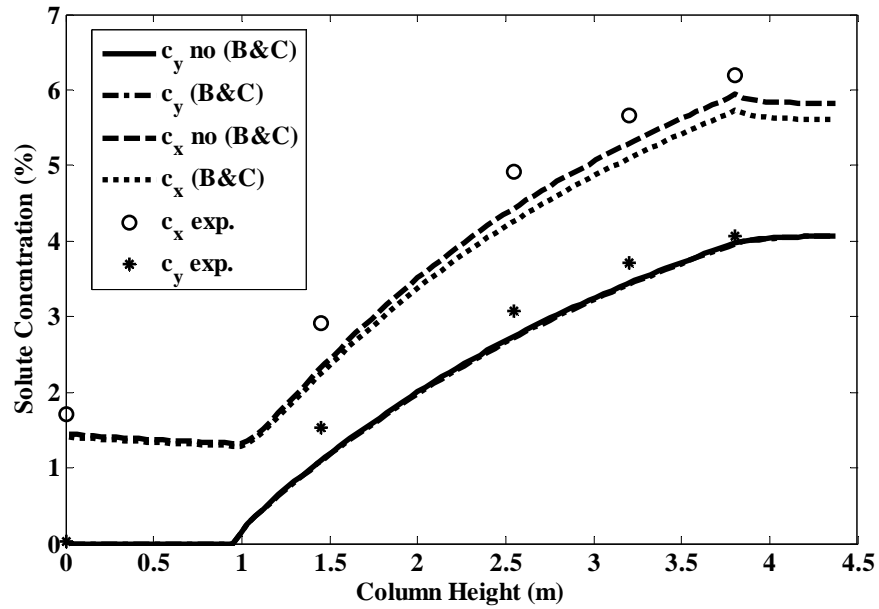


Fig.32. Simulated and experimental (Garthe, 2006) solute concentration profiles as function of the column height. Mass transfer from continuous to dispersed.

5. DYNAMIC MODELLING AND SIMULATION OF EXTRACTION COLUMNS

Liquid-liquid extraction plays an important role in separation processes that received a wide industrial application in many fields of engineering such as food, hydrometallurgical, nuclear and pharmaceutical industries (Bart, 2001; Lo et al., 1983). Nevertheless, the design and control of extraction columns is tedious and is still based on laboratory scale pilot plant experiments and depends on scale up methods which are time consuming and expensive (Bart et al., 2008; Drumm, 2010).

The extraction process presents a strongly non-linear behaviour and time-varying dynamics, particularly when the operation is approaching the flooding point at which the column operates at its highest efficiency (Bonnet and Jeffreys, 1985; Camurdan et al., 1991). Accordingly, a great attention has been emerged to focus on the modelling, simulation, and control of liquid-liquid extraction columns (Hufnagl et al., 1991; Zamponi, 1996; Weinstein et al., 1998; Mjalli et al., 2005); [I; II; XVIII, Jaradat et al., 2012a, 2012b, Attarakih et al., 2008b]. This was also elicited by the unavoidableness needs to understand the process behaviour under start up, shut down, and stable operation of the column (Weinstein et al., 1998; Mjalli, 2007; Gomes et al., 2009). However, reviewing the modelling literature reveals strong simplification by severe assumptions that limit their application to only very limited cases of the process range of operation (Mjalli, 2007); [I; II; XVIII, Jaradat et al., 2012a, 2012b, Attarakih et al., 2008b].

Better understanding of the dynamic behaviour of liquid-liquid extraction columns can be gained taking into account the droplet behaviour (Oliveira et. al., 2008) in the design of process control strategy or the start-up and shutdown procedures (Hufnagl et al., 1991; Weinstein et al., 1998; Mjalli, 2005; Xiaojin et al., 2005; Attarakih et al., 2008c); [I; II; XVIII, Jaradat et al., 2012a, 2012b, Attarakih et al., 2008b]. Droplet population balances consider the macroscopic (droplet breakage and coalescence) dispersed phase interactions as well as the microscopic interphase mass transfer occurring in the continuously turbulent flow field result in a distributed population of droplets. This population is distributed not only in the spatial domain of the contacting equipment, but also randomly distributed with respect to the droplet internal properties such as size and concentration (Ramkrishna, 2000; Attarakih et al., 2006b).

For optimal control of liquid-liquid extraction columns it is necessary to take into account the strong coupling between hydrodynamics and mass transfer phenomena occurring in the column (Chouai et al., 2000). Robust rigours mathematical models are required to predict effectively the influence of process variable changes in extraction columns and simulate the dynamic behaviour of the equipment [I; II; XVIII, Jaradat et al., 2012a, 2012b, Attarakih et al., 2008b]. These models are very important in the determination of the length of time required to reach steady state after a process disturbance occurs, the development of transfer functions for process control loops, and the simulation of interrelated processes which include extraction columns in a dynamic computer control system (Biery and Boylan, 1963). Therefore, the main objective of this work is to develop

a reduced mathematical model based on the bivariate population balance equation that is capable of describing the dynamic behaviour of liquid-liquid extraction columns.

The spatially distributed bivariate population balance equation (SDBPBE) has emerged as a powerful tool for extraction column modelling (Ramkrishna, 2000; Attarakih et al., 2006a); [I-X, Jaradat et al., 2012a, 2012b, 2012c, 2012d, 2011a, 2011b, 2011c, 2011d, 2010a, 2010b]. These transport equations range from integro-partial differential to integro-differential equations with no general analytical solutions (Attarakih et al., 2006b). The general form of the PBM is too complex and it is not feasible to use it for dynamic and online control purposes. To reduce the complexity of these models without losing the dynamic information, the concept of the primary and secondary particle method [XVI, Attarakih et al., 2009b] is utilized to reduce the bivariate population balance model to a self-contained dynamic one. In this work the concept of primary particles and secondary particle (PSPM) is used (Attarakih et al., 2009a); [I; II; IV; X, Jaradat et al., 2012a, 2012b, 2012d, 2010b].

5.1. Dynamic behaviour of stirred extraction column

In this work, a Kühni pilot plant liquid-liquid extraction column is considered. The technical specifications of this column are given in Table 11. The chemical test system water-acetone (solute)-toluene is used, which is recommended by the EFCE. The physical properties of this system are given in Table 3. The effect of varying (positive and negative step changes) the rotor speed (*rpm*), volumetric flow rates and the solute concentrations on the holdup, droplet size distribution and concentration profile also has been investigated to illuminate particular aspects in the column response to these step changes from steady state conditions given in Table 12.

Table 11. Kühni column geometry (Zamponi, 1996)

Column active height	2.520 m
Column diameter	0.15 m
Rotor diameter	0.085 m
Height of compartment	0.070 m
Number of compartments	36
Relative free opening area	27%

Table 12. Operating conditions

	Q_1	Q_2	Q_3
Continuous phase flow rate (<i>l/h</i>)	112.5	125.0	137.5
Dispersed phase flow rate (<i>l/h</i>)	144.0	160.0	176.0
Solute concentration in the continuous phase (%)	0.00	5.00	0.00
Solute concentration in the dispersed phase (%)		0.00	
Rotor speed (min^{-1})		160.0	
Total Load ($m^3.m^{-2}.h^{-1}$)	14.4	16.0	17.6
Phase ratio		0.78	

The experimental data from literature (Gomes et al., 2009; Gomes et al., 2005; Zamponi, 1996) were used for validation. In the experimental work of Zamponi, 1996 and Gomes et al., 2005, 2009 the same Kühni pilot plant column geometry (see Fig.33) is used to conduct the dynamic

experimental study. Here (see Fig.33) the holdup was measured using a non-invasive ultrasonic technique, where as a photoelectric technique was used to measure the droplet size and for the concentration profiles in both phases a special probes as described by Hufnagl, (1991) and finally density transducers were used to monitors the densities.

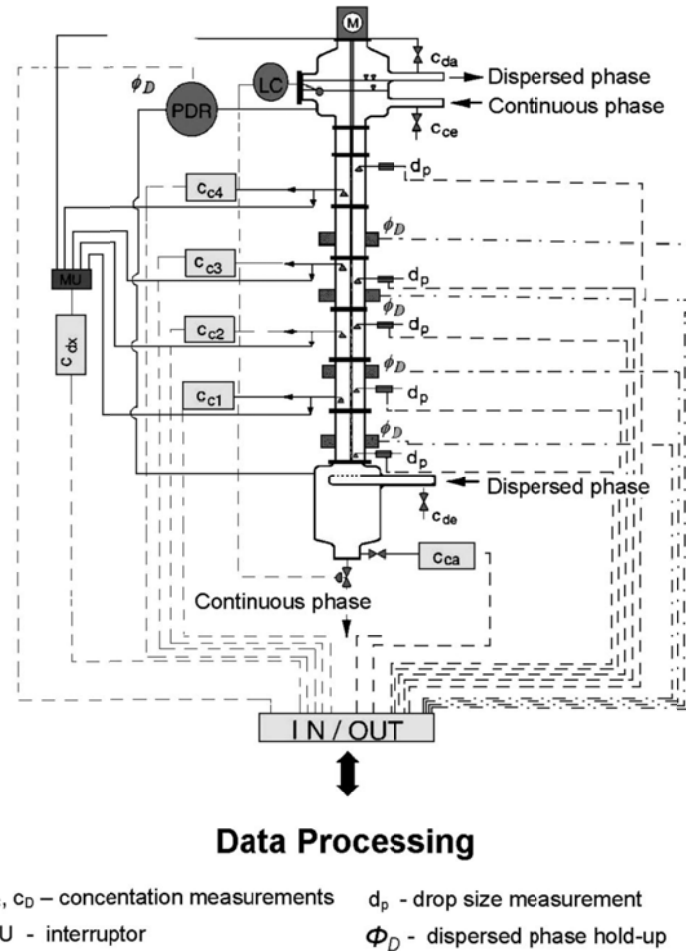


Fig.33. Scheme of the Kühni column with its measurement equipment (Gomes et al., 2009)

5.1.1. Dynamic behaviour due to a disturbance in the flow rate of both phases

Fig.34 shows the dynamic response of solute concentration in the raffinate at different positions along the column height due to a positive step change in the continuous phase flow rate (Q_c) by +20% (see Table 12). The step change is occurred at $t = 0$ s, the change is from $Q_c = 125$ to 150 $l.h^{-1}$. The experimental (Zamponi, 1996) and the simulation results along the column height are according to the measuring points as in Fig.33. Both in the experiment (Zamponi, 1996) and in the simulation, the concentration profiles indicate that the solute concentration is increased in the raffinate with increasing the simulation time. Since the disturbances in Q_c affects abruptly the entire column, no dead time can be observed at the individual measuring points due to the incompressibility of the flow of this phase. This is also true for the continuous phase outlet, since the extraction rate decreased along the extractor height. Conversely, near the feed point of the

continuous phase ($C_{c,5}$) the change in the concentration is the lowest since the inlet (feed) continuous phase concentration has not changed. At the outlet of the continuous phase ($C_{c,1}$), the mixing effect results in a significant reduction of the disturbance effect at the lower part of the column. In addition, after such disturbance the extractor is still in a favourable operating condition, so that the outlet concentration attained the continuous raffinate and increases only moderately. However, the mixing effect at the lower part of the separator is reproduced correctly by the model. Finally at steady state, after about 6000 s, a new concentration profile has generated corresponding to the disturbance. The disturbance in Q_c affects only slightly the holdup profile, so that the presentation of holdup results is dispensed.

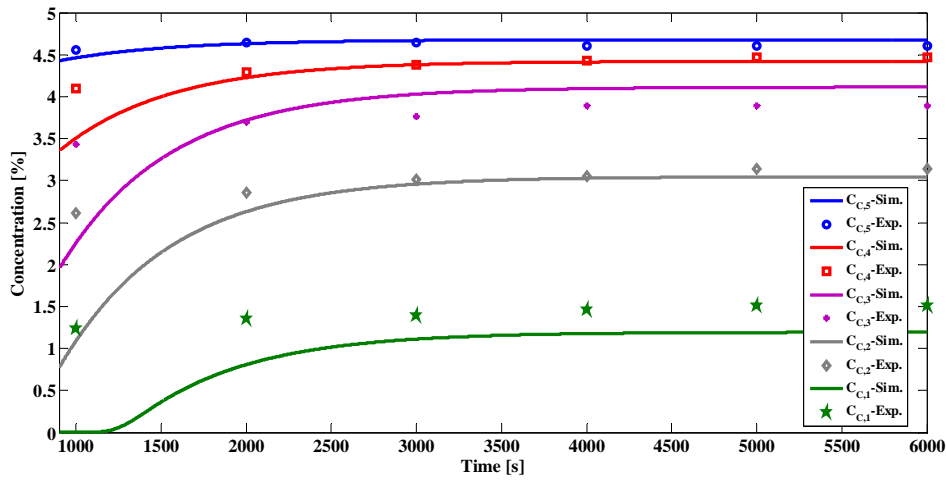


Fig.34. Simulated and experimental (Zamponi, 1996) transient solute concentration in the continuous phase due to a positive step change in Q_c

After a disturbance in Q_c by -20% (negative step change), see Fig.35, the transient behaviour of the extractor is analogous to the behaviour in the case of positive disturbance. The simulation of this figure carried out under the Q_2 operating conditions (see Table 12). The step change is occurred at $t = 0$ s, the change is from $Q_c = 125$ to 100 l.h^{-1} . Thus Fig.35 shows the corresponding results to proof the good reproducibility of the model. The negative disturbance by -20% in Q_c (Fig.35) leads to lower the flow rate and as compared to the results in Fig.34 the column has a slightly slower dynamics. The model predictions are moderately accurate, since the calculated concentration profiles are slightly below the measured values.

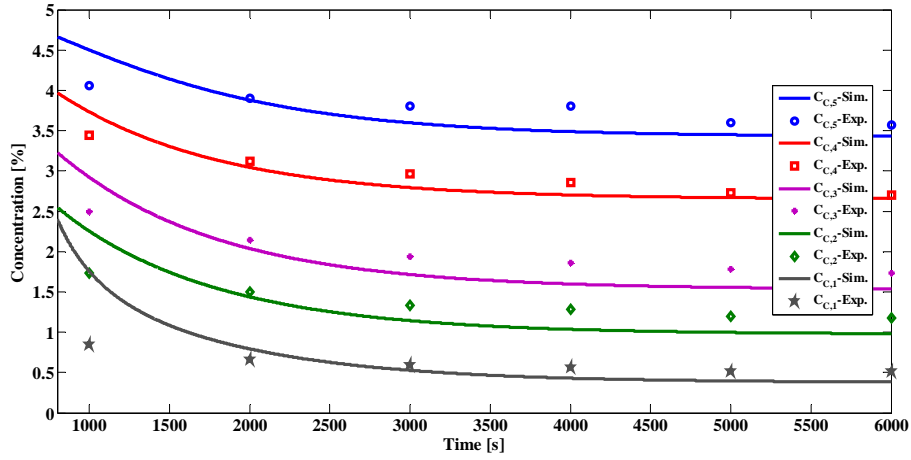


Fig.35. Simulated and experimental (Zamponi, 1996) transient solute concentration in the continuous phase due to a negative step change in Q_c

Fig.36 presents the dynamic evolution of the holdup profiles due to a negative step change in the dispersed phase flow rate (Q_d). The simulation results were compared to the experimental one (Gomes et al., 2009) with a good agreement. Notice that the dispersed phase holdup is decreased by decreasing Q_d , due to the presence of a lower amount of dispersed phase. The simulation and the experiment were carried out under the following operating conditions: $Q_C = 125 \text{ l.h}^{-1}$, $\text{rpm} = 140 \text{ min}^{-1}$ without mass transfer. The negative step change in Q_d is from 208 to 112 l.h^{-1} after 1000 s.

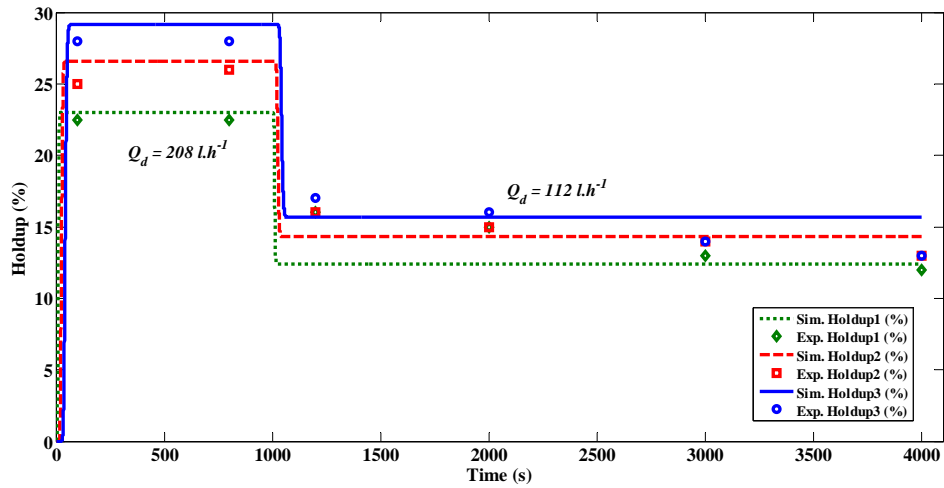


Fig.36. Simulated dynamic holdup profiles compared to the experimental one (Gomes et al., 2009) due to a negative step change in Q_d

Fig.37 depicts the simulated and the experimental (Zamponi, 1996) dynamic holdup profile after an abrupt disturbance on Q_d (combined step change). The simulation of this figure carried out under the Q_2 operating conditions, however, without mass transfer (see Table 12). At $t = 200 \text{ s}$ a positive step change in Q_d is from 160 to 190 l.h^{-1} , and at $t = 1100 \text{ s}$ followed by a negative step change from $Q_d = 190$ to 160 l.h^{-1} prior to final negative step change from $Q_d = 160$ to 130 l.h^{-1} at $t = 1900 \text{ s}$. The response of the holdup profile after the first disturbance shows a dead time, which

increases with increasing the distance from the measuring point of the disturbance's consignment. The dispersed phase flow behaviour causes an increase in the dead time of the system response. Contrary to the continuous phase, the flow of the dispersed phase is determined through the rising velocity of the individual droplets. Once they enter the column and leave the dispersed phase distributor, the droplets move through the column according to their individual condition and depending on the surrounding environment. As a consequence, the response to an increase in Q_d , which occurs at the lower end of the column just above the distributor, is delayed at the upper section of the column. The variation of the individual droplets rise velocities leads to different residence times and with higher residence time the effect of the disturbance is smearing out. The abrupt nature of the imposed disturbance is superimposed more and more from the mixing behaviour of the column.

From holdup evolution in Fig.37 it can be observed that at the measuring points that are far away from the disturbance consignment (Holdup 3), the system response is delayed (lag time) and become slower (sluggish), the holdup increases more slowly, and that the holdup significantly sets later on to a new steady state value. The reason for both phenomena is the proportion of small dispersed droplets that has the small size distribution. Smaller droplets flow significantly slower through the extractor and lead to increase the holdup gradually at the top of the column. In addition, the proportion of small droplets increases further with the flow through the column height due to the redispersion in each stirred cells, so that the above mentioned effects are amplified further in the extractor. The complex hydrodynamics behaviour of the dispersed phase, results in increasing the dead time, increasing the smearing of the stepped profile and decreasing the gradient that is resulting in new steady state profiles. However, the model is able to reproduce all of these phenomena correctly. After 1100 s, Q_d throttled back to its nominal value at 160 l.h^{-1} , so that after about 300 s the holdup profile sets back to the initial operating point. Also after this disturbance in the operating conditions the same effects are observed, which is explained by the same as the first disturbance effects. The model reflects the experimental behaviour well again. After a total test time of 1900 s of operation, the extractor is disturbed through reducing Q_d by -20% compared to the operating point. The last procedure causes a transient response, which is very similar to the response due to the disturbance at 1100 s. basically, it should be noted that the extraction column responds to a variation in Q_d much more sensitive to a change in Q_c . This is, as stated, due to the complex flow behaviour of the droplet swarm.

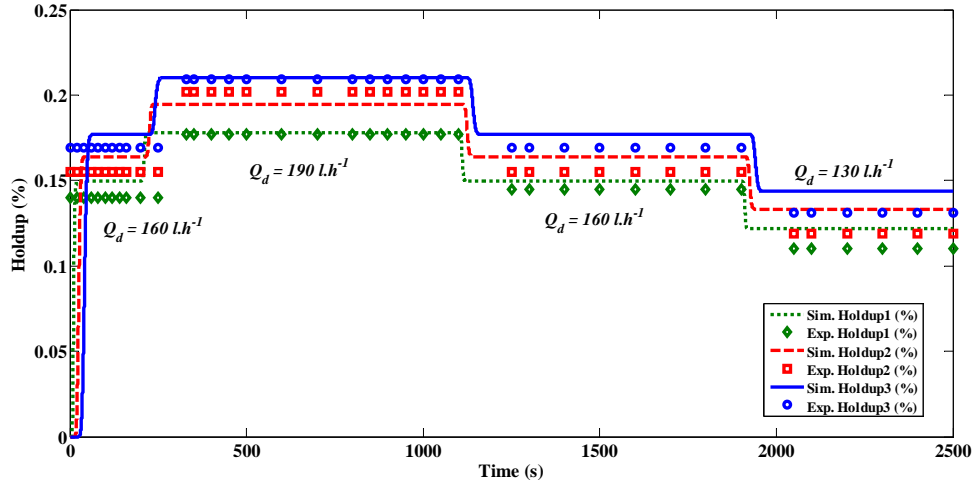


Fig.37. Simulated dynamic holdup evolution compared to the experimental one (Zamponi, 1996) due to a combined (positive and negative) step change in Q_d

The simulated and experimental (Zamponi, 1996) dynamic evolution of solute concentration in the raffinate due to a positive step change in Q_d is depicted in Fig.38. The simulation of this figure is carried out under the Q_2 operating conditions (see Table 12). At $t = 0$ s a positive step change is occurred from $Q_d = 160$ to 190 l.h^{-1} . By increasing Q_d the mass transfer rate increases accordingly. In the column, this leads to a decrease in acetone concentration in the continuous phase (raffinate) in all measuring points. The disturbance shifts the solute (acetone) concentration profiles in the middle of the column at the greatest, while they decrease out at the extractor end. At the upper end of column, the inlet of the continuous phase (constant inlet concentration) prevents any significant change in the continuous phase concentration at the measuring point $C_{c,5}$. At the lower end of the column the continuous phase, which is leaving already before the disturbance is nearly in balance with the incoming dispersed solvent, so that the concentration $C_{c,1}$ is changed only slightly. It is noticeable that with all measuring points, except at the raffinate concentration outlet, approximately the same dead time is observed. However, the dynamic concentration profile does not exhibit this behaviour. This apparent contradiction can be explained with the regulatory approach of the hydrodynamics of the extractor, which is explained in detail in section 4.4. Due to the sudden increased of Q_d , which occurs at the lower end of the extractor, the phase interface rises up at the top of the column. Consequently, the phase interface controller restricts the incoming continuous phase flow rate at the top of the extractor, so that shortly after the disturbance the dispersed phase ratio is shifted and increased not only by increasing the flow of solvent, but also through the controller caused by reducing Q_c . Thus, the disturbance is amplified with respect to the phase ratio. This two-fold intervention, affected the hydrodynamics along the extractor height, manifest their effects increases rapidly throughout the column height, and the dead time is the same on the entire column. After about 5000 s in the extractor a new steady state concentration profile is obtained. In comparison with the experimental results (Zamponi, 1996) the model reflects well the real column behaviour and the effects of the corresponding control approach.

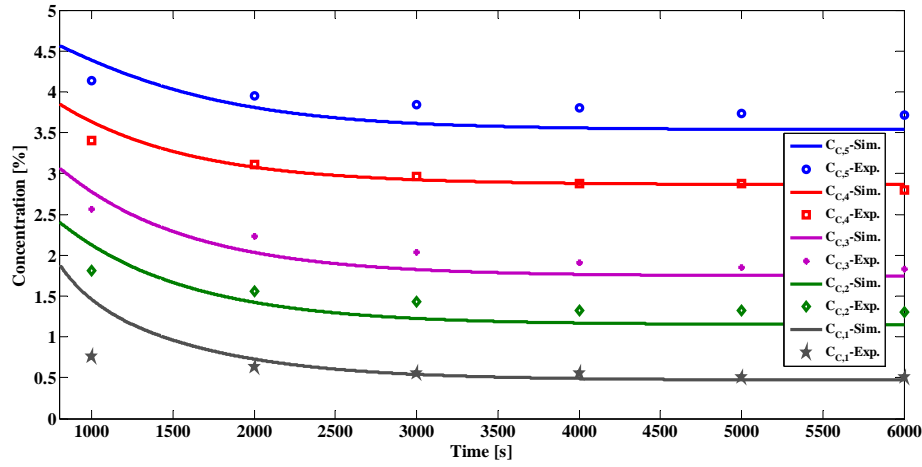


Fig.38. Simulated and experimental (Zamponi, 1996) transient solute concentration in the continuous phase (raffinate) due to a positive step change in Q_d

Fig.39 presents the dynamic behaviour of the holdup profile in the column due to a combined (positive and negative) step changes in the total load. The simulation of this figure carried out under the Q_2 operating conditions, but without mass transfer (see Table 12). At $t = 200$ s a positive step change in the total throughput is from 16 to $17.6 \text{ m}^3 \cdot \text{m}^{-2} \cdot \text{h}^{-1}$, and at $t = 1500$ s a negative step change in the total throughput is from 17.6 to $16 \text{ m}^3 \cdot \text{m}^{-2} \cdot \text{h}^{-1}$ followed by another negative step change in the total throughput from 16 to $14.4 \text{ m}^3 \cdot \text{m}^{-2} \cdot \text{h}^{-1}$ at $t = 1900$ s.

Starting from steady state after 200 s, the total throughput increases of both phases by $+10\%$. However, the holdup profile is increased after an increase in the dispersed phase flow only (see Fig.37). Notice that the holdup gradient is increased; particularly at the upper measurement points somewhat it is the largest. Such disturbance leads to a sudden increase in Q_c throughout the column, as discussed in section 4.1. The reason for this behaviour is that whilst there is an increase in Q_d an increase in Q_c is occurred. This in turn results in a greater residence time of the dispersed phase. The simultaneous increase of Q_d causes a further increase in the holdup. After 1500 s the total throughput of the column is brought back again to the value of the operating point, and after 2700 s, the total throughput is throttled by -10% . After the first load reduction the extractor attempting to return back to its original state (starting point) can be clearly seen. The response of the hydrodynamics in the column after a reduction in the total throughput shows the same pattern after an increase of the total load. The model is able to reproduce correctly the column transient hydrodynamics behaviour due to a combined (negative and positive) step change in the total load (throughput), where the model dynamic simulation agree well to the corresponding experimental results (Zamponi, 1996). The simulation results show that the holdup response in comparison to the experimental data (Zamponi, 1996) is slightly less sensitive to load changes. Nevertheless, the mass transfer takes place in the extractor does not show any significant response to the tested load changes.

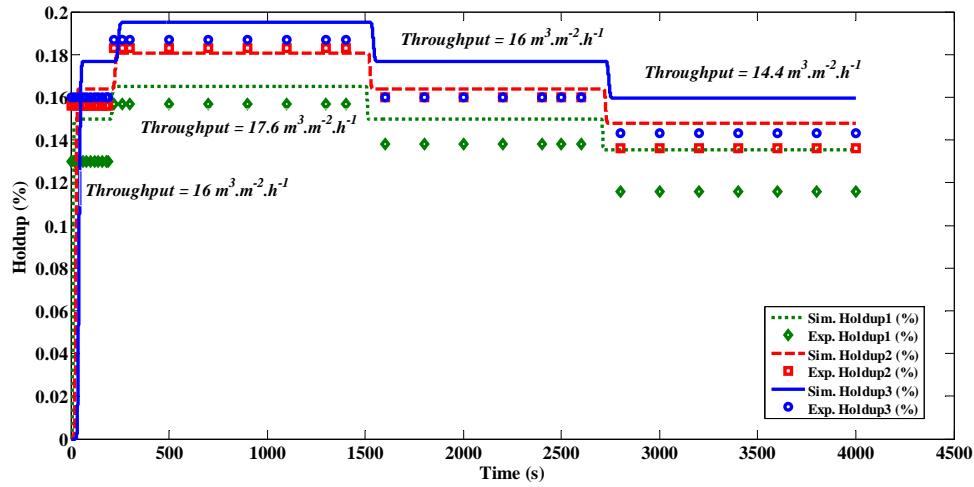


Fig.39. Simulated dynamic holdup evolution compared to the experimental one (Zamponi, 1996) due to a combined (positive and negative) step change in the total throughput

5.1.2. Column dynamic behaviour due to the variation in the rotor speed

Fig.40 shows the comparison between the simulated and experimental (Gomes et al., 2009) holdup profiles at different positions along the column height due to a negative step change in rpm from 170 to 140 min^{-1} after 1500 s . The simulation carried out under the following conditions: $Q_c = 94$ & $Q_d = 120 \text{ l.h}^{-1}$, $C_{c,in} = 5.7$ & $C_{d,in} = 0.0 \%$. It is noticeable that, after such negative disturbance in rpm , the droplet volume fraction of the larger droplets increases mainly at the upper section of the column, where a droplet population of smaller sized droplets is predominant. The interpretation of this phenomena is due to the greater increase of the coalescence to breakage frequency ratio where the holdup is higher, the presence of solute results in an increase in smaller droplets, but mainly at the upper part of the column (Gomes et al., 2009), that is after a sufficiently long residence time of the droplets within the agitated flow field. Contradictory, with $rpm = 140 \text{ min}^{-1}$ the solute's presence results in an increase in the larger droplets, due to the relatively higher coalescence frequencies, the presence of the solute lower the interfacial tension values, which leads to a greater deformability of the colliding droplets (Gomes et al., 2009).

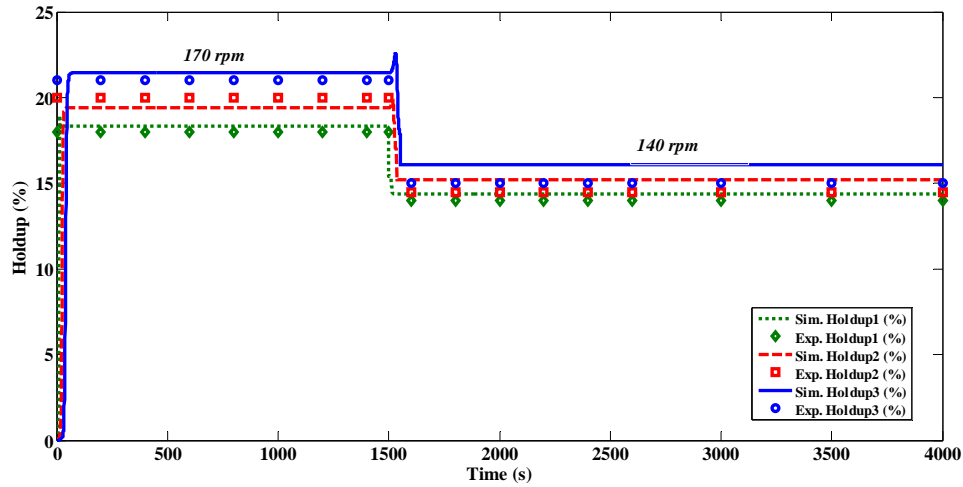


Fig.40. Simulated dynamic holdup profiles compared to the experimental one (Gomes et al., 2009) due to a negative step change in rpm

Fig.41 depicts the holdup dynamic behaviour at the lower (bottom) and the upper (top) measuring points (see Fig.33) due to a combined (positive and negative) step change in the stirrer speed. The simulation of this figure carried out under the Q_2 operating conditions, but without mass transfer (see Table 12). The step changes are occurred at $t = 800\text{ s}$ from $rpm = 160$ to 190 min^{-1} , at $t = 4600\text{ s}$ from $rpm = 190$ to 160 min^{-1} and $t = 5700\text{ s}$ from $rpm = 160$ to 130 min^{-1} . On the basis of Fig.41, the Kühni column hydrodynamics response is clearly sensitive to the changes in the energy input. This also means that the stirrer speed is a suitable control variable of the hydrodynamic behaviour for the purpose of extraction column control. After 800 s from the steady state operation the stirrer speed is increased by +20%. The dead time in the holdup response in the column in each stirred cell is the same, because the agitator speed of all stirred cells is changed simultaneously. However, again in Fig.41 the holdup at the highest measuring point adjusted significantly later to an approximately constant value. The small droplets are increased by increasing the energy input. As discussed in detail in section 4.2, they have a slower flow through the extractor, and this results in a gradually increase in the holdup especially in the column's upper part.

The proportion of small droplets increases steadily due to the high stirrer speed. Again, this process is clear especially at the top of the extractor, since the number of small droplets increases with the flow through each stirred cell, and thus this effect is accumulative and is visible mainly at the top measuring point. In this case, the column already is in a critical state, since these small droplets leave the column hardly, preferring to accumulate in the upper region of the column. This provides a steady and very slow increase of the volume fraction of dispersed phase, which would result in flooding of the column (Zamponi, 1996). The simulated transient holdup response due to an increase in the stirrer speed matches the experimental results (Zamponi, 1996) well again. Also the simulation shows a significantly delay in holdup response that is increases at the top of the column. Further increases in rpm causes an increase in the holdup, furthermore; the velocity of the droplets swarm will decrease therefore continuously.

After returning the stirrer speed to its nominal value of 160 min^{-1} , after a time period of 4600 s, the holdup value remains slightly high at the top measuring point in comparison to the initial steady state value. The reason for this observation is the existence of this very small droplets, which hardly coalesce or been slowly transported out of the active portion of the column. This explains the significant difference between simulation and experimental results (Zamponi, 1996) concerning the upper column holdup in the corresponding time frame. Only with a further decrease of the energy input by -20% below the standard value of the operating point, after 5700 s, the smallest droplet can be reduced through increasing the droplet-droplet coalescence. In addition, the lower energy input resulted of a short residence time of the droplet because the toroidal flow around the stirrer is less pronounced. However, the calculated holdup decreases in the experiment significantly slower than in the simulation, implying that the droplet-droplet coalescence is the time-determining step in this complex process is not described sufficiently precise (Zamponi, 1996).

The continuous phase inlet flow rate illustrates the control strategy of the extractor. Through entering this stream the height of the interface maintained constant at the top of the column. By increasing the stirrer speed, the droplet diameter decrease, which leads to reduce the droplets rise velocity with a lower Q_d and leads to an increase in the holdup. To compensate for the higher content of dispersed phase, the residence time of the incoming continuous phase is decreased. When the stirrer speed is reduced, the control of the interfacial level responds contrary. With the larger droplets diameter the flow rate of dispersed phase leaving the column is increased, the holdup is decreased, and the controller compensates for this disturbance by increasing the continuous phase inlet flow rate. However, it can be seen clear that the control procedure of the extractor and its impact on the dynamic behaviour of the column are reproduced from the model.

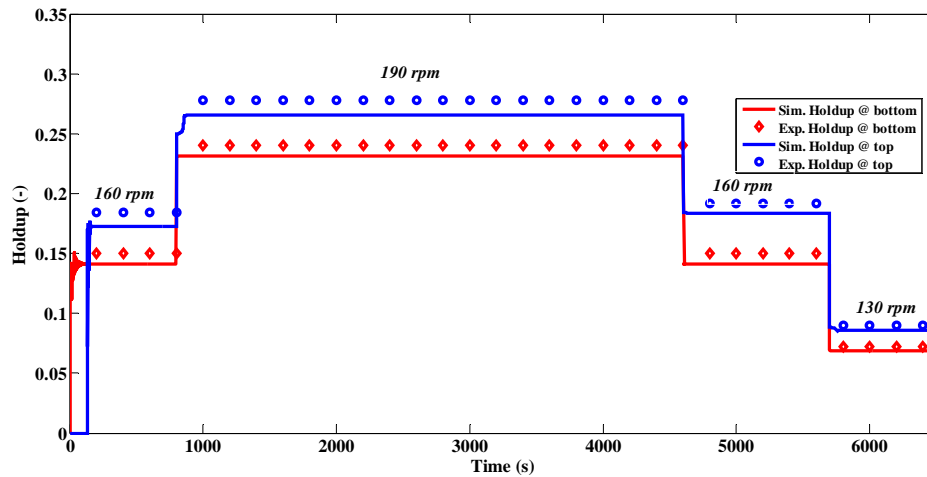


Fig.41. Simulated dynamic holdup evolution compared to the experimental (Zamponi, 1996) one due to a combined (positive and negative) step change in *rpm*

5.1.3. Dynamic behaviour due to a disturbance in both phases inlet concentrations

Changing the inlet concentration in the feed or in the solvent are the most common practice in the disturbances. They act primarily on the mass transfer efficiency in the extractor, also lead to a

change in the physical properties, which in turn affects the flow behaviour of the extractor, especially the droplets breakage, coalescence or dispersion. In the following the dynamic concentration profile after an abrupt increase in the continuous phase inlet concentration ($C_{c,in}$) of 5.0 % to 7.0 % is discussed. Fig.42 gives the simulation and experimental results (Zamponi, 1996) of the dynamic profiles of acetone concentration in the continuous phase at the four measuring points along the active part of the extractor and again in the raffinate outlet. The simulation of this figure carried out under the Q_2 operating conditions (see Table 12). The step change is occurred at $t = 0$ s, the change is from $C_{c,in} = 5.0$ to 7.0 %. With increasing the distance from the feed point of the disturbance the dead time increases in the concentration profile, while the disturbance decreases in the acetone concentration. The latter effect is caused by the mixing effect of the continuous phase which is subjected to flow through the extractor. Furthermore, increasing the concentration of acetone in the raffinate leads to an increase in mass transfer rate. It is clear that the delay and mixing effects in the column are reproduced also by the model. These results demonstrate the usefulness of the dynamic model.

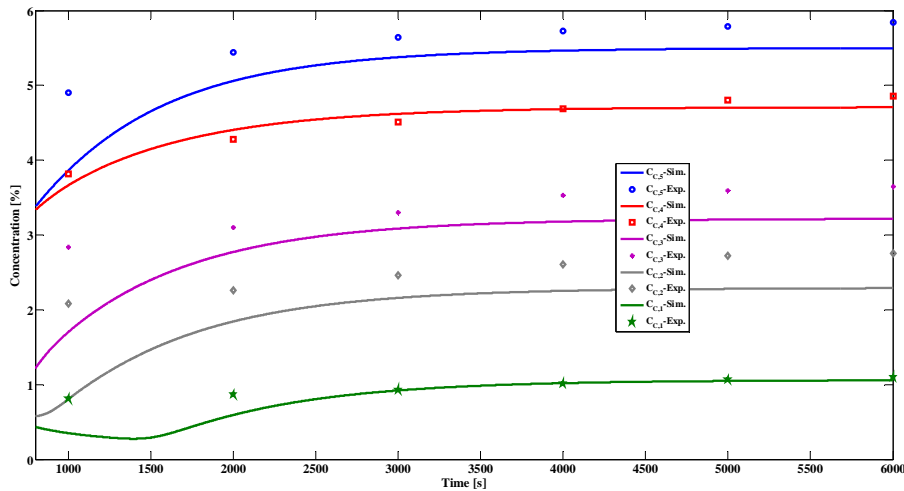


Fig.42. Simulated and experimental (Zamponi, 1996) transient solute concentration in the continuous phase due to a positive step change in $C_{c,in}$

Fig.43 depicts the simulated and experimental (Zamponi, 1996) dynamic concentration profile in the continuous phase after a positive step change in the dispersed phase inlet concentration ($C_{d,in}$) from 0.0 to 1.0 %. The simulation of this figure carried out under the Q_2 operating conditions (see Table 12). The step change is occurred at $t = 0$ s, the change is from $C_{d,in} = 0.00$ to 1.0 %. It is noticeable in this case that not only the internal concentration profile in the extractor is shifted. Rather, the disturbance in the concentration is the largest at the raffinate outlet, which is the feed point of the disturbance. After the massive disturbance in $C_{d,in}$ that is occurring in the lower part of the column the corresponding solute equilibrium concentration is shifted. As a consequence, the raffinate leaving the extractor is significantly higher loaded with acetone than before the disturbance. The increase in the continuous phase outlet concentration is predominantly at the lower part of the column, which causes the response to delay (dead time) with increasing the column height. At a greater distance from the feed point of the dispersed phase a reduction of the

disturbance influence is seen as is expected. The dispersed phase in this area of the extractor is in contact with the continuous phase, which still comprises a relatively high acetone concentration. Accordingly, there is slower response. In the upper section of the extractor the influence of the incoming continuous phase dominates, which maintains the concentration profile even after disturbance. A change in the dispersed phase inlet solute concentration has much stronger impact on the raffinate outlet concentration than the previously discussed cases (disturbance in $C_{c,in}$). The model gives the concentration profile in the continuous phase after the disturbance rather correct. The calculated continuous phase outlet concentration profiles respond to the disturbance slightly faster, as it is observed with the experiments (Zamponi, 1996).

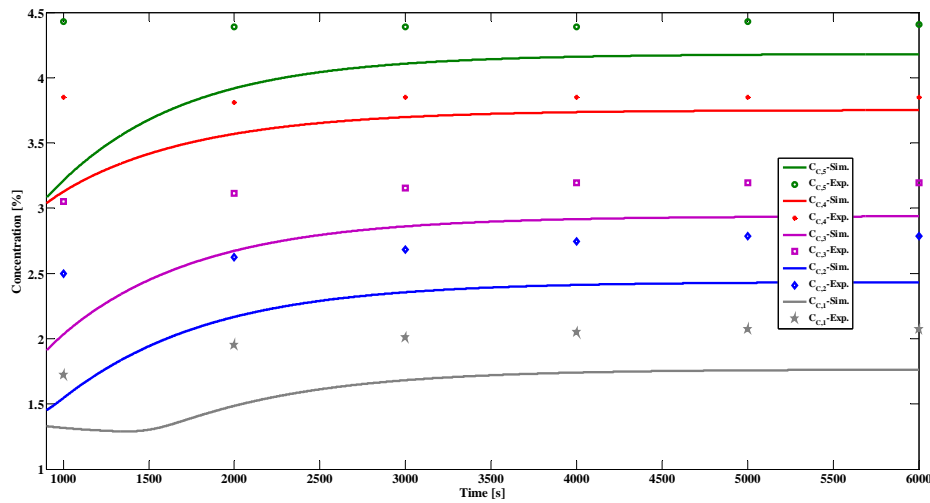


Fig.43. Simulated and experimental (Zamponi, 1996) transient solute concentration in the continuous phase due to a positive step change in $C_{d,in}$

5.1.4. Dynamic behaviour during start-up of the extractor

Fig.44 shows the variation of holdup at the four measuring points along the column height (see Fig.33) during the start-up of the column. The dead time (lag time) of the holdup is increase along the active part of the extraction column. The overshoot in the holdup is clear particularly noticeable during the start-up process, which is more pronounced with increasing the distance between the measuring point and the feeding point of the dispersed phase. The simulation of this figure carried out under the Q_2 operating conditions without mass transfer (see Table 12). At $t = 0$ s a positive step change is occurred in Q_d from 0 to 160 l.h^{-1} (start-up) and at $t = 1500$ s the system subjected to a negative step change in Q_d from 160 to 0 l.h^{-1} (shutdown).

The hydrodynamics simulation of the start-up process is extremely difficult to perform (Zamponi, 1996); in cases when Q_d is greater than Q_c (see Table 12). Despite that the phase interface controller reduces the flow of continuous phase at this time to zero; this phase ratio cannot prevent the phase interface at the top of the column to increases transiently (for a short time). The volume balance around the extractor cannot be satisfied at the start-up time, sufficient dispersed phase exits before the top of the column. In order to calculate the starting up process, the simulation of Q_d during the first 300 s is rising linearly started up from zero to its nominal value

(160 l.h^{-1}). At this point already a sufficiently large flow rate of dispersed phase enters at the head of the extractor, so that the simulator satisfies the volume balance at any time. The system of equations that describes the state of the column always comprises a solution. However, the calculated holdup profile deviates significantly from the experimental (Zamponi, 1996) profiles at the start-up procedure.

Apart from the problems in the illustration of the start-up control process, the model is not able to predict the overshoot in the holdup profiles due to the complex dispersed phase behaviour. To explain this behaviour further experimental investigations are needed (Zamponi, 1996). Analogous to starting up behaviour in the shutdown process, the column responds to the disturbance at the nearest measuring point at the extractors bottom. The dead times at the individual measuring points correspond approximately to those which are observed during start-up. The portion of small droplets, which can flow very slowly through the extractor to the top leads to the fact that during the shutdown process the holdup initially decreases rapidly at the top of the extractor. A residual fraction of dispersed phase leaves the column, but only very slowly. This effect is observed most clearly at the highest measuring point, because the dispersion of the droplets during their motion through the column to the top increases the fraction of small droplets. In contrast to the starting up of the extractor, the shutdown procedure after 1500 s the holdup profile is reproduced very well by the model (see Fig.44). The calculated dead time at the individual measuring points correspond to experimental data (Zamponi, 1996).

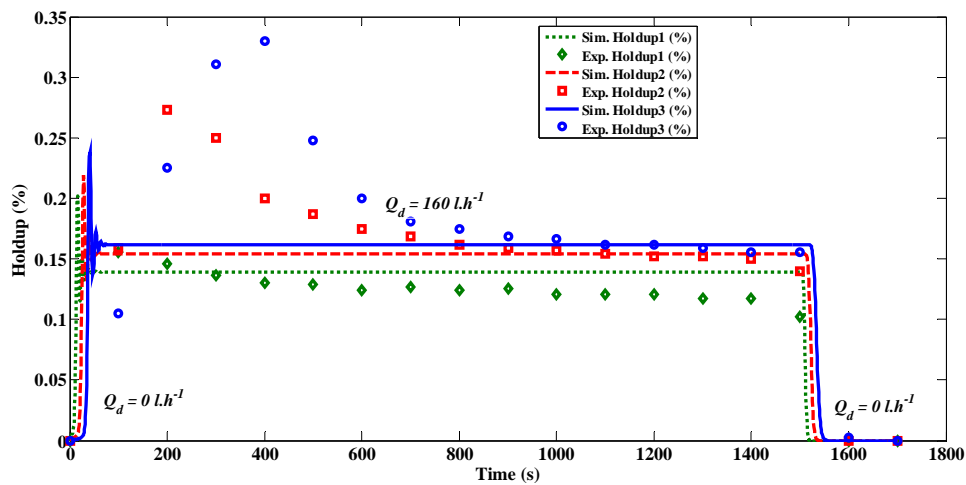


Fig.44. Simulated dynamic holdup evolution compared to the experimental one (Zamponi, 1996) during start-up and shutdown of the column

The experimental observation (Zamponi, 1996) reveals that the holdup decreases significantly slower in the upper measuring points during shutdown, which is in agree with the calculated results. In the simulation, after Q_d is reduced abruptly to zero the holdup initially increasing slightly then start to decrease. The reason for this deviation again lies in the concept of model based control for the representation of the extractor hydrodynamics. The abruptly deficient inflow stream of the dispersed phase at the lower part of the separator is compensated by entering the continuous phase at the top of the separator; hence Q_c increases in the whole column. The

residence time of the droplets increases, correspondingly increasing the dispersed phase residence time, which leads to the observed increase in the holdup.

Fig.45 presents both the simulation and experimental results (Zamponi, 1996) for the column start-up performance with respect to mass transfer behaviour. At the beginning of the experiment the entire column filled with the continuous phase with $C_{c,in} = 4.5\%$ acetone. The simulation of this figure carried out under the Q_2 operating conditions with $C_{c,in} = 4.5\%$ (see Table 12). The step change is occurred at $t = 0\text{ s}$, the change is from $Q_d = 0$ to 160 l.h^{-1} . At the time $t = 0\text{ s}$ the dispersed solvent begins to flow into the extraction column.

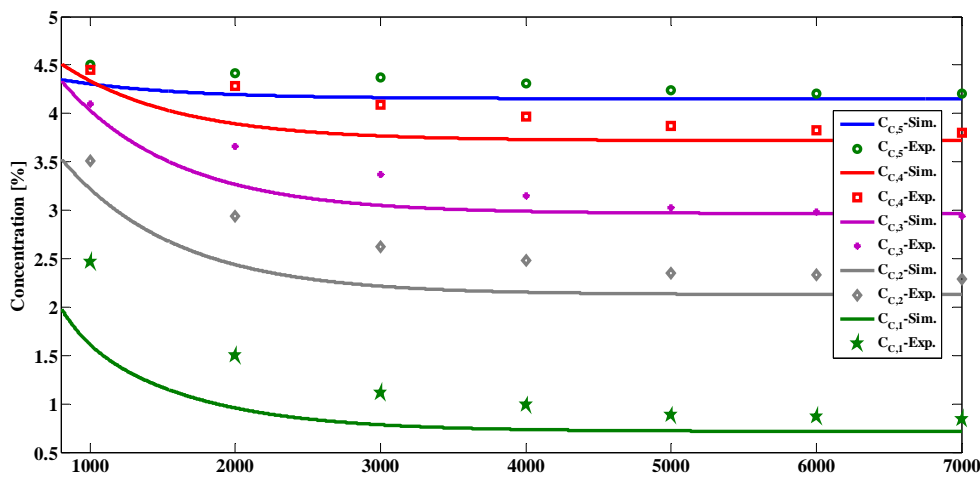


Fig.45. Simulated and experimental (Zamponi, 1996) transient solute concentration in the continuous phase during the column start-up

According to the relative distance from the inlet point of the dispersed phase the acetone concentration starts to decrease in the continuous phase at the individual measurement points. The dead time in the system response increases with increasing the distance in the direction of the dispersed phase flow. The change in the raffinate outlet concentration is the greatest, because there the continuous phase is already flows through the entire extractor and depleted, on the other hand at the lower end of the extractor the continuous phase is in contact with unloaded solvent. In contrast, the change in the concentration in the vicinity of the continuous phase inlet point is negligible, because before arriving in this region of the column the dispersed phase already has included significant amount of acetone. Despite there are some discrepancies, the model predicted quite well the hydrodynamics and mass transfer behaviour compared to the experimental results (Gomes et al., 2005, 2009; Zamponi, 1996). The hydrodynamics in the extractor, as illustrated Fig.44, reaches the steady state after a period of about 1100 s. Nevertheless, the steady state concentration profiles are established in the extractor only after about 6200 s of the start-up. However, the mass transfer profiles demonstrate significantly a sluggish mass transfer dynamics in comparison to the prompt response in the hydrodynamics behaviour.

5.2. Dynamic behaviour of pulsed columns

Conducting experimental work is very necessary in order to describe the dynamic behaviour of chemical process equipment such as extraction columns to achieve better design of automatically controlled systems. To get ride from the experimental work, there is an obvious need for a rigours and robust mathematical model that is capable to describe the real behaviour of extraction column. Hence, the present work was undertaken to provide a rigours and robust mathematical model for the dynamic behaviour of extraction column, the model simulation results were compared with experimental one over the entire range of column flow conditions.

The transient analysis of columns allows the study of the effect of disturbances or specific changes in the operating conditions on the column behaviour. In this work, the mathematical investigation of the dynamic behaviour of a pulsed liquid-liquid extraction column is reported. The pulsation intensity and the flow rates of the influent and effluent streams are used to control the pulsed (sieve plate and packed) extraction columns. Changing these variables causes the holdup to vary with time and position in the column.

Table 13. Pulsed sieve plate column geometry (Foster et al., 1970)

Dimension	Value
Height of the column	1.84 (m)
Inlet for the continuous phase	1.58 (m)
Inlet for the dispersed phase	0.35(m)
Column diameter	0.051 (m)
Diameter of sieve tray (d_{st})	50 (mm)
Diameter of holes (d_h)	3.2 (mm)
Relative free cross-sectional area (ϕ_{st})	0.23 ($m^2.m^{-2}$)
plate spacing (h_{st})	56 (mm)
Number of sieve plates	22 (-)

Fig.46 depicts the validation of LLECMOD transient simulation for pulsed sieve plate column, the column dimensions are given in Table 13, the simulation transient results compared to the experimental data (Foster et al., 1970). The simulation results agree with the experimental data (Foster et al., 1970) fairly well. The test system used here is water- methyl isobutyl ketone (w-MIBK); the physical properties of the test system are given in Table 14 (Sehmel and Babb, 1963). This figure shows the dynamic evolution of dispersed phase holdup due to a positive step change in the dispersed phase volumetric flow rate. The operating conditions used in this dynamic simulation are given in Table 15.

Table 14. Physical properties of the test system (w-MIBK) (Sehmel and Babb, 1963)

$\rho_x (kg.m^{-3})$	$\rho_y (kg.m^{-3})$	$\mu_x (kg.m^{-1}.sec^{-1})$	$\mu_y (kg.m^{-1}.sec^{-1})$	$\sigma (N.m^{-1})$
990.9	800.5	0.001163	0.000554	0.001

Table 15. Operating conditions for pulsed sieve plate column (dynamic simulation)

$Q_c (l/h)$	$Q_d (l/h)$	Pulse amplitude (m)	Pulse frequency (s)	No mass transfer
18.36	17.43	0.032	1.67	

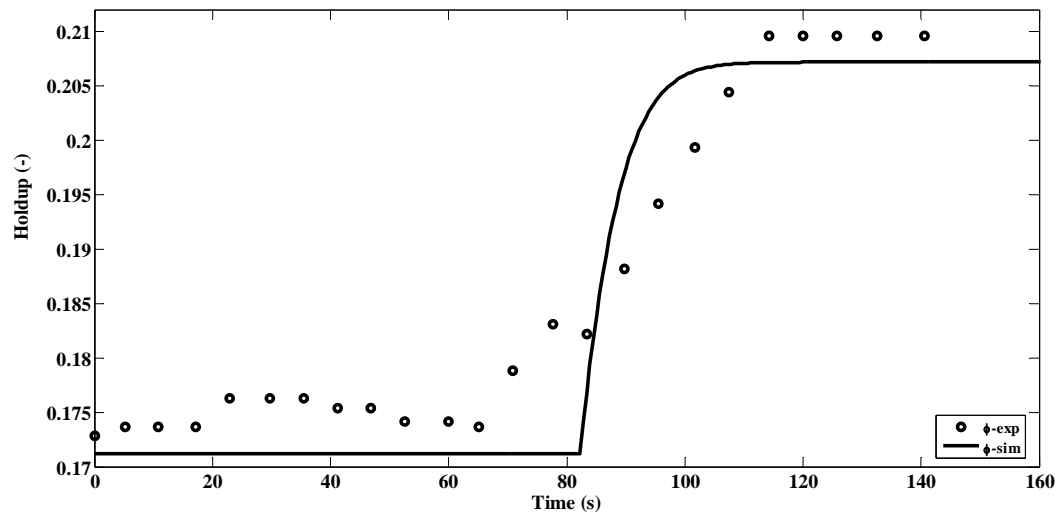


Fig.46. Dynamic evolution of holdup profile in pulsed sieve plate column compared to the experimental data (Foster et al., 1970).

6. CONCLUSIONS

Pulsed columns: In part of this doctoral thesis work, a comprehensive model for the dynamic and steady state simulation tool of extraction in pulsed (packed and sieve plate) columns is developed. The two pulsed extraction column modules (namely: pulsed packed and pulsed sieve plate column) are integrated into the LLECMOD program for the simulation of coupled hydrodynamics and mass transfer for liquid-liquid extraction columns. The LLECMOD non-equilibrium bivariate (in solute concentration and droplet diameter) population balance model is found capable of simulating new types of extraction columns; namely, pulsed and un-pulsed (packed and sieve tray) columns in addition to the stirred ones (Kühni & RDC types). The user-friendly input dialogs and the user functions input modules make the program very general and simple to use. The model has been successfully validated against experimental data. This model base on a non-equilibrium bivariate population balance model to describe the complex (steady state and dynamic) coupled hydrodynamics and mass transfer phenomena in extraction columns. In this work the pulsed/ un-pulsed (packed and sieve plate) are considered. Now the present version of LLECMOD offers the simulation of pulsed/ un-pulsed (sieve plate and packed) columns and the stirred (RDC and Kühni) columns. The steady state performance of the above-mentioned columns is studied using a detailed population balance framework as an alternative to the commonly applied dispersion and back-mixing models. The model has been validated against the experimental data and good agreements were achieved. The model has been found to predict accurately the real behaviour of the agitated and non-agitated extraction columns.

Optimum operating conditions can be obtained by varying the pulsation intensity. Greater efficiency can be obtained with the proper pulsation intensity. The variation of the dispersed phase holdup with height and the effect of operating conditions were studied and compared to the experimental results in this work. The results were compared with similar studies carried out in other extraction columns and a complete analysis of influence of operating conditions on the holdup profile of a pulsed (packed and sieve plate) columns was given. The results show that with increasing height, the holdup increases. With increasing the flow rate of each phase, the holdup increases but the effect of dispersed flow rate is more than the flow rate of continuous phase. Pulse velocity has a direct influence on holdup but at high pulse velocity, they have inverse relation to each other. In these studies, the systems with high interfacial tension (water-acetone-toluene) presented the most significant changes in column performance with the variation of pulsation intensity. While the system with low interfacial tension presented the most significant changes in column performance with the variation of volumetric flow rates. Moreover, LLECMOD was successfully validated against industrial extraction column data and even transient analysis gave no problems. In general, LLECMOD provides a useful tool for the scale up and simulation of agitated liquid extraction columns considering a more realistic conception of the dispersed phase discrete nature.

Effect of mass transfer direction and phase dispersion: It is shown in other part of this doctoral thesis work that the performance of Rotating Disk Contactor (RDC) depends strongly on the dispersed phase properties that dictate the interfacial area available for mass transfer. Since this interfacial area depends on the evolution of the dispersed phase population, classical or lumped models fail when competing with detailed population balance modelling. The effect of the spatial change of dispersed phase properties and their mutual influence on column hydrodynamics and mass transfer is now possible in the LLECMOD program. The present version of LLECMOD offers the options of dispersing either the light or heavy phases where reduced mean droplet diameter is found to persist when the heavy phase is dispersed. The steady state performance of an RDC extraction column is studied using a detailed population balance framework as an alternative to the commonly applied dispersion and backmixing models. So, one can draw the following conclusions:

- (1) The experimental and simulation results show that there is a profound effect of mass transfer direction on the liquid–liquid extraction column performance. This is generally cannot be simulated without taking into account droplet size distribution and the coupled hydrodynamics and mass transfer through the system interfacial tension.
- (2) With respect to the mass transfer direction it is found that the extractor efficiency is higher when the direction of mass transfer is from the continuous to the dispersed phase, which agrees with the published experimental data.
- (3) The predicted steady state mean properties of the dispersed phase were found less accurate than that of the continuous phase mean properties when compared to the experimental data. This may be attributed to the accuracy of the measuring techniques used in the experiments.

Stirred columns: Also in other part of this doctoral thesis work, a multivariate population balance model is developed and extended to include the momentum balance to calculate the droplet velocity; the model is used to predict the performance of liquid-liquid extraction columns. The population balance model is reduced using the SQMOM with only one secondary particle and a variable number of primary particles. The use of multi-primary particles can be viewed as a multi-fluid model in Eulerian frame of reference. Unlike previously published models, the present model has two basic advantages: First, the droplet velocity is predicted in a more fundamental way by deriving momentum balance equation for each primary particle (or fluid phase). Hence, the model avoids the use of algebraic velocity models used to correlate single droplet terminal velocity. Second, the reduced model is consistent in terms of number, volume and solute concentrations by solving directly coupled system of conservation laws. In this way, the population balance solver is free of classical finite difference schemes which are internally inconsistent. Numerical results show the rapid convergence of the droplet number and volume concentration profiles by increasing the number of primary particles. Actually, 10 to 20 primary particles are found enough to get reliable solutions. The mean droplet diameter (here it is d_{30}) is found insensitive to the number of primary particles. This is a great advantage when the need for the full distribution is relaxed. The mean dispersed phase velocity calculated from the momentum balance equation results in a jump in the dispersed phase holdup and the total number

concentration at the injection point due to the small relaxation time of the primary particles. This jump cannot be predicted using the steady state algebraic velocity models. The high coupling between the model equations through the primary particle velocity, and the nonlinearity of the conservation laws call for special CFD solvers. Here, a first-order finite volume method with flux vector splitting is used. To increase the time step, the present structure of the momentum balance allows the use of semi-implicit scheme, which is first-order in time for this purpose. The steady state results (holdup, mean droplet diameter and mass transfer profiles) in a pilot plant RDC column) are subjected to experimental validation, this validation show a very good agreement. As a final conclusion, the present model can be considered as an advanced engineering tool for simulating extraction columns in one dimension without neglecting its discrete and multi-scale nature.

Transient behaviour: Moreover, in other part of this doctoral thesis work, a rigours and robust mathematical dynamic model based on the bivariate population balance is developed and extended to include the momentum balance to calculate the droplet velocity. The model is used to predict and analyse the dynamic performance and behaviour of Kühni liquid-liquid extraction columns. The population balance model is reduced using the PSPM with only one secondary particle and a variable number of primary particles. Unlike previously published models, the present model has two basic advantages: First, the droplet velocity is predicted in a more fundamental way by deriving the momentum balance equation for each primary particle (or fluid phase). Hence, the model avoids the use of algebraic velocity models used to correlate the single droplet terminal velocity. Second, the reduced model is consistent in terms of number, volume and solute concentrations by solving directly coupled system of conservation laws. In this way, the population balance solver is free of classical finite difference schemes which are internally inconsistent. The high coupling between the model equations through the primary particle velocity, and the nonlinearity of the conservation laws call for special numerical solvers. Here, a first-order finite volume method with flux vector splitting is used. To increase the time step, the present structure of the momentum balance allows the use of semi-implicit scheme, which is first-order in time.

The numerical results reveal that the dynamic behaviour of the dispersed and continuous phases shows a lag time that increases away from the feed points of both phases. The solute concentration response shows a highly nonlinear behaviour due to both positive and negative step changes of equal magnitude in the input variables. The unsteady state analysis reveals the fact that the largest time constant (slowest response) is in the solute concentration of the continuous phase. The dynamic simulation results (holdup and mass transfer profiles) obtained from the rigors model in a pilot plant Kühni column are subjected to experimental validation showing a very good agreement. As a final conclusion, the present model can be considered as an advanced engineering tool for the dynamic simulation and analysis of extraction columns in one dimension without neglecting the discrete and multi-scale nature of the droplet swarm.

List of Symbols

a	Pulsation amplitude, m
A_c	Column cross sectional area, m ²
af	Pulsation intensity, m.s ⁻¹
a_{15}, a_{16}	Adjustable parameters, -
a_{PK}	Volumetric surface area of a packing, m ² .m ⁻³
C_i	Constant parameter, -
C_D	Drag coefficient, -
C_{IP}	Interface instability parameter, -
c	Solute concentration, Kg.m ⁻³
c_x, c_y	Solute concentration (continuous and dispersed phase), kg.m ⁻³
c_x, \bar{c}_y	Solute concentration (continuous and dispersed phase), kg.m ⁻³
$c_{x,in}, c_{y,in}$	Inlet solute concentration (continuous and dispersed phase), kg.m ⁻³
d, d'	Mean droplet diameter, m
d_{30}	Mass-number mean droplet diameter, m
\bar{D}_x, \bar{D}_y	Axial dispersion coefficient (continuous and dispersed phase), m ² .s ⁻¹
d_A	Shaft diameters, m
d, d_m, d', d''	Droplet diameter, m
d_{\min}, d_{\max}	Minimum and maximum droplet diameters, mm
D_c, D_r, D_s	Column, rotor and stator diameters, m
d_{100}	Characteristic droplet diameter due to a breakage probability of 100 %, m
d_{stab}	Stable droplet diameter, m
d_{crit}	Critical droplet diameter, m
d_{vs}	Sauter mean droplet diameter, m
f	Pulsation frequency, s ⁻¹
$f_{d,c_y} \partial d \partial c_y$	Number of droplets with d and $c_y \in [d, d + \partial d] \times [c_y, c_y + \partial c_y]$, m ⁻³
$g(d, d')$	Daughter droplet distribution based on droplet number, m ⁻¹
$h(d, d', \phi)$	Coalescence frequency, s ⁻¹
H_{cd}	Hamaker coefficient, Nm
H_{PK}	Height of a packing, m
H	Column height, m
H_C, h_c	Compartment height, m
k_v	Slowing factor, -
K_{ox}, K_{oy}	Continuous and dispersed phase overall mass transfer coefficient, m.s ⁻¹

k_x, k_y	Individual mass transfer coefficient (continuous and dispersed phase), m.s^{-1}
m	Solute distribution coefficient, -
m'	Modified solute distribution coefficient, -
m_0, m_3	Zero and third moments of the distribution, -
N_{sp}, N_{pp}	Number of secondary and primary particles, -
N_y	Droplet number concentrations, m^{-3}
N, n_R	Rotor speed, min^{-1}
N_{crit}	Critical rotor speed, min^{-1}
n	Swarm velocity exponent, -
N_P	Dimensionless power number, -
N_z, \bar{N}_z	Number and average number of daughter droplets, -
$p(d), P_r, P_B$	Breakage probability, -
P_C	Coalescence probability, -
Q	Volumetric flow rate, $\text{m}^3.\text{s}^{-1}$
Q_{bot}	Total flow rate at bottom of the column, $\text{m}^3.\text{s}^{-1}$
Q_{top}	Dispersed phase flow rate at top of the column, $\text{m}^3.\text{s}^{-1}$
$Q_{x,in}, Q_{y,in}$	Inlet flow rate (continuous and dispersed phase), $\text{m}^3.\text{s}^{-1}$
t	Time, s
u	Velocity, m.s^{-1}
\bar{u}_r	Relative droplet (slip) velocity, m.s^{-1}
\bar{u}_t	Terminal droplet velocity, m.s^{-1}
\bar{u}_x, \bar{u}_y	Relative velocity (continuous and dispersed phase), m.s^{-1}
$v(d)$	Droplet volume, m^3
V_T	Compartment volume, m^3
X, x	Total solute concentration in continuous phase, kg.m^{-3}
Y, y	Total solute concentration in dispersed phase, kg.m^{-3}
z	Space coordinate, m
z_c, z_x	Continuous phase inlet, m
z_d, z_y	Dispersed phase inlet, m

Greek Symbols

α	Volume concentrations, -
$\beta(d, d')$	Daughter droplet distribution based on droplet number, m^{-1}
$\Gamma(d)$	Breakage frequency, s^{-1}
Δt	Time interval, s
ε	Mean specific input energy, $\text{m}^2.\text{s}^{-3}$
ζ	Time and space vector, -
$\lambda(d, d', \phi)$	Coalescence efficiency, -

μ_r	r^{th} moment, -
μ	Viscosity, $\text{kg}\cdot\text{m}^{-1}\cdot\text{s}^{-1}$
μ_x, μ_y	Viscosity (continuous and dispersed phase), $\text{kg}\cdot\text{m}^{-1}\cdot\text{s}^{-1}$
π_0	Source term that accounts for the net number of drops per unit volume generated by breakage π_0^b and coalescence π_0^c , s^{-1}
π_3	Source term that accounts for the net number of drops per unit volume generated by breakage π_3^b and coalescence π_3^c , s^{-1}
ρ_x, ρ_y	Density (continuous and dispersed phase), $\text{kg}\cdot\text{m}^{-3}$
ρ	Density, $\text{kg}\cdot\text{m}^{-3}$
σ	Interfacial tension, $\text{N}\cdot\text{m}^{-1}$
Σ	Standard deviation, m
τ_c	Continuous phase local shear stress, $\text{N}\cdot\text{m}^{-2}$
τ_p	Droplet relaxation time, s
v, v'	Droplet volumes, m^3
v_{\min}, v_{\max}	Minimum and maximum droplet volume, m^3
ξ_i	Parameter, -
Υ	Source term that represents the net number of droplet produced by breakage and coalescence, $\text{m}^{-3}\cdot\text{s}^{-1}$
ϕ	Holdup, -
ϕ_e	Dispersed phase hold up entrained with the continuous phase-
ϕ_x, ϕ_y	Hold up (continuous and dispersed phase), -
$\vartheta(d')$	Mean number of daughter droplets, -
Υ	Source term that represents the net number of droplet produced by breakage and coalescence $\text{m}^{-3}\cdot\text{s}^{-1}$
$\Upsilon.\partial\zeta$	Source term, $\text{m}^{-3}\cdot\text{s}^{-1}$
φ_s	Relative free cross-sectional area of a sieve tray plate, $\text{m}^2\cdot\text{m}^{-2}$
ψ	Internal and external coordinates vector $[d \ c_y \ z \ t]$, -
$\omega(d, d')$	Coalescence frequency, $\text{m}^3\cdot\text{s}^{-1}$
$\omega_R, \omega_{R, \text{crit}}$	Rotor and critical rotor speeds respectively, s^{-1}

Dimensionless numbers

π_{af}	Pulsation intensity, -
π_{ap}	Volumetric surface area of a packing, -
π_d	Droplet diameter, -
π_{hp}	Height of a packing, -
π_σ	Interfacial tension, -

Re	Droplets Reynolds number, –
We_{mod}	Modified Weber number, -

Subscript

avg	Average
c, x	Continuous phase
d, y	Dispersed phase
max	Maximum
min	Minimum
r	Relative
s	Slip
t	Terminal

Superscript

in	Inlet
–	Mean value
*	Equilibrium

Abbreviations

BVSQMOM	: Bivariate Sectional Quadrature Method of Moments
CFD	: Computational Fluid Dynamic
CM	: Classes Method
CQMOM	: Cumulative Quadrature Method Of Moments
DPBM	: Droplet Population Balance Model
DQMOM	: Direct Quadrature Method of Moments
EFCE	: European Federation of Chemical Engineering
FDS	: Finite Difference Scheme
FVS	: Flux Vector Splitting
GFP	: General Fixed Pivot technique
LLEC	: Liquid-Liquid Extraction Column
LLECMOD	: Liquid-Liquid Extraction Column Module
MCM	: Monte Carlo Method
MOM	: Method Of Moments
MPOSPM	: Multi Primary One Secondary Particle Method
OPOSPM	: One Primary One Secondary Particle Method
PBE	: Population Balance Equation
PBM	: Population Balance Model
PDF	: Probability Density Function
PSD	: Particle Size Distribution
PSPM	: Primary and Secondary Particle Method
QMOM	: Quadrature Method Of Moments
RDC	: Rotating Disk Contactor
SDBPBE	: Spatially Distributed Bivariate Population Balance Equation
SMM	: Standard Method of Moment
SQMOM	: Sectional Quadrature Method Of Moments

References

- Aarts, D.G.A.L.; Lekkerkerker, H.N.W., (2008). Droplet coalescence: drainage, film rupture and neck growth in ultralow interfacial tension systems. *J. Fluid Mech.*, 606, 275-294.
- Al Khani, S.D.; Gourdon, C.; Casamatta, G., (1988). Simulation of hydrodynamics and mass transfer of a disk and rings pulsed column. *Ind. Eng. Chem. Res.*, 27(2), 329-333.
- Al Khani, S.D.; Gourdon, C.; and Casamatta, G., (1989). Dynamic and steady state simulation of hydrodynamics and mass transfer in liquid-liquid extraction column. *Chem. Eng. Sci.*, 44, 1295-1305.
- Alopaeus, V.; Koskinen, J.; Keskinen, K.I., (2002). Simulation of the population balances for liquid-liquid systems in a nonideal stirred tank. Part 2 Parameter fitting and the use of the multiblock model for dense dispersions. *Chem. Eng. Sci.*, 57, 1815-1825.
- Andersson, R.; Andersson, B., (2006a). Modeling the breakup of fluid particles in turbulent flows. *AIChE. J.*, 52(6), 2031-2038.
- Attarakih, M. M.; Bart, H.-J.; and Faqir, N. M., (2003). Solution of the population balance equation for liquid-liquid extraction columns using a generalized fixed-pivot and central difference schemes. *Computer-Aided Chemical Engineering*, 14, 557-562.
- Attarakih, M. M.; Bart, H.-J.; and Faqir, N. M., (2004a). Solution of the droplet breakage equation for interacting liquid-liquid dispersions: a conservative discretization approach. *Chem. Eng. Sci.*, 59, 2547-2565.
- Attarakih, M. M.; Bart, H.-J.; and Faqir, N. M., (2004b). Numerical solution of the spatially distributed population balance equation describing the hydrodynamics of interacting liquid-liquid dispersions. *Chem. Eng. Sci.*, 59, 2567-2592.
- Attarakih, M.; Bart, H.J.; Faqir, N., (2006a). Numerical Solution of Bivariate Population Balance Equation for the Interacting Hydrodynamics and Mass Transfer in Liquid-Liquid Extraction Columns. *Chem. Eng. Sci.*, 61, 113-123.
- Attarakih, M. M.; Bart, H.-J.; and Faqir, N. M., (2006b). A Hybrid scheme for the solution of the bivariate spatially distributed population balanced equation. *Chem. Eng. Technol.*, 29, 435-441.
- Attarakih, M.M.; Bart, H.-J.; and Faqir, N.M., (2006c). LLECMOD: A windows-based program for hydrodynamics simulation of liquid-liquid extraction columns. *Chem. Eng. Process*, 45(2), 113-123.
- Attarakih, M.M.; Bart, H.-J.; Steinmetz, T.; Dietzen, M.; and Faqir, N.M., (2008a). LLECMOD: A bivariate population balance simulation tool for liquid- liquid extraction columns. *Open Chem. Eng. J.*, 2, 10-34.
- Attarakih, M.M.; Jaradat, M.; Allaboun, H.; Bart, H.-J.; Faqir, N.M.; (2008b). *Dynamic Modelling of a Rotating Disk Contactor Using the Primary and Secondary Particle Method (PSPM)*. In Bertrand Braunschweig & Xavier Joulia (Eds.), 18th European Symposium on Computer Aided Process Engineering–ESCAPE 18. Lyon - France: Elsevier.
- Attarakih, M.; Zeidan, D.; Drumm, C.; Tiwari, S.; Kuhnert, J.; Allaboun, H.; Bart, H.-J., (2008c). Dynamic Modelling of Liquid Extraction Columns using the Direct Primary and Secondary Particle Method (DPSPM). In: Proceedings of the 6th International Conference on Computational Fluid Dynamics in the Oil & Gas, Metallurgical and Process Industries, Johansen S.T, Olsen J.E, Ashrafi A, Eds., Trondheim, Norway.

- Attarakih, M.; Drumm, C.; Bart, H.-J., (2009a). Solution of the population balance equation using the sectional quadrature method of moments (SQMOM). *Chem. Eng. Sci.*, 64, 742-752.
- Attarakih, M.; Jaradat, M.; Drumm, C.; Bart, H.-J.; Tiwari, S.; Sharma, V.K.; Kuhnert, J.; Klar, A., (2009b). *Solution of the Population Balance Equation using the One Primary and One Secondary Particle Method (OPOSPM)*. In J. Jeżowski & J. Thullie (Eds.), 19th European Symposium on Computer Aided Process Engineering–ESCAPE19. Cracow - Poland: Elsevier.
- Attarakih, M.; Jaradat, M.; Drumm, C.; Bart, H.-J.; Tiwari, S.; Sharma, V.K.; Kuhnert, J.; Klar, A., (2009c). *A Multivariate Population Balance Model for Liquid Extraction Columns*. In J. Jeżowski & J. Thullie (Eds.), 19th European Symposium on Computer Aided Process Engineering–ESCAPE19. Cracow - Poland: Elsevier.
- Attarakih, M.M.; Jaradat, M.; Bart, H.-J.; Kuhnert, J.; (2010a). *Solution of the population balance equation using the Cumulative Quadrature Method of Moments (CQMOM)*. Proc. 4th International Conference on Population Balance Modelling, September 15 - 17, 2010, Berlin - Germany.
- Attarakih, M.M.; Jaradat, M.; Drumm, C.; Bart, H.-J.; Tiwari, S.; Sharma, V.K.; Kuhnert, J.; Klar, A., (2010b). *A multivariate sectional quadrature method of moments for the solution of the population balance equation*. Proc. of 20th European Symposium on Computer-Aided Process Engineering-ESCAPE 20, Ischia, Naples - Italy, June 2010.
- Attarakih, M.M., (2010c). System and method for simulating and modeling the distribution of discrete systems, United States Patent Application: 0100106467, April 29, 2010.
- Attarakih, M.; Jaradat, M.; Hlawitschka, M.; Bart, H.-J.; Kuhnert, J., (2011). Integral Formulation of the Population Balance Equation using the Cumulative Quadrature Method of Moments (CQMOM). *Computer Aided Chemical Engineering*, 29, 81-85.
- Azizi, Z.; Rahbar, A.; and Bahmanyar, H., (2010). Investigation of packing effect on mass transfer coefficient in a single drop liquid extraction column. *Iran. J. Chem. Eng.*, 7, 3-11.
- Bahmanyar, H.; and Slater, M.J., (1991). Studies of drop break up in liquid-liquid systems in a rotary disc contactor, part I: conditions of no mass transfer. *Chem. Eng. Technol.*, 14, 79-89.
- Bahmanyar, H.; Ghasempour, F.; and Safdari, J., (2007). Dispersed phase hold-up in a vertical mixer settler in with and without mass transfer conditions. *J. Chem. Eng. Jpn.*, 40, 17-25.
- Bailes, P.J.; Winward, A., (1972). Progress in liquid-liquid extraction. *Trans. Inst. Chem. Eng.*, 50, 240-258.
- Bapat, P.M.; and Tavlarides, L.L., (1985). Mass Transfer in a Liquid-Liquid CFSTR. *AIChE J.*, 31(4), 659-666.
- Barrett, J.C.; Webb, N.A., (1998). A comparison of some approximate methods for solving the aerosol general dynamic equation. *J. Aerosol Sci.*, 29, 31-39.
- Bart, H.-J.; and Stevens, G., (2004). Reactive Solvent Extraction. In: *Ion Exchange and Solvent Extraction*, Kertes, M.; Sengupta, A.K. (Eds.), 17, 37-82, Marcel Dekker: New York.
- Bart, H.-J.; Drumm, C.; Attarakih, M., (2008). Process Intensification with Reactive Extraction Columns. *Chem. Eng. Process.*, 47, 745-754.
- Bart, H.-J., (2001). *Reactive Extraction (Heat and Mass Transfer)*. Springer-Verlag: Heidelberg.

- Bart, H.-J., (2006). From Single Droplet to Column Design. *Tsinghua Sci. Technol.*, 11(2), 212-216.
- Bastani, D., (2004). Stagewise Modeling of Liquid-Liquid Extraction Column (RDC). *IJE Transactions B: Applications*, 17(1), 7-17.
- Batey, W.; and Thornton, J.D., (1989). Partial mass-transfer coefficients and packing performance in liquid-liquid extraction. *Ind. Eng. Chem. Res.*, 28, 1096-1101.
- Bauer, R., (1976). Die Längsvermischung beider Phasen in einer gerührten Fest-Flüssig-Extraktionskolonne. Dissertation, ETH Zurich, Zurich, Switzerland.
- Bensalem, A.K., (1985). Hydrodynamics and Mass Transfer in a Reciprocating Plate Extraction Column. Dissertation, Swiss Federal Institute of Technology, Zurich, Switzerland.
- Bhawsar, P.C.M.; Pandit, A.B.; Sawant, S.B.; and Joshi, J.B., (1994). Enzyme mass transfer coefficient in a sieve plate extraction column. *Chem. Eng. J.*, 55, B1-B17.
- Biery, J.C.; Boylan, D.R., (1963). Dynamic Simulation of Liquid-Liquid Extraction Column. *Ind. Eng. Chem. Fundam.*, 2, 44-50.
- Blass, E.; and Zimmerman, H., (1982). Mathematische Simulation und Experimentelle Bestimmung des Instationären Verhaltens einer Flüssigkeitspulsierten Siebbodenkolonne zur Flüssig-Flüssig-Extraktion. *Verfahrenstechnik*, 16, 652-690.
- Bonnet, J.C.; Jeffreys, G.V., (1985). Hydrodynamics and mass transfer characteristics of a Scheibel extractor. Part I: Drop size distribution, holdup, and flooding. *AIChE J.*, 31, 788-794.
- Borba Costa, C.B.; Wolf Maciel, M.R.; Filho, R.M., (2007). Considerations on the crystallization modeling: Population balance solution. *Compt. Chem. Eng.*, 31(3), 206-218.
- Brandt, H.W.; Reissinger, K.-H.; Schröter, J., (1978). Moderne Flüssig/Flüssig-Extraktoren–Übersicht und Auswahlkriterien. *Chem. Ing. Tech.*, 50(5), 345-354.
- Cabassud, M.; Gourdon, C.; Casamatta, G., (1990). Single Drop Breakup in a Kühni Column. *Chem. Eng. J.*, 44, 27-41.
- Cameron, I.T.; Wang, F.Y.; Immanuel, C.D.; Stepanek, F., (2005). Process systems modelling and applications in granulation: A review. *Chem. Eng. Sci.*, 60, 3723-3750.
- Camurdan, M.C.; Taylor, P.A.; Baird, M.H.I., (1991). Adaptive control of hydrodynamic holdup in a Kar extraction column. *Can. J. Chem. Eng.*, 69, 578-587.
- Casamatta, G.; and Vogelpohl, A., (1985). Modelling of fluid dynamics and mass transfer in extraction columns. *Ger. Chem. Eng.*, 8, 96-103.
- Casamatta, G., (1981). Comportement de la population des gouttes dans une colonne d'extraction: Transport, rupture, coalescence, transfer de matiere. PhD Thesis, Institut National Polytechnique De Toulouse, Toulouse, France.
- Cauwenberg, K.; Degreve, J.; and Slater, M.J., (1997). The Interaction of Solute Transfer, Contaminants and Drop Break-up in Rotating Disc Contactors: Part II. The Coupling of the Mass Transfer and Breakage Processes via Interfacial Tension. *Can. J. Chem. Eng.*, 75, 1056-1066.
- Cauwenberg, V.; Degreve, J.; and Slater, M.J., (1997). The Interaction of Solute Transfer, Contaminates and Drop Break-Up in Rotating Disc Contactors: Part I. Correlation of Drop Breakage Probabilities. *Can. J. Chem. Eng.*, 75, 1046-1055.
- Cavatorta, O.N.; Böhm, U.; and Giorgio, A.M.C., (1999). Fluid-Dynamic and mass-transfer behaviour of static mixers and regular packings. *AIChE J.*, 45, 938-948.

- Chantry, W.A.; Von Berg, R.L.; Wiegandt, H.F., (1955). Application of pulsation to liquid-liquid extraction. *Ind. Eng. Chem.*, 47, 1153-1159.
- Chatzi, E.; Lee, J.L., (1987). Analysis of interaction for liquid-liquid dispersion in agitated vessels. *Ind. Eng. Chem. Res.*, 26, 2263-2267
- Chesters, A.K., (1991). The modelling of coalescence processes in fluid-liquid dispersions. A review of current understanding. *Trans IChemE.*, 69(A), 259-281.
- Chouai, A.; Cabassud, M.; Le Lann, M.V.; Gourdon, C.; Casamatta, G., (2000). Multivariable Control of a Pulsed Liquid-Liquid Extraction Column by Neural Networks. *Neural Comput. Applic.*, 9, 181-189.
- Clift, R.; Grace, J. R.; Weber, M. E., (1978). *Bubbles, Drops, and Particles*. Academic Press: New York.
- Colella, D.; Vinci, D.; Bagatin, R.; Masi, M., (1999). A study on coalescence and breakage mechanisms in three different bubble columns. *Chem. Eng. Sci.*, 54, 4767-4777.
- Coulaloglou, C.A.; Tavlarides, L.L., (1977). Description of interaction processes in agitated liquid-liquid dispersions. *Chem. Eng. Sci.*, 32, 1289-1297.
- Diemer, R.B.; Olson, J.H., (2002). A moment methodology for coagulation and breakage problems: Part 3 – generalized daughter distribution functions. *Chem. Eng. Sci.*, 57, 4187-4198.
- Diemer, R.B.; Olson, J.H., (2002a). A moment methodology for coagulation and breakage problems: Part 1- analytical solution of the steady-state population balance. *Chem. Eng. Sci.*, 57, 2193-2209.
- Diemer, R.B.; Olson, J.H., (2002b). A moment methodology for the coagulation and breakage problems: Part 2-moment models and distribution reconstruction. *Chem. Eng. Sci.*, 57, 2211-2228.
- Drumm, C.; Attarakih, M.; Hlawitschka, M.W.; Bart, H.-J., (2010). One-Group Reduced Population Balance Model for CFD Simulation of a Pilot-Plant Extraction Column. *Ind. Eng. Chem. Res.*, 49, 3442-3451.
- Drumm, C., (2010). Coupling of Computational Fluid Dynamics and Population Balance Modelling for Liquid-Liquid Extraction. Dissertation; Technischen Universität Kaiserslautern, Kaiserslautern, Germany.
- Dutta, B.K., (2007). *Principles of mass transfer and separation processes*. Prentice-Hall of India, New Delhi.
- Efendiev Y.; Zachariah, M., (2002). Hybrid Monte Carlo method for simulation of two-component aerosol coagulation and phase segregation. *J. Colloid Interface Sci.*, 249, 30-43.
- Fan, R.; Marchisio, D.L.; Fox, R.O., (2004). Application of the direct quadrature method of moments to polydisperse gas-solid fluidized beds. *Powder Technol.*, 139, 7-20.
- Foster Jr., H.R.; McKEE, R.E.; and Babb, A.L., (1970). Transient holdup behaviour of a pulsed sieve plate solvent extraction column. *Ind. Eng. Chem. Process Des. Dev.*, 9(2), 272-278.
- Fox, M.H.; Ralph, S.J.; Sithebe, N.P.; Buchalter, E.M.; Riordan, J.J., (1998). Comparison of some aspects of the performance of a Bateman pulsed column and conventional box-type mixer-settlers. *ALTA 1998 Nickel/cobalt pressure leaching and hydrometallurgy forum*. Perth Western Australia, Australia.
- Galla, U.; Goldacker, H.; Schlenker, R.; and Schmieder, H., (1990). Improved U/PU separation in pulsed columns by optimized pulsation conditions and use of two consecutive extraction columns. *Sep. Sci. Technol.*, 25, 1751-1761.

- Garcia, A.L.; van den Broeck, C.; Aertsens M.; Serneels, R., (1987). A Monte Carlo simulation of coagulation. *Physica, A Stat. Theor. Phys.*, 143(3), 535-546.
- Garg, M.O.; and Pratt, H.R.C., (1984). Measurement and modelling of droplet coalescence and breakage in a pulsed-plate extraction column. *AIChE J.*, 30, 432-441.
- Garthe, G., (2006). *Fluid Dynamics and Mass Transfer of Single Particles and Swarms of Particles in Extraction Column*. Dr. Hut Verlag: München.
- Gautschi, W., (1994). Algorithm 726: ORTHPOL-a package of routines for generating orthogonal polynomials and Gauss-type quadrature rules. *ACM Trans. Math. Software*, 20(1), 21-62.
- Gerstlauer, A., (1999). *Herleitung und Reduktion populationsdynamischer Modelle am Beispiel der Flüssig-Flüssig-Extraktion*. Fortschritt-Berichte VDI Verlag, Düsseldorf.
- Gillespie, D.T., (1972). The stochastic coalescence model for cloud droplet growth. *J. Atmos. Sci.*, 29, 1496-1510.
- Gillespie, D.T., (1975). An exact method for numerically simulating the stochastic coalescence process in a cloud. *J. Atmos. Sci.*, 32, 1977-1989.
- Gillespie, D.T., (1976). A general method for numerically simulating the stochastic time evolution of coupled chemical reactions. *J. Comput. Phys.*, 22, 403-434.
- Godfrey, J.C.; and Slater, M.J., (1991). Slip velocity relationships for liquid-liquid extraction columns. *Trans. Inst. Chem. Eng.*, 69, 130-141.
- Godfrey, J.C.; Slater, M.J., (1994). *Liquid-Liquid Extraction Equipment*. John Wiley and Sons, New York.
- Golub G.H.; Welsh, J.H., (1969). Calculation of Gauss quadrature rules. *Math. Comp.*, 23(106), 221-230.
- Gomes, L.N.; Guimarães, M.L.; Stichlmair, J.; Cruz-Pinto, J.J., (2005). Study of Dynamic Simulation and Its Influence on the Control of an Agitated Liquid-Liquid Kühni Extraction Column. Proceedings of the International Solvent Extraction Conference, Beijing China, ISEC05, September 19-23, 2005, 965-970.
- Gomes, L.N.; Guimarães, M.L.; Stichlmair, J.; Cruz-Pinto, J.J., (2009). Effects of Mass Transfer on the Steady State and Dynamic Performance of a Kühni Column - Experimental Observations. *Ind. Eng. Chem. Res.*, 48, 3580-3588.
- Gooch J.R.P.; Hounslow, M.J., (1996). Monte Carlo simulation of size-enlargement mechanisms in crystallization. *AIChE J.*, 42(7), 1864-1874.
- Goodson, M.J.; Kraft, M., (2004). Simulation of coalescence and breakage: an assessment of two stochastic methods suitable for simulating liquid-liquid extraction. *Chem. Eng. Sci.*, 59, 3865-3881.
- Goodson, M.J., (2007). Stochastic Solution of Multi-Dimensional Population Balances. Dissertation, Trinity College-University of Cambridge, Cambridge, United Kingdom.
- GORDON, R.G., (1968). Error bounds in equilibrium statistical mechanics. *J. Math. Phys.*, 9, 655-672.
- Gottlieb, K.; Grinbaum, B.; Chen, D.; and Stevens, G.W., (2000). The use of pulsed perforated plate extraction column for recovery of sulphuric acid from copper tank house electrolyte bleeds. *Hydrometallurgy*, 58, 203-213.
- Gourdon, C.; Casamatta, G., (1991). Influence of mass transfer direction on the operation of a pulsed sieve-plate pilot column. *Chem. Eng. Sci.*, 46-11, 2799-2808.

- Gourdon, C.; Casamatta, G.; and Muratet, G., (1994). Population balance based modelling of solvents extraction columns, In: *Liquid-liquid extraction equipment*. Godfrey, J.C.; Slater, M.J.; (Eds.), Wiley & Sons, New York, 137-226.
- Gourdon, C., (1989). Les Colonnes d'Extraction par Solvant: Modèles et comportement. Dissertation, Institute National Polytechnique de Toulouse, Toulouse, France.
- Grace, J.R.; Wairegi, T.; and Nguyen, T.H., (1976). Shapes and velocities of single drops and bubbles moving freely through immiscible liquids. *Trans. Inst. Chem. Eng.*, 54, 167-173.
- Green, D.W.; Perry, R.H., (2008). *Perry's Chemical Engineers' Handbook*. McGraw-Hill, New York.
- Grinbaum, B., (2006). The existing models for simulation of pulsed and reciprocating columns -how well do they work in the real world? *Solvent Extr. Ion Exch.*, 24, 796-822.
- Groothuis, H., and Zuideweg, F.J., (1960). Influence of mass transfer on coalescence of drops. *Chem. Eng. Sci.*, 12, 288-289.
- Hagesaether, L.; Jakobsen, H.A.; Svendsen, H.F., (2002). A model for turbulent binary breakup of dispersed fluid particles. *Chem. Eng. Sci.*, 57, 3251-3267.
- Handlos, A.E.; Baron, T., (1957). Mass and heat transfer from drops in liquid-liquid extraction. *AIChE J.*, 3, 127-136.
- Hanson, C., (1971). *Recent Advances in Liquid-Liquid Extraction*. Pergamon Press, Oxford, United Kingdom.
- Haverland, H.; Vogelpohl, A.; Gourdon, C.; and Casamatta, G. Simulation of fluid dynamics in a pulsed sieve plate column. *Chem. Eng. Technol.*, 1987, 10, 151-157.
- Henschke, M., (2004). *Auslegung pulsierter Siebboden-Extraktionskolonnen*. Shaker Verlag: Aachen.
- Hounslow, M.J.; Ryall, R.L.; Marshall, V.R., (1988). A discretized population balance for nucleation, growth and aggregation. *AIChE J.*, 34, 1821-1832.
- Huang, Y.-Y.; and Lu, M., (1999). Continuous Phase Mass Transfer Coefficients For Single Droplets Moving in an Infinite Droplet Chain. *Chem. Eng. Commun.*, 171(1), 181-194.
- Hufnagl, H.; McIntyre, M.; and Blas, E., (1991). Dynamic behaviour and simulation of a liquid-liquid extraction column. *Chem. Eng. Technol.*, 14, 301-306.
- Hulburt, H.M.; Katz, S., (1964). Some problems in particle technology. *Chem. Eng. Sci.*, 19, 555-574.
- Igarashi, L.; Kieckbusch, T.G.; and Franco, T.T., (2004). Mass transfer in aqueous two-phase system packed column. *J. Chromatogr. B.*, 807, 75-80.
- Ishii, M.; Mishima, K., (1984). Two-fluid model and hydrodynamic constitutive relations. *Nucl. Eng. Des.*, 82, 107-126.
- Jahya, A.B.; Clive Pratt, H.R.; and Stevens, G.W., (2005). Comparison of the performance of a pulsed disc and doughnut column with a pulsed sieve plate liquid extraction column. *Solvent Extr. Ion Exch.*, 23, 307-317.
- Jaradat, M.; Allaboun, H.; Bart, H.-J.; Attarakih, M., (2012a). Dynamic modelling and simulation of Kühni extraction columns. *Computer Aided Chemical Engineering*, 30, 1073-1077.
- Jaradat, M.; Attarakih, M.; Bart, H.-J., (2012b). Transient modelling and simulation of Kühni extraction column: hydrodynamics and mass transfer using population balance model. *Chem. Eng. Technol.*, DOI: 10.1002/ceat.201200164.

- Jaradat, M.M.; Attarakih, M.M.; Steinmetz, T.; Bart, H.-J., (2012c). LLECMOD: A Bivariate Population Balance Simulation Tool for Pulsed (Packed and Sieve Plate) Liquid-Liquid Extraction Columns. *Open Chem. Eng. J.*, 6, 8-31.
- Jaradat, M.; Attarakih, M.; Bart, H.-J., (2012d). RDC Extraction Column Simulation using the Multi-Primary One Secondary Particle Method: Coupled Hydrodynamics and Mass Transfer. *Comput. Chem. Eng.*, 37(10), 22-32.
- Jaradat, M.; Attarakih, M.; Bart, H.-J., (2011a). Population Balance Modelling of Pulsed (Packed and Sieve Plate) Extraction Columns: Coupled Hydrodynamic and Mass Transfer. *Ind. Eng. Chem. Res.*, 50 (24), 14121-14135.
- Jaradat, M.; Attarakih, M.; Bart, H.-J., (2011b). Advanced Prediction of Pulsed (packed and sieve plate) Extraction Columns Performance Using Population Balance Modelling. *Chem. Eng. Res. Des. - IChemE*, 89(12), 2752-2760.
- Jaradat, M.; Attarakih, M.; Bart, H.-J., (2011c). Detailed Mathematical Modelling of Liquid-Liquid Extraction Columns. *Computer Aided Chemical Engineering*, 29, 1-5.
- Jaradat, M.; Attarakih, M.; Bart, H.-J., (2011d). Advanced Prediction of Pulsed Extraction Column Performance using LLECMOD. (CM)² young researcher symposium proceeding, 45-49, 15 February 2011, Kaiserslautern - Deutschland.
- Jaradat, M.; Attarakih, M.; Bart, H.-J., (2010a). Effect of Phase Dispersion and Mass Transfer Direction on Steady State RDC Performance using Population Balance Modelling. *Chem. Eng. J.*, 165, 2, 379-387.
- Jaradat, M.; Attarakih, M.; Hlawitschka, M.; Bart, H.-J.; (2010b). *A multivariate population balance model for liquid extraction columns*. Proc. 4th International Conference on Population Balance Modelling, September 15 - 17, 2010, Berlin - Germany.
- Johnson, H.F.; and Bliss, H., (1946). Liquid-liquid extraction in spray towers. *Trans. Am. Inst. Chem. Eng.*, 42, 331-358.
- Kelishami, AR.; Bahmanyar, H.; Nazari, L.; and Moosavian, M.A., (2009). Development of an effective diffusivity model for regular packed liquid extraction columns. *Aust. J. Basic Appl. Sci.*, 3, 407-417.
- Kentish, S.E.; Stevens, G.W.; Pratt, H.R.C., (1998). Estimation of coalescence and breakage rate constants within a Kühni column. *Ind. Eng. Chem. Res.*, 37, 1099-1106.
- Kleczek, F.; Cauwenberg, V.; and Rompay, P.V., (1989). Effect of Mass Transfer on Droplet Size in Liquid-liquid Dispersions. *Chem. Eng. Technol.*, 12, 395-399.
- Klee, A.J.; and Treybal, R.E., (1956). Rate of rise or fall of liquid drops. *AIChE J.*, 2, 444-447.
- Komazawa, J.; and Ingham, J., (1978). Effect of System Properties on the Performance of Liquid-Liquid Extraction Columns-II. *Chem. Eng. Sci.*, 33, 479-485.
- Konno, M.; Matsunaga, Y.; Arai, K.; Saito, S., (1980). Simulations model for breakup process in an agitated tank. *J. Chem. Eng. Japan* 13, 67-73.
- Korschinsky, W.J.; and Young, C.H., (1989). Modelling drop-side mass transfer in agitated polydispersed liquid-liquid systems. *Chem. Eng. Sci.*, 40, 2355-2361.
- Korschinsky, W.J.; Azimzadeh-Khatayloo, S., (1976). An improved stagewise model of counter-current flow liquid-liquid contactors. *Chem. Eng. Sci.*, 31(10), 871-875.
- Kostoglou, M.; Karabelas, A. J., (1994). Evaluation of zero order methods for simulating particle coagulation. *J. Colloid Interface Sci.*, 163, 420-431.

- Kronberger, T.; Ortner, A.; Zulehner, W.; and Bart, H.-J., (1994). Numerical Determination of Droplet Size in Extraction Columns. In: 7th European Conference on Mathematics in Industry, Fasano A., Primerico M., Eds., Teubner Stuttgart, 247-254.
- Kronberger, T.; Ortner, A.; Zulehner, W.; and Bart, H.-J., (1995). Numerical Simulation of Extraction Columns using a Drop Population Model. *Comput. Chem. Eng.*, 19, 639-644.
- Kronig, R.; and Brink, J., (1950). On the theory of extraction from falling droplets. *Appl. Sci. Res.*, A2, 142-154.
- Kruis, F.E.; Maisels, A.; Fissan, H., (2000). Direct simulation Monte Carlo method for particle coagulation and aggregation. *AIChE J.*, 46(9), 1735-1742.
- Kumar, S.; Ramkrishna, D., (1996a). On the solution of population balance equations by discretization-I. A fixed pivot technique. *Chem. Eng. Sci.*, 51, 1311-1332.
- Kumar, S.; Ramkrishna, D., (1996b). On the solution of population balance equations by discretization-II. A moving pivot technique. *Chem. Eng. Sci.*, 51, 1333-1342.
- Kumar, A.; Hartland, S., (1999). Correlations for prediction of mass transfer coefficients in single drop systems and liquid-liquid extraction columns. *Chem. Eng. Res. Des.*, 77, 372-384.
- Kumar, A.; Hartland, S., (1996). Unified Correlation for the Prediction of Drop Size in Liquid-Liquid Extraction Columns. *Ind. Eng. Chem. Res.*, 35, 2682-2695.
- Kumar, A.; and Hartland, S., (1995). A unified correlation for the prediction of dispersed-phase hold-up in liquid-liquid extraction columns. *Ind. Eng. Chem. Res.*, 34, 3925-2695.
- Kumar, A.; and Hartland, S., (1994). Empirical prediction of operating variables. In: Godfrey, J.C.; and Slater, M.J.; (eds.), Liquid-Liquid extraction equipment, Wiley & Sons, Chichester, United Kingdom, 141-226.
- Kumar, A.; and Hartland, S., (1994). Prediction of drop size, dispersed phase holdup, slip velocity and limiting throughputs in packed extraction columns. *Chem. Eng. Res. Des.*, 72, 89-104.
- Kumar, A.; and Hartland, S., (1988). Mass Transfer in a Kühni Extraction Column. *Ind. Eng. Chem. Res.*, 27, 1198-1203.
- Kumar, A.; and Hartland, S., (1986). Prediction of drop size in pulsed perforated-plate extraction columns. *Chem. Eng. Commun.*, 44, 163-182.
- Kumar, A.; and Hartland, S., (1986). Prediction of Drop Size in Rotating Disc Extractors. *Can. J. Chem. Eng.*, 64, 915-924.
- Lambin P.; Gaspard, J.P., (1982). Continued-fraction technique for tight-binding systems. A generalized-moments method. *Phys. Rev. B*, 26(8), 4356-4368.
- Lasheras, J.C.; Eastwood, C.; Martínez-Bazán, C.; Montañés, J.L., (2002). A review of statistical models for the break-up of an immiscible fluid immersed into a fully developed turbulent flow. *Int. J. Multiphase Flow*, 28, 247-278.
- Laso, M.; Steiner, L.; Hartland, S., (1987). Dynamic simulation of agitated liquid-liquid dispersions-II. Experimental determination of breakage and coalescence rates in a stirred tank. *Chem. Eng. Sci.*, 42(10), 2437-2445.
- Lattuada, M.; Wu H.; Morbidelli, M., (2003). A simple model for the structure of fractal aggregates. *J. Colloid Interface Sci.*, 268, 106-120
- Lee K.; Matsoukas, T., (2000). Simultaneous coagulation and break-up using constant-N Monte Carlo. *Powder Technol.*, 110, 82-89.

- Lehr, F.; Mewes, D., (2001). A Transport Equation for the Interfacial Area Density Applied to Bubble Columns. *Chem. Eng. Sci.* 56, 1159-1166.
- Lehr, F.; Millies, M.; Mewes, D., (2002). Bubble-size distributions and flow fields in bubble columns. *AIChE. J.* 48, 2426-2442.
- Leveque, R.J., (2004). *Finite Volume Methods for Hyperbolic Problems*. Cambridge University Press, Cambridge, United Kingdom.
- Liao, Y. and Lucas, D., (2010). A literature review on mechanisms and models for the coalescence process of fluid particles. *Chem. Eng. Sci.*, 65, 10, 2851-2864.
- Liao, Y.; Lucas, D., (2009). A literature review of theoretical models for drop and bubble breakup in turbulent dispersions. *Chem. Eng. Sci.*, 64(15) 3389-3406.
- Liffman, K., (1992). A direct simulation Monte-Carlo method for cluster coagulation. *J. Comput. Phys.*, 100(1), 116-127.
- Lin, Y.; Lee K.; Matsoukas, T., (2002). Solution of the population balance equation using constant-number Monte Carlo. *Chem. Eng. Sci.*, 57, 2241-2252.
- Litster, J.D.; Smit, D.J.; Hounslow, M.J., (1995). Adjustable discretization population balance for growth and aggregation. *AIChE. J.*, 41, 591-603.
- Lo, T.C.; Baird, M.H.I.; Hanson, C., (eds.) (1983). *Handbook of Solvent Extraction*. John Wiley and Sons, New York, USA.
- Logsdaile, D. H.; and Thornton, J. D., (1957). Liquid-liquid Extraction. Part XIV: The Effect of Column Diameter upon the Performance and Throughput of Pulsed Plate Columns. *Trans. Inst. Chem. Eng.*, 35, 331-342.
- Lorenz, M.; Haverland, H.; and Vogelpohl, A., (1990). Fluid dynamics of pulsed sieve plate extraction columns. *Chem. Eng. Technol.*, 13, 411-422.
- Luo, H.; Svendsen, H.F., (1996). Theoretical model for drop and bubble breakup in turbulent dispersions. *AIChE. J.*, 42, 1225-1233.
- Luo, H. (1993). Coalescence, Breakup and Liquid Circulation in Bubble Column Reactors. PhD thesis, University of Trondheim, Trondheim, Norway.
- Madden, A.J.; and Damerell, G.L., (1962). Coalescence Frequencies in Agitated Liquid-Liquid Systems. *AIChE J.*, 8(2), 233-239.
- Mafield, F.D.; and Church, W.L., (1952). Liquid-liquid extractor design. *Ind. Eng. Chem.*, 44, 2253-2260.
- Maisels, A.; Einar Kruis F.; Fissan, H., (2004). Direct simulation Monte Carlo for simultaneous nucleation, coagulation, and surface growth in dispersed systems. *Chem. Eng. Sci.*, 59(11), 2231-2239.
- Maisels, A.; Kruis F.E.; Fissan, H., (2004). Coagulation in bipolar aerosol chargers. *J. Aerosol Sci.*, 35, 1333-1345.
- Marangoni, C., (1871). Sul principio della viscosita' superficiale dei liquidi stabilito dal sig. *II NuovoCimento*, 5-6(1), 239-273.
- Marangoni, C., (1878). Difesa della teoria dell'elasticita' superficiale dei liquidi Plasticita' superficiale. *II Nuovo Cimento*, 3(1), 193-211.
- Marchisio, D.L.; Fox, R.O., (2005). Solution of population balance equation using the direct quadrature method of moments. *J. Aerosol Sci.*, 36, 43-73.
- Marchisio, D.L.; Pikturna, J.T.; Fox, R.O.; Vigil, R.D.; Barresi, A.A., (2003a). Quadrature method of moments for population-balance equations. *AIChE. J.*, 49, 1266-1276.
- Marchisio, D.L.; Vigil, R.D.; Fox, R.O., (2003b). Implementation of the quadrature method of moments in CFD codes for aggregation-breakage problems. *Chem. Eng. Sci.*, 58, 3337-3351.

- Marchisio, D.L.; Vigil, R.D.; Fox, R.O., (2003c). Quadrature method of moments for aggregation-breakage processes. *J. Colloid Interface Sci.*, 258, 322-334.
- Marchisio, D.L.; Fox R.O.; Fan, R., (2004). Application of the direct quadrature method of moments to polydisperse gas-solid fluidized beds. *Powder Technol.*, 139, 7-20.
- Martínez-Bazán, C.; Montañés, J.L.; Lasheras, J.C., (1999a). On the breakup of an air bubble injected into a fully developed turbulent flow. Part 1. Breakup frequency. *J. Fluid Mech.*, 401, 157-182.
- Martínez-Bazán, C.; Montañés, J.L.; Lasheras, J.C., (1999b). On the breakup of an air bubble injected into a fully developed turbulent flow. Part 2. Size PDF of the resulting daughter bubbles. *J. Fluid Mech.*, 401, 183-207.
- Matsoukas T.; Friedlander, S.K., (1991). Dynamics of aerosol agglomerate formation. *J. Colloid Interface Sci.*, 146, 495-506.
- McGraw R.; Wright, D.L., (2002). Chemically resolved aerosol dynamics for internal mixtures by the quadrature method of moments. *J. Aerosol Sci.*, 34, 189-209.
- McGraw, R., (1997). Description of aerosol dynamics by the quadrature method of moments. *Aerosol Sci. Tech.*, 27, 255-265.
- Millies, M.; Mewes, D., (1999). Interfacial Area Density in Bubbly Flow. *Chem. Eng. Process.*, 38, 307-319
- Misek, T., (1978). Recommended Systems for Liquid-Liquid Extraction Studies. European Federation of Chemical Engineering, Working Party on Distillation, Absorption and Extraction, Eds.: The Institution of Chemical Engineers, Rugby, United Kingdom.
- Misek, T.; Berger, R.; and Schröter, J., (1985). Standard Test Systems for Liquid-Liquid Extraction. European Federation of Chemical Engineering. Working Party on Distillation, Absorption and Extraction, Eds.: The Institution of Chemical Engineers, Rugby, United Kingdom.
- Mjalli, F.S.; Abdel-Jabbar, N.M.; Fletcher, J.P., (2005). Modeling, simulation and control of a scheibel liquid-liquid contactor Part 1. Dynamic analysis and system identification. *Chem. Eng. Process.*, 44, 543-555.
- Mjalli, F.S., (2005). Neural network model-based predictive control of liquid-liquid extraction contactors. *Chem. Eng. Sci.*, 60, 239-253.
- Mjalli, F.S., (2007). Control of Stagewise Extractors Using Neural-Based Approximate Predictive Control as Compared to Nonlinear MPC. *Solvent Extr. Ion Exch.*, 24, 227-250.
- Modes, G.; Bart, H.J.; Perancho, R.D.; Bröder, D., (1999). Simulation of the fluid dynamics of solvent extraction columns from single droplet parameters. *Chem. Eng. Tech.*, 22, 231-236.
- Mohanty, S., (2000). Modeling of liquid-liquid extraction column: A Review. *Rev. Chem. Eng.*, 16, 199-248.
- Mostaedi, M.T.; Safdari, J.; and Ghaemi, A., (2010). Mass transfer coefficients in pulsed perforated-plate extraction columns. *Braz. J. Chem. Eng.*, 27, 243- 251.
- Narsimhan, G.; Gupta, J.P., (1979). A model for transitional breakage probability of droplets in agitated lean liquid-liquid dispersions. *Chem. Eng. Sci.*, 34, 257-265.
- Narsimhan, G.; Nejjfelt, G.; Ramkrishna, D., (1984). Breakage functions for droplets in agitated liquid-liquid dispersion. *AIChE J.*, 30(3), 457-467.
- Newman, A.B., (1931). The drying of porous solids diffusion and surface emission equations. *AIChE J.*, 27, 203-220.
- Nicmanis, M.; Hounslow, M.J., (1998). Finite-element methods for steady-state population balance equations. *AIChE. J.*, 44, 2258-2272.

- Oliveira, N.S. Moraes Silva, D.; Gondim, M.P.C.; and Borges Mansur, M.A., (2008). Study of the drop size distributions and hold-up in short Kühni columns. *Braz. J. Chem. Eng.*, 25, 729-741.
- Patruno, L.E.; Dorao, C.A.; Svendsen, H.F.; Jakobsen, H.A., (2009). Analysis of breakage kernels for population balance modelling. *Chem. Eng. Sci.*, 64(3), 501-508.
- Patruno, L.E.; Dorao, C.A.; Dupuy, P.M.; Svendsen, H.F.; Jakobsen, H.A., (2009). Identification of droplet breakage kernel for population balance modelling. *Chem. Eng. Sci.*, 64(4), 638-645.
- Pérez, A.; Elman, H.; and Morales, C., (2005). Fluid dynamics study of a liquid-liquid extraction process in a column packed with SMVP. *Sep. Sci. Technol.*, 40, 1513-1535.
- Pfennig, A.; Pilhofer, T.; Schröter, J., (2006). *Flüssig-Flüssig Extraktion*. In: Fluidverfahrenstechnik Band 2, Goedecke, R. (Hrsg.), Wiley-VCH, Weinheim.
- Pohorecki, R.; Moniuk, W.; Bielsky, P.; Zdrójkowski, A., (2001). Modelling of the coalescence/ redispersion processes in bubble columns. *Chem. Eng. Sci.* 56, 6157-6164.
- Prabhakar, A.; Sriniketan, G.; Varma, Y.B.G., (1988). Dispersed phase holdup and drop size distribution in pulsed plate columns. *Can. J. Chem. Eng.*, 66(2), 232-240.
- Pratt, H.R.C.; and Stevens, G.W., (1992). *Selection, design, pilot-testing and scale-up of extraction equipment*. In: Science and Practice in Liquid-Liquid Extraction; Thornton, J. D. (Ed.), Oxford University Press: New York.
- Prince, M. J.; Blanch, H.W., (1990). Bubble coalescence and break-up in air-sparged bubble columns. *AIChE J.*, 36, 1485-1499.
- Rahbar, A.; Azizi, Z.; Bahmanyar, H.; and Moosavian, M.A., (2011). Prediction of enhancement factor for mass transfer coefficient in regular packed liquid-liquid extraction columns. *Can. J. Chem. Eng.*, 89(3), 508-519.
- Ramkrishna, D.; Mahoney, A.W., (2002). Population balance modeling. Promise for the future. *Chem. Eng. Sci.*, 57, 595- 606.
- Ramkrishna, D., (1985). The Status of Population Balances. *Rev. Chem. Eng.*, 3, 49-95.
- Ramkrishna, D., (2000). *Population Balances Theory and Applications to Particulate Systems in Engineering*. Academic Press, London, United Kingdom.
- Randolph, A., (1964). A population balance for countable entities. *Can. J. Chem. Eng.*, 42, 208-281
- Reay, D.; Ramshaw, C.; Harvey, A., (2008). *Process Intensification: Engineering for Efficiency, Sustainability and Flexibility*. Butterworth-Heinemann, Oxford, United Kingdom.
- Ribeiro, L.M.; Regueiras, P.F.R.; Guimarães, M.M.L.; Madureira, C.M.N.; Cruz-Pinto, J.J.C., (1996). The dynamic behaviour of liquid-liquid agitated dispersions-II. Coupled hydrodynamics and mass transfer. *Comput. Chem. Eng.*, 21, 543-558.
- Richardson, J.F.; Zaki, W., (1954). Sedimentation and Fluidisation: Part I. *Chem. Eng. Res. Des.*, 32, 35-53.
- Rong, F.; Marchisio, D.; Fox, R.O., (2004). Application of the direct quadrature method of moments to polydisperse gas solid fluidized beds. *Powder Technol.*, 139, 7-20.
- Rosner, D.E.; Pyykonen, J.J., (2002). Bivariate Moment Simulation of Coagulating and Sintering Nano-particles in Flames. *AIChE J.*, 48(3), 476-491.
- Rosner D.E.; Yu, S., (2001). Monte Carlo simulation of aerosol aggregation and simultaneous spheroidization. *AIChE J.*, 47(3), 545-561.
- Rosner, D.E.; McGraw R.; Tandon, P., (2003). Multivariate population balances via moment and Monte Carlo simulation methods: an important sol reaction engineering bivariate

- example and mixed moments for the estimation of deposition, scavenging, and optical properties for populations of nonspherical suspended particles. *Ind. Eng. Chem. Res.*, 42, 2699-2711.
- Saboni, A.; Gourdon, C.; and Chesters, A.K., (1999). The influence of inter-phase mass transfer on the drainage of partially mobile liquid films between drops undergoing a constant interaction force. *Chem. Eng. Sci.*, 54, 461-473.
 - Sanvordenker, K.S., (1960). Engineering Study of a Perforated Plate Pulse Column. Dissertation, The University of Michigan, Michigan, USA.
 - Sattler, K.; Feindt, H., (1995). *Thermal Separation Processes, Principles and Design*. Wiley-VCH, Weinheim.
 - Sehmel, G.A.; Babb, A.L., (1963). Holdup studies in a pulsed sieve-plate solvent extraction column. *Ind. Eng. Chem. Process Des. Dev.*, 2(1), 38-42.
 - Schmidt, A.S.; Simon, M.; Attarakih, M.M.; Lagar, L.G.; and Bart, H.-J., (2006). Droplet Population Balance Modelling: Hydrodynamics and Mass Transfer. *Chem. Eng. Sci.*, 61, 246-256.
 - Schmidt, S.A., (2006). *Populationsdynamische Simulation gerührter Extraktionskolonnen auf der Basis von Einzeltropfen- und Tropfenschwarmuntersuchungen*. Dr.-Ing. Thesis, Shaker Verlag, Aachen.
 - Seader, J.D., (2006). *Separation Process Principles*. John Wiley & Sons, Hoboken.
 - Sege, G.; and Woodfield, F.W., (1954). Pulse column variables. *Chem. Eng. Prog.*, 50, 396-402.
 - Shen, Z.J.; Ramarao, N.V.; and Baird, M.H.I., (1985). Mass Transfer in a Reciprocating Plate Extraction Column - Effects of Mass Transfer Direction and Plate Material. *Can. J. Chem. Eng.*, 63(1), 29-36.
 - Slater, M.J., (1995). A Combined Model of Mass Transfer Coefficients for Contaminated Drop Liquid-Liquid Systems. *Can. J. Chem. Eng.*, 73, 462-469.
 - Smith, M.; Matsoukas, T., (1998). Constant-number Monte Carlo simulation of population balances. *Chem. Eng. Sci.*, 53, 1777-1786.
 - Smoot, L.D.; Mar, B.W.; and Babb, A.L., (195). Flooding characteristics and separation efficiencies of pulsed sieve-plate extraction columns experimental data applied to design of extraction columns. *Ind. Eng. Chem.*, 9(51), 1005-1010.
 - Soltanali, S.; Ziaie-Shirkolaei, Y., (2008). Experimental Correlation of Mean Drop Size in Rotating Disc Contactors (RDC). *J. Chem. Eng. Jpn.*, 41, 862-869.
 - Sovova, H., (1981). Breakage and Coalescence of Drops in a Batch Stirred Vessel- II Comparison of Model and Experiment. *Chem. Eng. Sci.* 36, 1567-1573.
 - Steiner, L.; Bertschmann, H.; and Hartland, S., (1995). A Model for Simulation of Hydrodynamics and Mass-Transfer in Extraction Columns Filled with a Regular Packing. *Chem. Eng. Res. Des.*, 73, 542-550.
 - Steinmetz, T.; Schmidt, S.A.; and Bart, H.-J., (2005). Modellierung gerührter Extraktionskolonnen mit dem Tropfenpopulationsbilanzmodell. *Chem. Ing. Tech.*, 77(6), 723-733.
 - Tandon, P.; Rosner, D.E., (1999). Monte Carlo Simulation of Particle Aggregation and Simultaneous Restructuring. *J. Colloid Interface Sci.*, 213, 273-286
 - Thornton, J.D., (1957). Liquid-Liquid Extraction Part XIII: The Effect of Pulse Wave Form and Plate Geometry on the Performance and Throughput of a Pulsed Column. *Trans. Inst. Chem. Eng.*, 35, 136-330.

- Thornton, D., (1992). *Science and Practice of Liquid-Liquid Extraction 2*. Oxford University Press, New York.
- Torab-Mostaedi, M.; and Safdari, J., (2009). Prediction of Mass Transfer Coefficients in a Pulsed Packed Extraction Column Using Effective Diffusivity. *Braz. J. Chem. Eng.*, 26, 685-694.
- Treybal, R., (1963). *Liquid Extraction*. McGraw-Hill, New York.
- Treybal, R., (1980). *Mass-Transfer Operations*. McGraw-Hill Book Company, New York.
- Tsouris, C.; Tavlarides, L.L., (1994). Breakage and Coalescence Models for Drops in Turbulent Dispersions. *AIChE J.*, 40, 395-406.
- Tsouris, C.; Kirou, V. I.; Tavlarides, L. L., (1994). Drop size distribution and holdup profiles in a multistage extraction column. *AIChE J.*, 40, 407-418.
- Tung, L.S.; and Luecke, R.H., (1986). Mass Transfer and Drop Sizes in Pulsed-Plate Extraction Columns. *Ind. Eng. Chem. Process Des. Dev.*, 25, 664-673.
- Valentas, K.J.; Amundson, N.R., (1966). Breakage and coalescence in dispersed phase systems. *Ind. Eng. Chem. Fundam.*, 5, 533-542.
- Valentas, K.J.; Bilous, O.; Amundson, N.R., (1966). Analysis of breakage in dispersed phase systems. *Ind. Eng. Chem. Fundam.*, 5, 271-279.
- Van Dijck, W. J. D., (1935). Tower with internal perforated plates suitable for extracting liquid by treatment with other liquids and for similar counter-current contact processes. U.S. Patent 2,011,186.
- Vanni, M., (2000). Approximate Population Balance Equations for Aggregation-Breakage Processes. *J. Colloid Interface Sci.*, 221, 143-160.
- Venkatanarasaiiah, D.; and Varma, Y.B.G., (1988). Dispersed phase holdup and mass transfer in liquid pulsed column. *Bioproc. Biosys. Eng.*, 18, 119-126.
- Vignes, A., (1965). Hydrodynamique des dispersions. *Genie Chimique*, 93, 129-142.
- Wang, T.; Wang, J.; Jin, Y., (2003). A novel theoretical breakup kernel function for bubbles/droplets in a turbulent flow. *Chem. Eng. Sci.*, 58, 4629-4637.
- Wang, F.; Mao, Z.-S., (2005). Numerical and experimental investigation of liquid-liquid two-phase flow in stirred tanks. *Ind. Eng. Chem. Res.*, 44, 5776-5787.
- Wang, Y.; Jing, S.; Wu, G.; and Wu, W., (2006). Axial mixing and mass transfer characteristics of pulsed extraction column with discs and doughnuts. *Trans. Nonferrous Met. Soc. Chin.*, 16, 178-184.
- Weinstein, O.; Semiat, R.; Lewin, D., (1998). Modelling, simulation and control of liquid-liquid extraction columns. *Chem. Eng. Sci.*, 53, 325-339.
- Weiss, J.; Steiner, L.; and Hartland, S., (1995). Determination of Actual Drop Velocities in Agitated Extraction Columns. *Chem. Eng. Sci.*, 50(2), 255-261.
- Wesselingh, J.A.; Bollen, A.M., (1999). Single particles, bubbles and drops: Their velocities and mass transfer coefficients. *Trans. Inst. Chem. Eng.*, 77, 89-96.
- Wolschner, B.H., (1980). *Konzentrationsprofile in Drehscheibenextraktoren*. Dissertation, Technische Universität Graz, Graz, Austria.
- Wright, D.L.; McGraw, R.; and Rosner, D.E., (2001). Bivariate extension of the quadrature method of moments for modeling simultaneous coagulation and sintering of particle populations. *J. Colloid Interface Sci.*, 236, 242-251.
- Xiaojin, T.; Guangsheng, L.; and Jiading, W., (2005). An improved dynamic combined model for evaluating the mass transfer performances in extraction columns. *Chem. Eng. Sci.*, 60, 4409-4421.

- Yadav, R.L.; and Patwardhan, A.W., (2008). Design aspects of pulsed sieve plate columns. *Chem. Eng. J.*, 138, 389 -415.
- Yoon, C.; McGraw, R., (2004). Representation of generally mixed multivariate aerosols by the quadrature method of moments: I. Statistical foundation. *J. Aerosol Sci.*, 35(5), 561-576.
- Yoon, C.; McGraw, R., (2004). Representation of generally mixed multivariate aerosols by the quadrature method of moments: II. Aerosol dynamics. *J. Aerosol Sci.*, 35, 577-598
- Zaccone, A.; Gäbler, A.; Maaß, S.; Marchisio, D.; Kraume, M., (2007). Drop breakage in liquid-liquid stirred dispersions-Modelling of single drop breakage. *Chem. Eng. Sci.*, 62, 6297-6307.
- Zamponi, G., (1996). *Das dynamische Verhalten einer gerührten Solventextraktionskolonne*. Shaker Verlag, Aachen.
- Zamponi, G.; Stichlmair, J.; Gerstlaur, A.; Gilles, E.D., (1996). Simulation of the transient behaviour of a stirred liquid-liquid extraction column. *Comp. Chem. Eng.*, 20, S963-S968.
- Zhao H.; Zheng, C., (2006). Monte Carlo solution of wet scavenging of aerosols by precipitation. *Atmos. Environ.*, 40(8), 1510-1525.
- Zhao, H.; Zheng, C.; Xu, M., (2005a). Multi-Monte Carlo method for coagulation and condensation/evaporation in dispersed systems. *J. Colloid Interface Sci.*, 286(1),195-208.
- Zhao, H.; Zheng C.; Xu, M., (2005b). Multi-Monte Carlo approach for general dynamic equation considering simultaneous particle coagulation and breakage. *Powder Technol.*, 154(2-3), 164-178.
- Zhao, H.; Zheng C.; Xu, M., (2005c). Multi-Monte Carlo method general dynamic equation considering particle coagulation. *Appl. Math. Mech.*, 26(7), 953-962.

Own publications

- I. **M. Jaradat**, H. Allaboun, H.-J. Bart and M. Attarakih (2012). Dynamic modelling and simulation of Kühni extraction columns. *Computer Aided Chemical Engineering*, 30, 1073–1077.
- II. **M. Jaradat**, M. Attarakih, H.-J. Bart (2012). *Transient modelling and simulation of Kühni extraction column: hydrodynamics and mass transfer using population balance model*. *Chem. Eng. Technol.*, DOI: 10.1002/ceat.201200164.
- III. **M.M. Jaradat**, M.M. Attarakih, T. Steinmetz, H.-J. Bart (2012). *LLECMOD: A Bivariate Population Balance Simulation Tool for Pulsed (Packed and Sieve Plate) Liquid-Liquid Extraction Columns*. *Open Chem. Eng. J.*, 6, 8-31.
- IV. **M. Jaradat**, M. Attarakih, H.-J. Bart (2012). *RDC Extraction Column Simulation using the Multi-Primary One Secondary Particle Method: Coupled Hydrodynamics and Mass Transfer*. *Comput. Chem. Eng.*, 37(10), 22–32.
- V. **M. Jaradat**, M. Attarakih, H.-J. Bart (2011). *Population Balance Modelling of Pulsed (Packed and Sieve Plate) Extraction Columns: Coupled Hydrodynamic and Mass Transfer*. *Ind. Eng. Chem. Res.*, 50 (24), 14121–14135.
- VI. **M. Jaradat**, M. Attarakih, H.-J. Bart (2011). *Advanced Prediction of Pulsed (packed and sieve plate) Extraction Columns Performance Using Population Balance Modelling*. *Chem. Eng. Res. Des. - IChemE*, 89(12), 2752-2760.
- VII. **M. Jaradat**, M. Attarakih and H.-J. Bart (2011). *Detailed Mathematical Modelling of Liquid-Liquid Extraction Columns*. *Computer Aided Chemical Engineering*, 29, 1-5.
- VIII. **M. Jaradat**, M. Attarakih, H.-J. Bart (2011). *Advanced Prediction of Pulsed Extraction Column Performance using LLECMOD*. (CM)² young researcher symposium proceeding, 45-49, 15 February 2011, Kaiserslautern - Deutschland.
- IX. **M. Jaradat**, M. Attarakih and H.-J. Bart (2010). *Effect of Phase Dispersion and Mass Transfer Direction on Steady State RDC Performance using Population Balance Modelling*. *Chem. Eng. J.*, 165, 2, pp. 379-387.
- X. **M. Jaradat**, M. Attarakih, M. Hlawitschka and H.-J. Bart (2010). *A multivariate population balance model for liquid extraction columns*. *Proc. 4th International Conference on Population Balance Modelling*, September 15 - 17, 2010, Berlin - Germany.
- XI. **M. Jaradat**, M. Attarakih and H.-J. Bart (2010). *Simulation gekoppelter Hydrodynamik und Stofftransport mittels einer Populationsbilanz*. *Chem. Ing. Tech.*, Vol. 82, Issue 9, 1390.
- XII. **M. Jaradat**, M. Attarakih and H.-J. Bart (2009). *Dynamische Simulation von Extraktionskolonnen auf der Grundlage einer multivariaten Populationsbilanz*. *Chem. Ing. Tech.*, Vol. 81, No. 8, 1061.
- XIII. M. Attarakih, **M. Jaradat**, M. Hlawitschka, H.-J. Bart and J. Kuhnert (2011). *Integral Formulation of the Population Balance Equation using the Cumulative Quadrature Method of Moments (CQMOM)*. *Computer Aided Chemical Engineering*, 29, 81-85.
- XIV. M.M. Attarakih, **M. Jaradat**, H.-J. Bart and J. Kuhnert (2010). *Solution of the population balance equation using the Cumulative Quadrature Method of Moments (CQMOM)*. *Proc. 4th International Conference on Population Balance Modelling*, September 15 - 17, 2010, Berlin - Germany.

- XV. M.M. Attarakih, **M. Jaradat**, C. Drumm, H.-J. Bart, S. Tiwari, V.K. Sharma, J. Kuhnert & A. Klar (2010). *A multivariate sectional quadrature method of moments for the solution of the population balance equation*. Proc. of 20th European Symposium on Computer-Aided Process Engineering-ESCAPE 20, Ischia, Naples - Italy, June 2010.
- XVI. M. Attarakih, **M. Jaradat**, C. Drumm, H.-J. Bart, S. Tiwari, V.K. Sharma (2009). *Solution of the Population Balance Equation using the One Primary and One Secondary Particle Method (OPOSPM)*. In J. Jeżowski & J. Thullie (Eds.), 19th European Symposium on Computer Aided Process Engineering-ESCAPE19. Cracow - Poland: Elsevier.
- XVII. M. Attarakih, **M. Jaradat**, C. Drumm, H.-J. Bart, S. Tiwari, V.K. Sharma (2009). *A Multivariate Population Balance Model for Liquid Extraction Columns*. In J. Jeżowski & J. Thullie (Eds.), 19th European Symposium on Computer Aided Process Engineering-ESCAPE19. Cracow - Poland: Elsevier.
- XVIII. M.M. Attarakih, **M. Jaradat**, H. Allaboun, H.-J. Bart & N.M. Faqir (2008). *Dynamic Modelling of a Rotating Disk Contactor Using the Primary and Secondary Particle Method (PSPM)*. In Bertrand Braunschweig & Xavier Joulia (Eds.), 18th European Symposium on Computer Aided Process Engineering-ESCAPE 18. Lyon - France: Elsevier.
- XIX. M. Mickler, S. Didas, **M. Jaradat**, M. Attarakih, H.-J. Bart (2011). *Tropfenschwarmanalytik mittels Bildverarbeitung zur Simulation von Extraktionskolonnen mit Populationsbilanzen*. Chem. Ing. Tech., 83, 3, pp. 227–236.
- XX. H.-J. Bart, M.W. Hlawitschka, M. Mickler, **M. Jaradat**, S. Didas, F. Chen, H. Hagen (2011). *Tropfenschwarmanalytik, Visualisierung und Simulation*. Chem. Ing. Tech. 83, 7, 965-978.
- XXI. M.W. Hlawitschka, F. Chen, M. Attarakih, **M. Jaradat**, J. Kuhnert, M. Mickler, H.-J. Bart (2011). *A CFD-Population Balance Model for the Simulation of Kühni Extraction Column*. Computer Aided Chemical Engineering, 29, 66-70.
- XXII. M.W. Hlawitschka, C. Drumm, M.M. Attarakih, **M. Jaradat**, H.-J. Bart (2010). *Simulation of a Kühni extraction column using a CFD and population balance model*. Proc. 4th International Conference on Population Balance Modelling, Berlin - Germany, September 15 - 17, 2010, September 15 - 17, 2010.
- XXIII. V.K. Sharma, S. Tiwari, M.M. Attarakih, **M. Jaradat**, A. Klar, J. Kuhnert & H.-J. Bart (2010). *A spatially meshfree population balance model for the simulation of liquid extraction columns*. Proc. 4th International Conference on Population Balance Modelling, Berlin-Germany, September 15 - 17, 2010.
- XXIV. V.K. Sharma, S. Tiwari, M. Attarakih, **M. Jaradat**, A. Klar, J. Kuhnert and H.-J. Bart, et al. (2009). *Simulation of two phase flow with incorporated population balance equation using a meshfree method*. In J. Jeżowski & J. Thullie (Eds.), 19th European Symposium on Computer Aided Process Engineering-ESCAPE19. Cracow - Poland: Elsevier.

Oral and poster presentations

Oral:

- **M. Jaradat**, (April 2008). *Investigation of Extraction Column (RDC) Performance using Population Balance Equation (PBE)*. Oral presentation at the annual meeting of the ProcessNet specialized committee extraction and the working group Phytoextrakte, Clausthal - Deutschland.
- **M. Jaradat**, (May 2008). *Liquid-Liquid Extraction Column Simulation Module (LLECMOD)*. Oral presentation at the ReDrop Workshop, RWTH Aachen - Deutschland.
- **M. Jaradat**, (March 2009). *Effect of Mass Transfer Direction on Extraction Column Performance using Population Balance Equation (PBE)*. Oral presentation at the ProcessNet Fachausschüsse CFD, Extraktion & Mischvorgänge, Fulda - Deutschland.
- **M. Jaradat**, (May 2009). *Advanced Prediction of Extraction Column Performance Using Population Balance Equation (PBE)*. Oral presentation at theACHEMA 2009, Frankfurt - Deutschland.
- **M. Jaradat**, (June 2009). *Solution of the Population Balance Equation using the One Primary and One Secondary Particle Method (OPOSPM)*. Oral presentation at the 19th European Symposium on Computer Aided Process Engineering – ESCAPE19, Cracow - Poland.
- **M. Jaradat**, (September 2009). *Dynamic Simulation of Liquid-Liquid Extraction Columns*. Oral presentation at the ProcessNet Jahrestagung, Mannheim - Deutschland.
- **M. Jaradat**, (March 2010). *Liquid-Liquid Extraction Columns Simulation Based on the Bivariate Population Balance and the Multi-primary Particle Concept*. Oral presentation at the ProcessNet Jahrestagung, Frankfurt - Deutschland.
- **M. Jaradat**, (February 2011). *Advanced Prediction of Pulsed Extraction Column Performance using LLECMOD*. Oral presentation at the (CM)² young researcher symposium, Kaiserslautern - Deutschland.
- **M. Jaradat**, (March 2011). *Simulation of Liquid-Liquid Extraction Columns Using LLECMOD*. Oral presentation at the Jahrestreffen der ProcessNet-Fachausschüsse Extraktion, Fluidverfahrenstechnik, Mehrphasenströmungen und Phytoextrakte, Fulda - Deutschland.
- **M. Jaradat**, (May 2011). *Detailed Mathematical Modelling of Liquid-Liquid Extraction Columns*. Oral presentation at the ESCAPE 21. Chalkidiki - Greece.
- **M. Jaradat**, (May 2011). *Integral Formulation of the Population Balance Equation Using the Cumulative QMOM (CQMOM)*. Oral presentation at the ESCAPE 21. Chalkidiki - Greece.
- **M. Jaradat**, (September 2011). *Pulsed Columns Performance Prediction using LLECMOD*. Oral presentation at the 8th ECCE. Berlin – Germany.

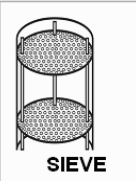
Posters:

- **M. Jaradat**, (September 2010). *Multivariate Population Balance for Liquid Extraction Columns*. Poster presentation at the 4th International Conference on Population Balance Modelling (PBM 2010), Berlin -Germany.
- **M. Jaradat**, (September 2010). *Simulation of Coupled Hydrodynamics and Mass Transfer Using a Bivariate Population Balance*. Poster presentation at the 28. DECHEMA - Jahrestagung der Biotechnologen und ProcessNet-Jahrestagung. Aachen - Germany.
- **M. Jaradat**, (March 2011). *Coupled Hydrodynamics and Mass Transfer Simulation Using the Multi-Primary One Secondary Particle Method*. Poster presentation at the Jahrestreffen der ProcessNet-Fachausschüsse Extraktion, Fluidverfahrenstechnik, Mehrphasenströmungen und Phytoextrakte, Fulda - Deutschland.
- **M. Jaradat**, (May 2011). *Detailed Mathematical Modelling of Liquid-Liquid Extraction Columns*. Poster presentation at the ESCAPE 21. Chalkidiki - Greece.
- **M. Jaradat**, (June 2012). *Dynamic modelling and simulation of Kühni extraction columns*. Poster presentation at the ESCAPE 22. London – United Kingdom.

Appendices

Figures

SIEVE



SIEVE

Pulse Amplitude [m]

0.0200

Pulse Frequency [1/Sec]

1.0000

Dispersion coefficient (active zone of the column)

Dispersion coeff. aqueous [m²/s]

0.0001000

Dispersion coeff. organic [m²/s]

0.0001000

☒ constant values ☐ internally calculated

Dispersion coefficient (settling zone of the column)

Dispersion coeff. aqueous [m²/s]

1.0000000

Dispersion coeff. organic [m²/s]

0.00010000

Close and continue

Column Internals Sieve Plate

Number of Plates [-]

15.0000

Plate Spacing [m]

0.1500

Orifice Diameter [m]

0.0020

Number of Orifices [-]

20.0000

Downcomer Diameter [m]

0.0150

Downcomer Height [m]

0.1000

Sieve Tray Diameter [m]

0.0790

Fractional Free Area [m]

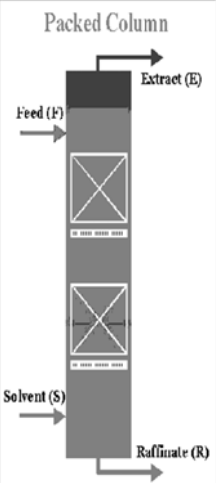
0.2300

Sieve Tray Thickness [m]

0.0010

Fig.III.1. Input dialogue for pulsed sieve plate column internal geometry

PACKED COLUMN



PACKED COLUMN

Height of a Packings [m]

0.1000

Diameter of a Pacing [m]

0.0790

Volumetric Surface Area [m²/m³]

350.0000

Void Fraction [m³/m³]

0.9700

Hole Diameter of Punched Sheets [m]

0.0040

Pulse Amplitude [s]

0.0500

Pulse Frequency [1/Sec]

1.0000

OK

Cancel

Fig.III.2. Input dialogue for pulsed packed column internal geometry

II

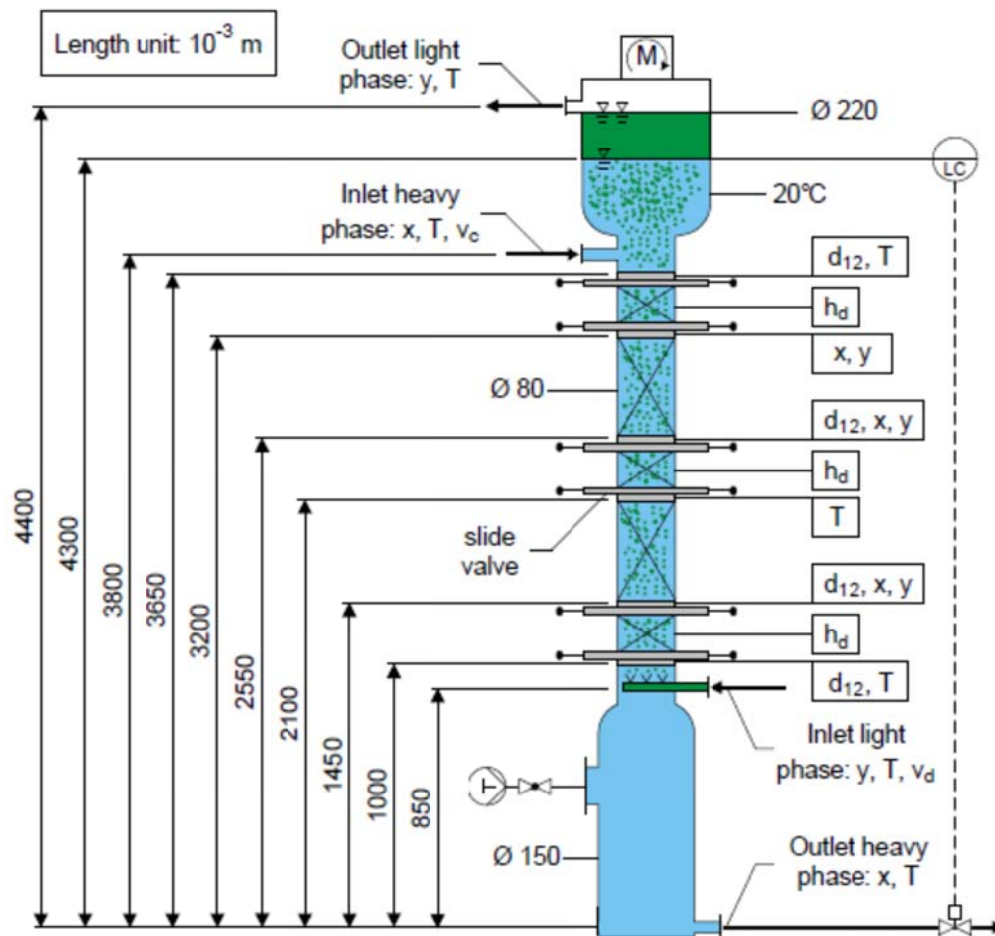


Fig.III.3. Pilot plant extraction column used in the experimental study of Garthe, 2006.

Transient Analysis

☐ Step response ☐ Multi-Step response ☐ Exponential Response OK

Transient change of rotational frequency *

Time step [s]	Rotational frequency [rpm]	Time step [s]	Rotational frequency [rpm]
at 1 to 1	at 1 to 1	at 1 to 1	at 1 to 1

Flow rate*

Flow rate (aqueous)

Time step [s]	Flow rate [litre/h]	Time step [s]	Flow rate [litre/h]
at 1 to 1	at 1 to 1	at 1 to 1	at 1 to 1

Flow rate (organic)

Time step [s]	Flow rate [litre/h]	Time step [s]	Flow rate [litre/h]
at 1 to 1	at 1 to 1	at 1 to 1	at 1 to 1

Concentration*

Concentration (aqueous)

Time step [s]	Concentration [kg/m ³]	Time step [s]	Concentration [kg/m ³]
at 1 to 1	at 1 to 1	at 1 to 1	at 1 to 1

Concentration (organic)

Time step [s]	Concentration [kg/m ³]	Time step [s]	Concentration [kg/m ³]
at 1 to 1	at 1 to 1	at 1 to 1	at 1 to 1

Concentration*

Concentration (aqueous)

Initial Time [s]	Time [min]
at 1 to 1	at 1 to 1

Concentration (organic)

Initial Time [s]	Time [min]
at 1 to 1	at 1 to 1

Exponential Function

$Y = A1 * \text{EXP} \{X1 / T1\} + A2 * \text{EXP} \{X2 / T2\} + Y0$

A1 1 A2 1 T1 1 T2 1 Y0 1

Input of initial conditions at main page

Graph showing concentration vs. time. The y-axis is labeled 'Concentration [kg/m³]' and ranges from 0.00 to 0.01. The x-axis is labeled 'Time [min]' and ranges from 0 to 20. The curve shows a rapid increase in concentration, reaching a plateau around 0.008 kg/m³ after approximately 10 minutes.

Fig.III.4. Input mask for transient analysis

Breakage Model: Aachen Sieve

A breakage model sieve column (Aachen)

OK Cancel

xi_2 1.1 xi_5 2.0 d_um (m) 4.366d-3

xi_3 0.3 xi_6 1.05 alpha_um 10.0d0

xi_4 2.00 xi_7 -0.45 alpha_gr 8.0d0

a_15 2.239d0

a_16 1.824d0

Stable droplet diameter
dstab,3 and dstab,4 are calculated internally

$$d_{stab,34} = \left(d_{stab,3}^{\zeta_2} + d_{stab,4}^{\zeta_2} \right)^{1/\zeta_2}$$

Average number of daughter drops
dstab and v_inf are calculated internally

$$\bar{n}_z = 2 + \zeta_3 \left[\left(\frac{d_M}{d_{stab}} \right)^{\zeta_4} - 1 \right] \left(\frac{af}{\phi v_\infty} + 1 \right)^{\zeta_4}$$

Breakage frequency

$$Ps = \zeta_6 \left(1 - \exp \left[\zeta_7 (\bar{n}_z - 2) \right] \right)$$

Fig.III.5. Input dialog for breakage Henschke (2004) model in pulsed sieve plate columns

Breakage Model: Aachen Packed

A breakage model packed column (Aachen)

OK Cancel

Breakage constant (ks) 2275

Time interval (delta t) 0.1

Exponent (a1) 1.5

Packing Angle (alpha) 45.0

Packing folding distance (X) 0.014

Packing folding height (Z) 0.008

Breakage frequency

$$P_s = k_s \frac{\pi}{8} \frac{\Delta h_T d_m^2 \sin(2\alpha)}{x^2 z} (2af + v_{abs}) d_m \left(\frac{d_m - d_{stab}}{d_m} \right)^{a_1}$$

Fig.III.6. Input dialog for Henschke (2004) breakage model in pulsed packed column

Breakage Model: Garthe 2006

Breakage model

Breakage Model (Garthe, 2006)

Model Parameter C1 (-) 1.98 Model Parameter C3 (-) 1.39

Model Parameter C2 (-) -0.08 Model Parameter C4 (-) 0.8

Breakage Probability

$$P(d) = C_1 \pi_{df}^{C_2} \frac{\left(\frac{(d - d_{stab})}{(d_{100} - d_{stab})} \right)^{C_3}}{C_4 + \left(\frac{(d - d_{stab})}{(d_{100} - d_{stab})} \right)^{C_3}}$$

d100 (mm) 4.5

dstab (mm) 2.0

Fig.III.7. Input dialog for Garthe (2006) breakage model in pulsed (packed and sieve plate) columns

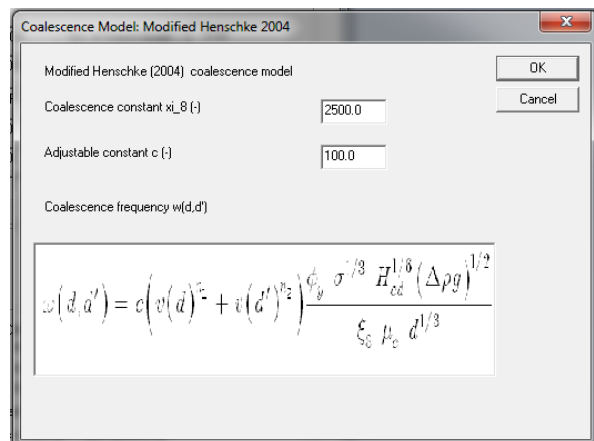


Fig.III.8. Input dialog for Henschke (2004) modified coalescence model in pulsed (packed and sieve plate) columns

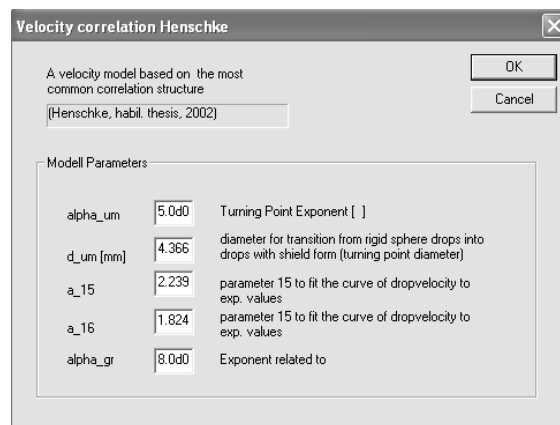


Fig.III.9. Input parameters for Henschke (2004) velocity model

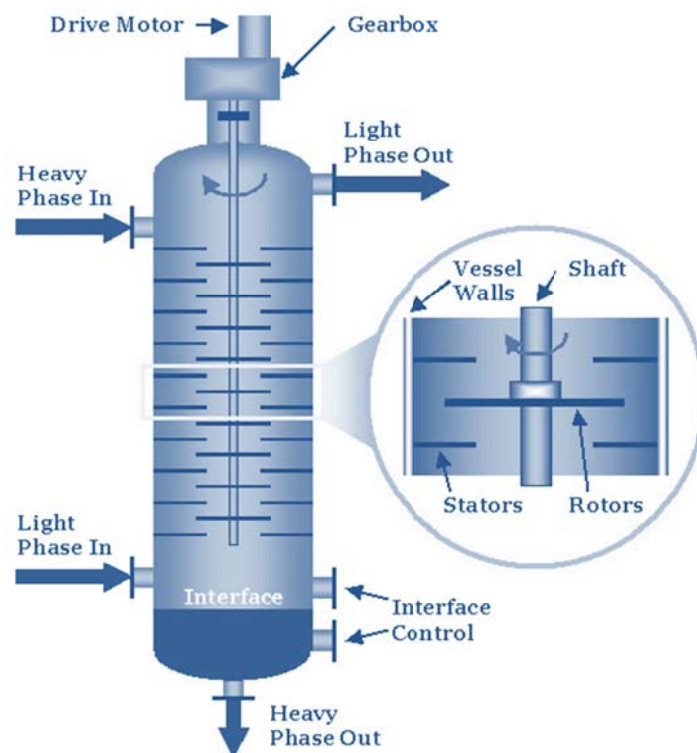


Fig.III.10: RDC; Source: <http://www.liquid-extraction.com/rdc-column.htm>

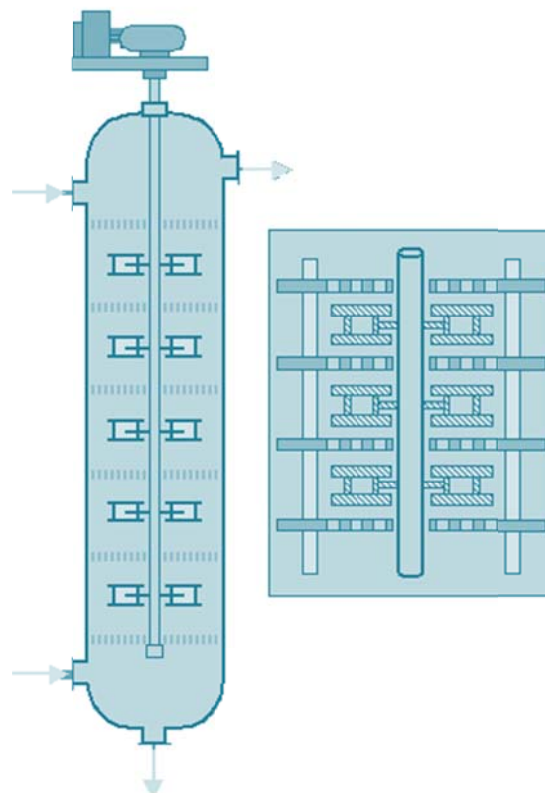


Fig.III.11: Kühni; Source: http://www.separationprocesses.com/Extraction/SE_039.htm

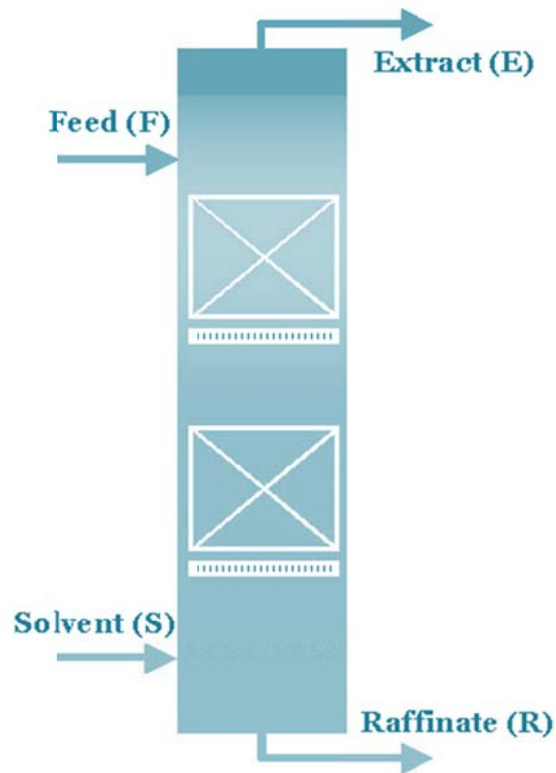


Fig.III.12: Packed; Source: <http://www.liquid-extraction.com/packed-column-random.htm>

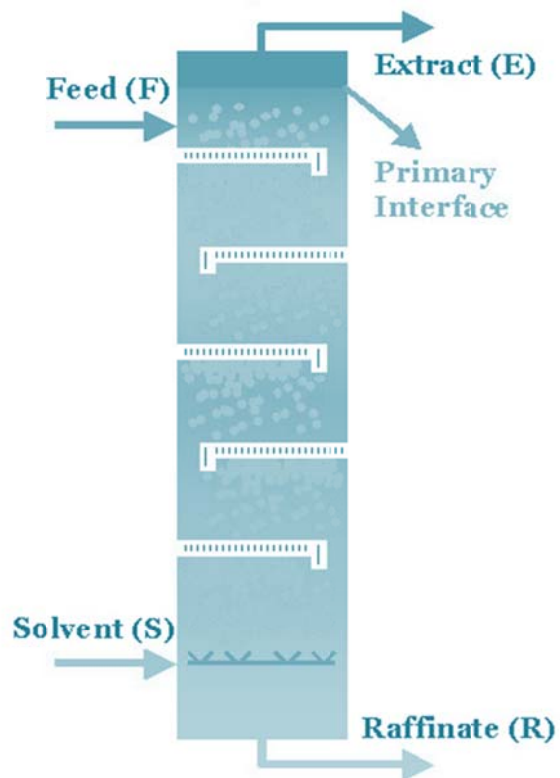


Fig.III.13: Sieve plate; Source: <http://www.liquid-extraction.com/sieve-tray-column.htm>

Curriculum Vitae

M. Sc. Eng. Moutasem Jaradat

Education:

10. 2007 - 07.2012 Ph.D. Candidate: The University of Kaiserslautern, Faculty of Mechanical and Process Engineering, Chair of Separation Science and Technology, Kaiserslautern - Germany.
09. 2004 - 06. 2007 Master Degree: Jordan University of Science and Technology, Faculty of Engineering, Chemical Engineering Department, Irbid - Jordan.
09. 1998 - 0.6. 2002 Bachelor Degree: Al -Balqa' Applied University, Faculty of Engineering Technology, Chemical Engineering Department, Amman - Jordan.

Professional Experience:

- 10.2007 - 10.2011 Research Associate/ Fellow, The University of Kaiserslautern, Faculty of Mechanical and Process Engineering, Chair of Separation Science and Technology, Kaiserslautern - Germany.
08. 2007 - 10.2007 Visiting Scholar, The University of Kaiserslautern, Faculty of Mechanical and Process Engineering, Chair of Separation Science and Technology, Kaiserslautern - Germany.
09. 2004 - 06. 2007 Teaching Assistant (TA), Jordan University of Science and Technology, Faculty of Engineering, Chemical Engineering Department, Irbid - Jordan.
09. 2003 - 07. 2004 Design & Installation (project) Engineer, Alwadi Establishment for Trading (Water Purification and Treatment Systems), Hofuf – Saudi Arabia
02. 2003 - 08. 2003 Design & Operation Engineer, Water Authority, Irbid Waste Water Treatment Station, Irbid - Jordan

Language:

- 1-Arabic: mother tongue.
- 2-English: very good.
- 3-German: good.